Course of Geodynamics

Dr. Magdala Tesauro

Course Outline:

1. Thermo-physical structure of the continental and oceanic crust
2. Thermo-physical structure of the continental lithosphere
3. Thermo-physical structure of the oceanic lithosphere and oceanic ridges
4. Strength and effective elastic thickness of the lithosphere
5. Plate tectonics and boundary forces
6. Hot spots, plumes, and convection
7. **Subduction zones systems**
8. Orogens formation and evolution
9. Sedimentary basins formation and evolution

Convergent plate margins of the Earth

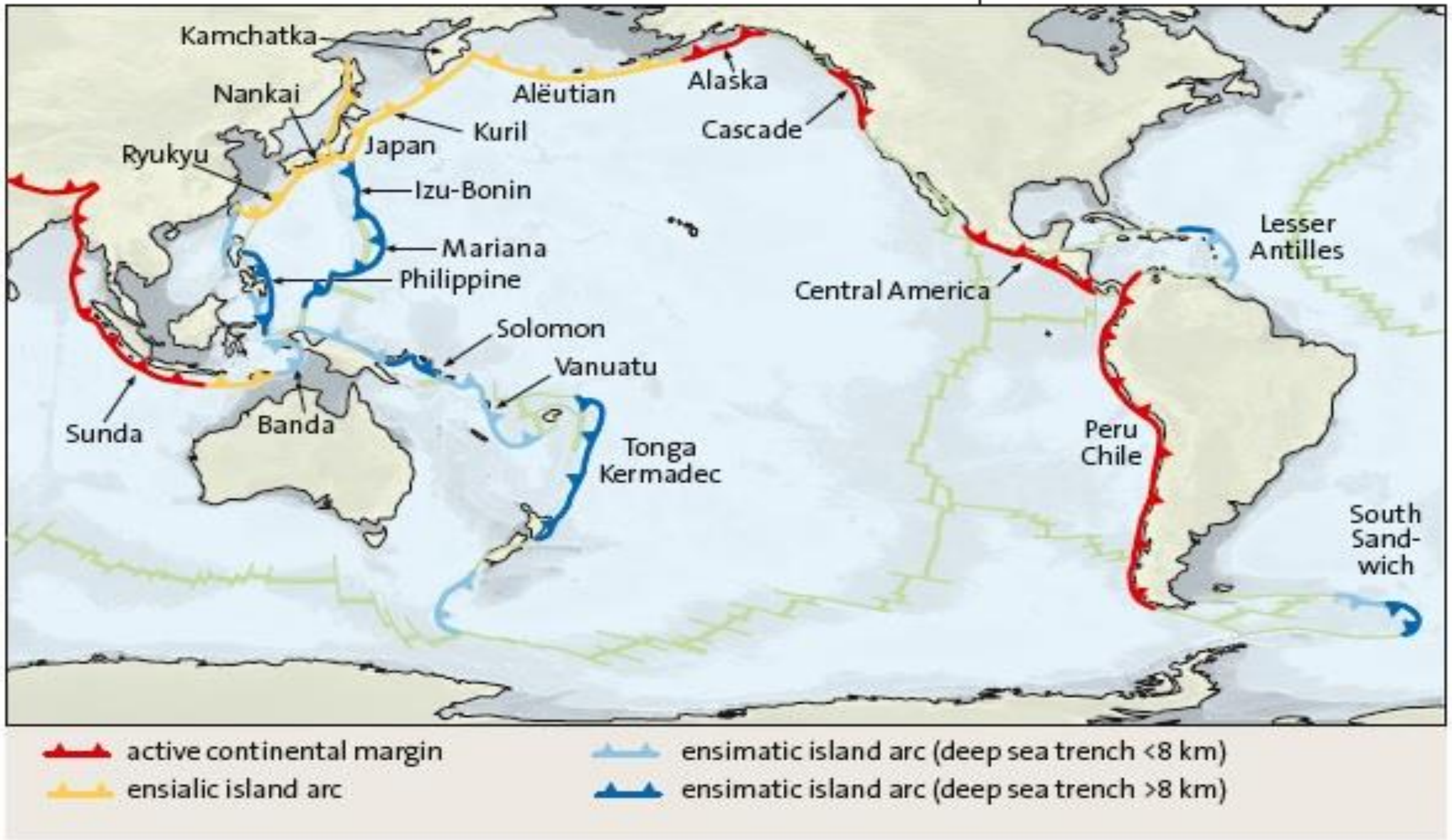

Global subduction zones sums to more than 55,000 km

- The total length of these subduction zones amounts to some 48,800 km, while the total length of incipient subduction zones amounts to some 10,550 km.
- Most collision zones are found along the Alpine–Himalayan chain and the total length of these collision zones amounts to some 23,000 km. This results in a total of 82,350 km of convergent plate boundaries on Earth.

Convergent plate margins of the Earth

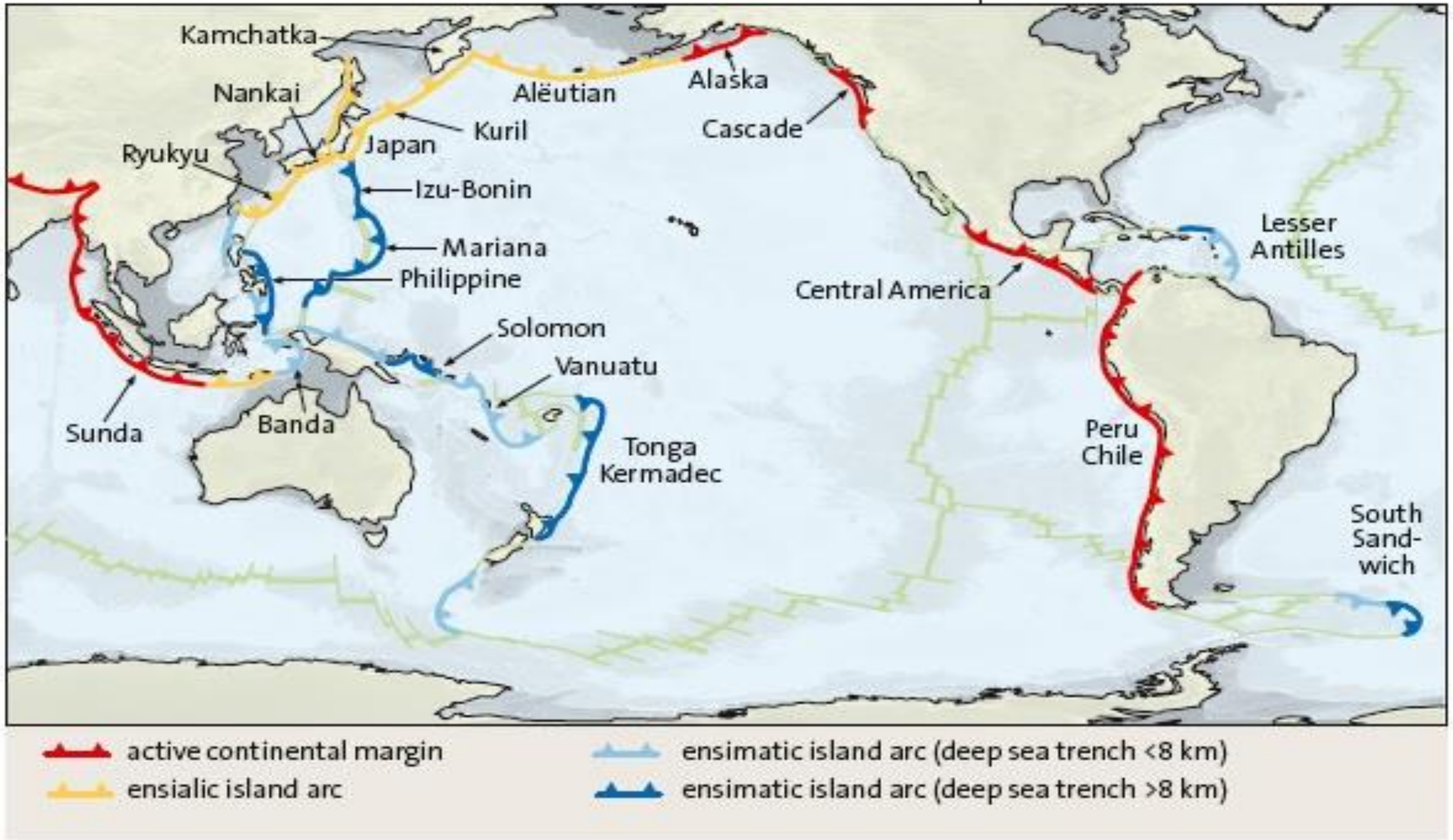

- **Ensimatic island arc:** it refers to a volcanic island arc system built on oceanic crust (ocean lithosphere is subducted below other ocean lithosphere).
- **Ensialic island arc:** it refers to an island arc underlain by continental crust (oceanic lithosphere is subducted beneath continental lithosphere).
- **The arc is built directly on the adjacent continent**: There is an active continental margins where oceanic lithosphere is subducted beneath continental lithosphere without a marine basin behind the volcanic arc.

Convergent Plate Margins

Two types of convergent plate margins: subduction zones (A and B) and collision zones (C and D)

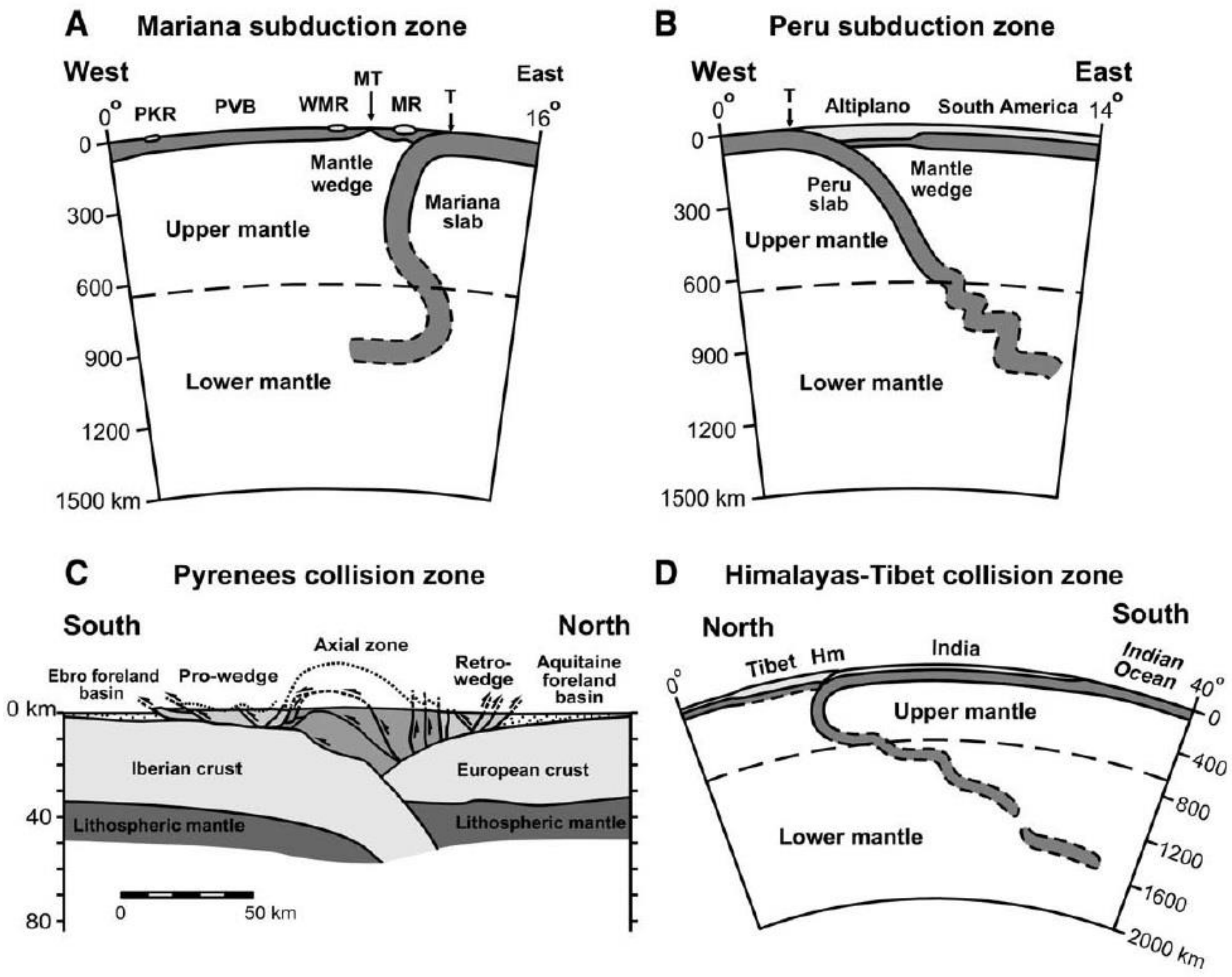

Slab geometry reconstructed from seismic tomography

- (A) The Marianna subduction zone as an example of an ocean–ocean subduction zone with an oceanic overriding (upper) plate (Philippine plate) and an oceanic subducting (lower) plate (Pacific plate).
- (B) The Peru subduction zone: ocean–continent subduction zone with a continental overriding (upper) plate (South American plate) and an oceanic subducting (lower) plate (Nazca plate).
- (C) The Pyrenees mountain belt: continent–continent collision zone, with two converging continental plates (Iberian plate and Eurasian plate).
- (D) The Himalayas–Tibet mountain belt: continent–continent collision zone between the Indian plate and the Eurasian plate with apparent penetration of Indian lithosphere into the sub-lithospheric mantle down to >600 km.

Schellart and Rawlinson, 2010, Tectonophysics, 483

Types of plate margins with subduction zones

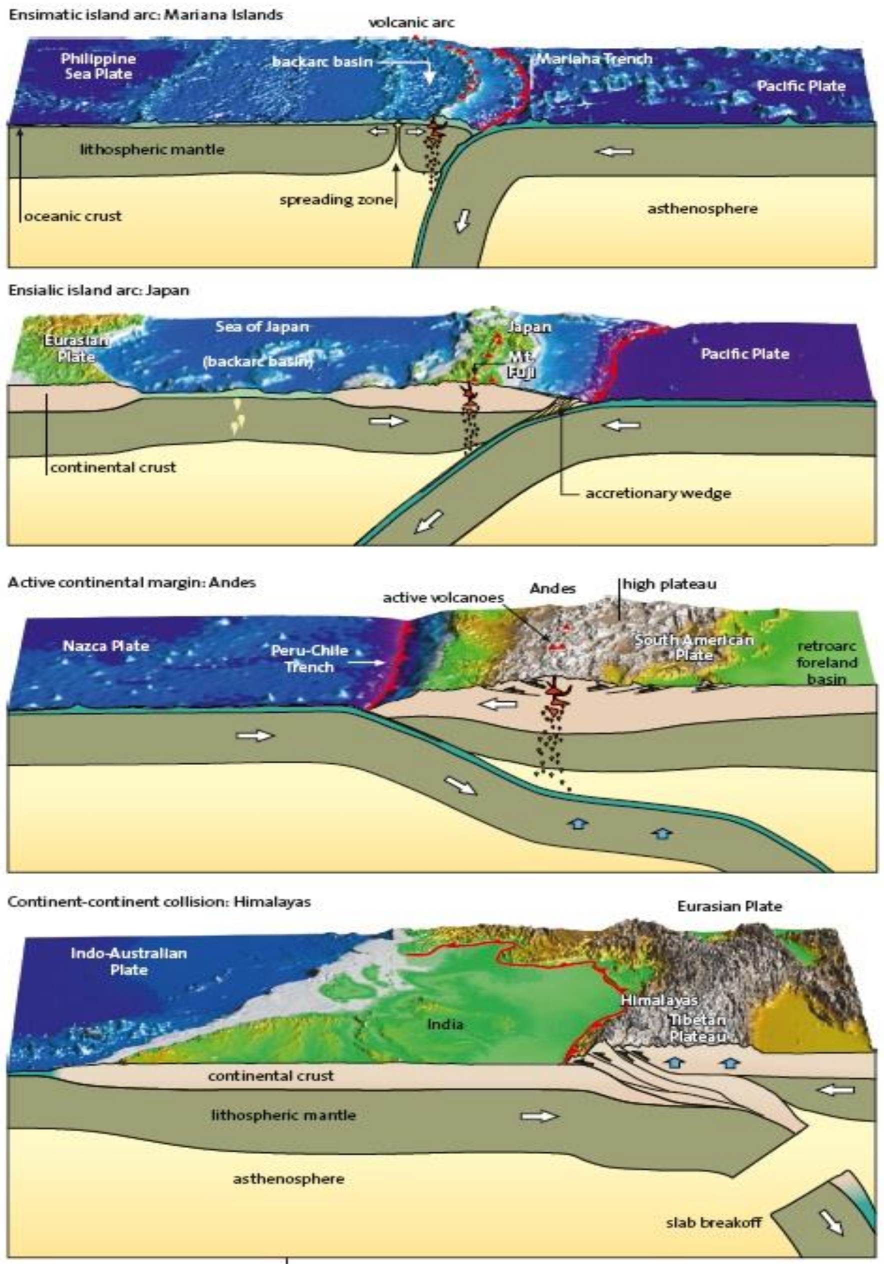

1. Intraoceanic subduction zone, ensimatic island arc (Mariana Islands).

2. Oceanic lithosphere is subducted beneath continental lithosphere, with a marine basin behind the ensialic island arc (Japanese Islands and the eastern Sunda Arc).

3. Oceanic lithosphere is subducted beneath continental lithosphere without a marine basin behind the ensialic island arc built directly on the adjacent continent (Andes, SE Alaska).

4. Zones of continent-continent collision resulting in «slab breakoff» of the oceanic part of the subducting plate and in formation of mountain ranges (e.g., the Himalayas or the Alps).

Structure of a subduction system

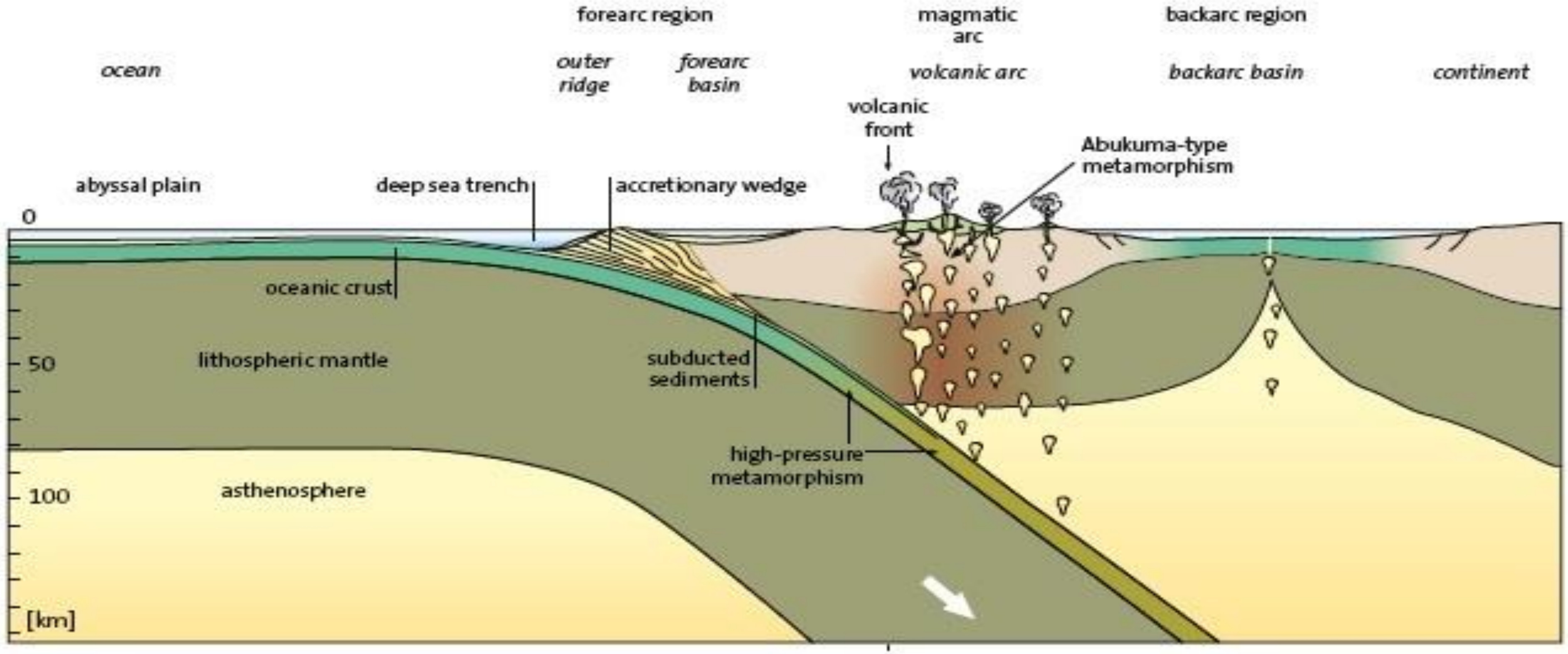

Oceanic trenches:

Are direct manifestation of underthrusting lithosphere. Trenches depth (up to 10-11 km) is controlled by the age of the oceanic lithosphere. Sediment fill of trenches vary greatly depending on proximity of continental areas.

Forarc basin:

Underlain by thinned continental and ocenaic crust, contain a variable thickness of sediments marine and derived from volcanic arc.

Volcanic arc:

It is located 100-150 km far from the trench, has an average width of 100 km, and is the central part of the island arc or the active continental margin.

Gravity and heat flow in the subduction zones

- The forearc area shows a negative gravity anomaly (due to the bending of the subducting plate resluting in a trench filled with water and water-satured sediments) and adjacent positive anomaly (due to the dense subducting plate and overthrusting upper plate).
- Volcanic front shows also a positive gravity anomaly which gradually decreases to normal gravity values towards the backarc basin (due to the contribution of the lighter asthenosphere).
- Heat flow increases abruptly in the magmatic arc and back-arc basin from 50 mW/m^2 to 80–150 mW/m^2

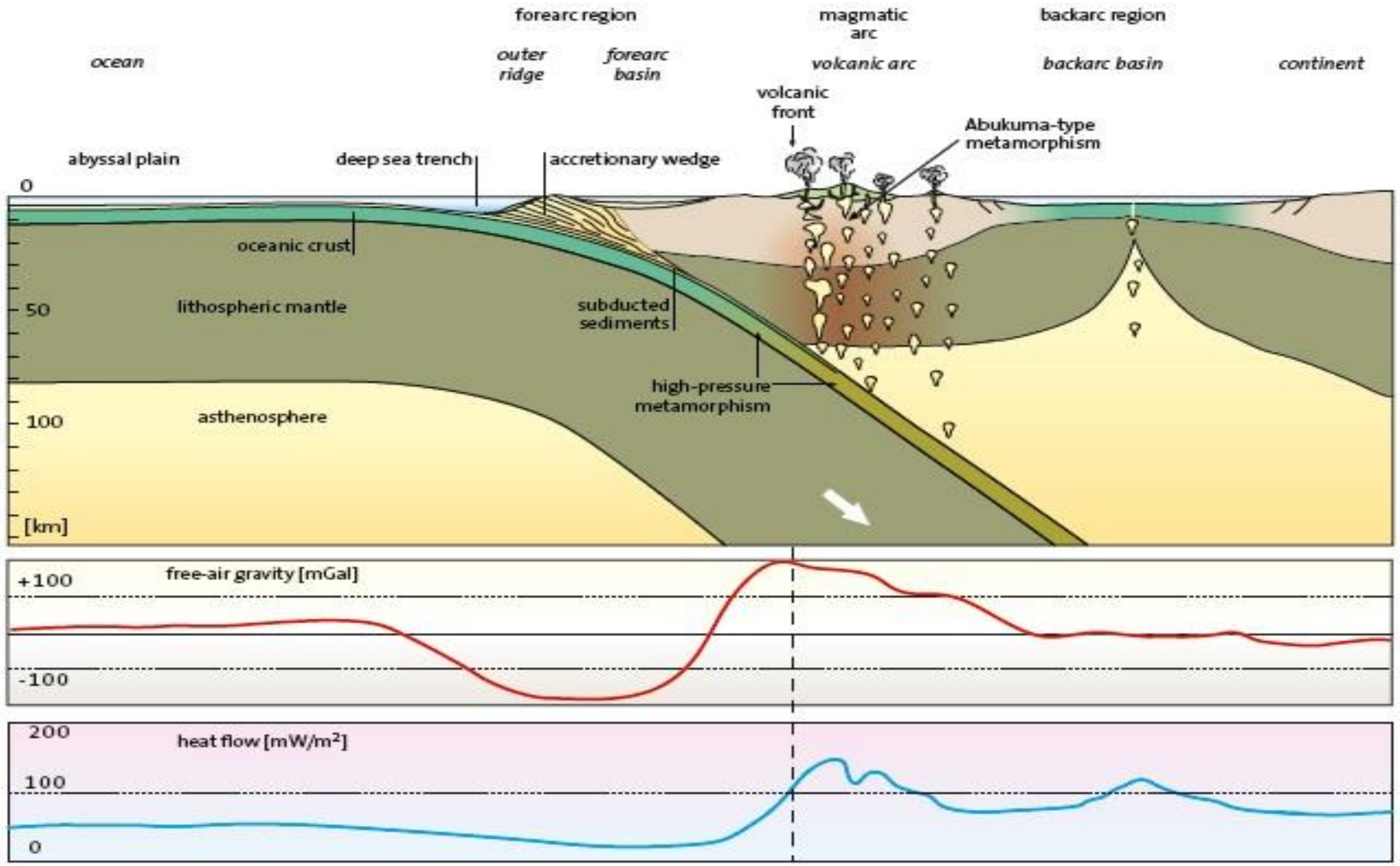

Subduction conditions

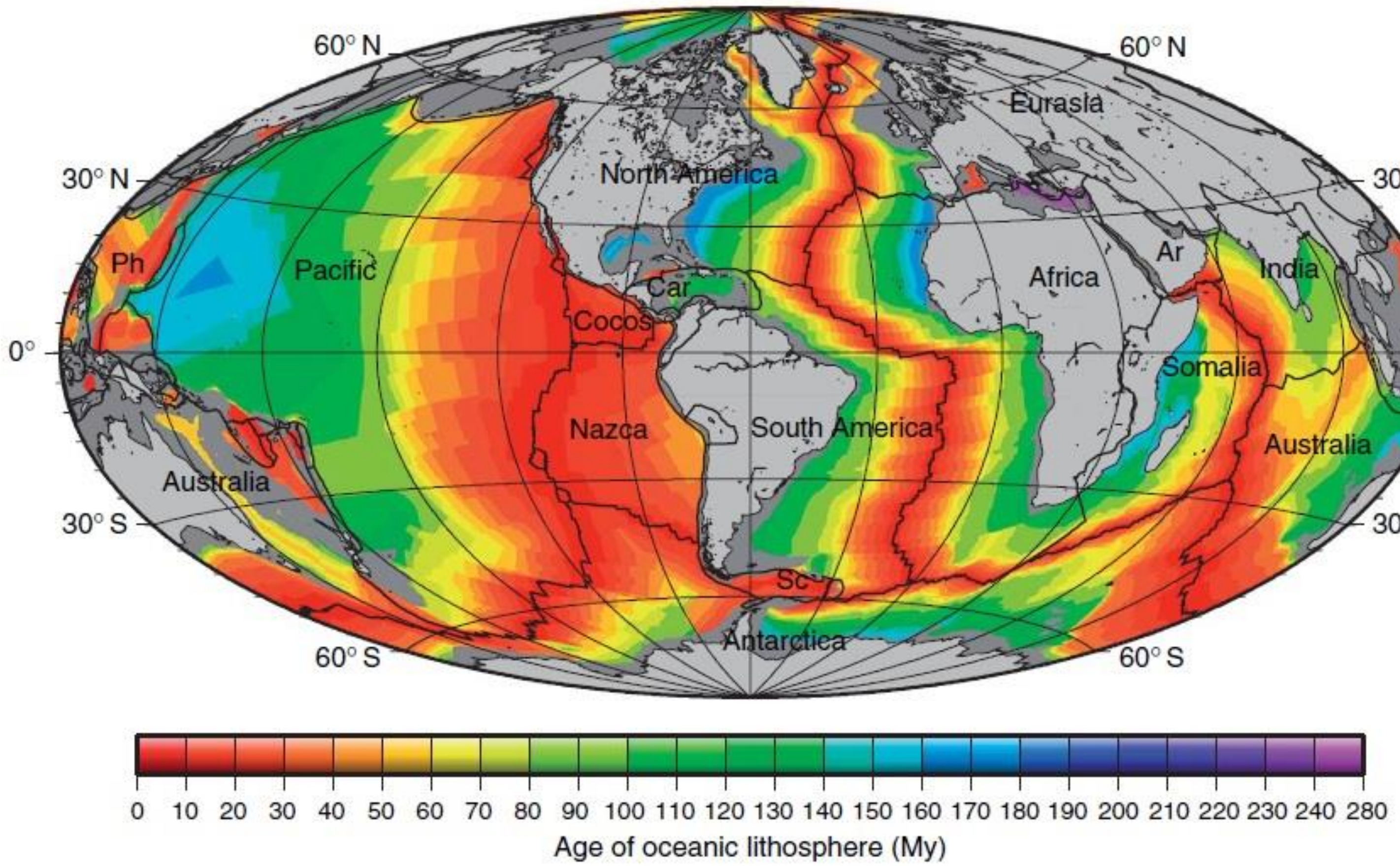

Favour subduction

- Excess of density is necessary to create the vertical forces that are capable of initiating spontaneous subduction (western rim of the Pacific plate, age > 100 Myr).
- Young oceanic lithosphere (eastern margin of the Pacific plate < 50 Myr) forced to subduction by compressional forces.

Against subduction

- Forces exerted on the subducting slab by the flow of the asthenosphere (causing uplift).

Dip of the slab and type of subduction

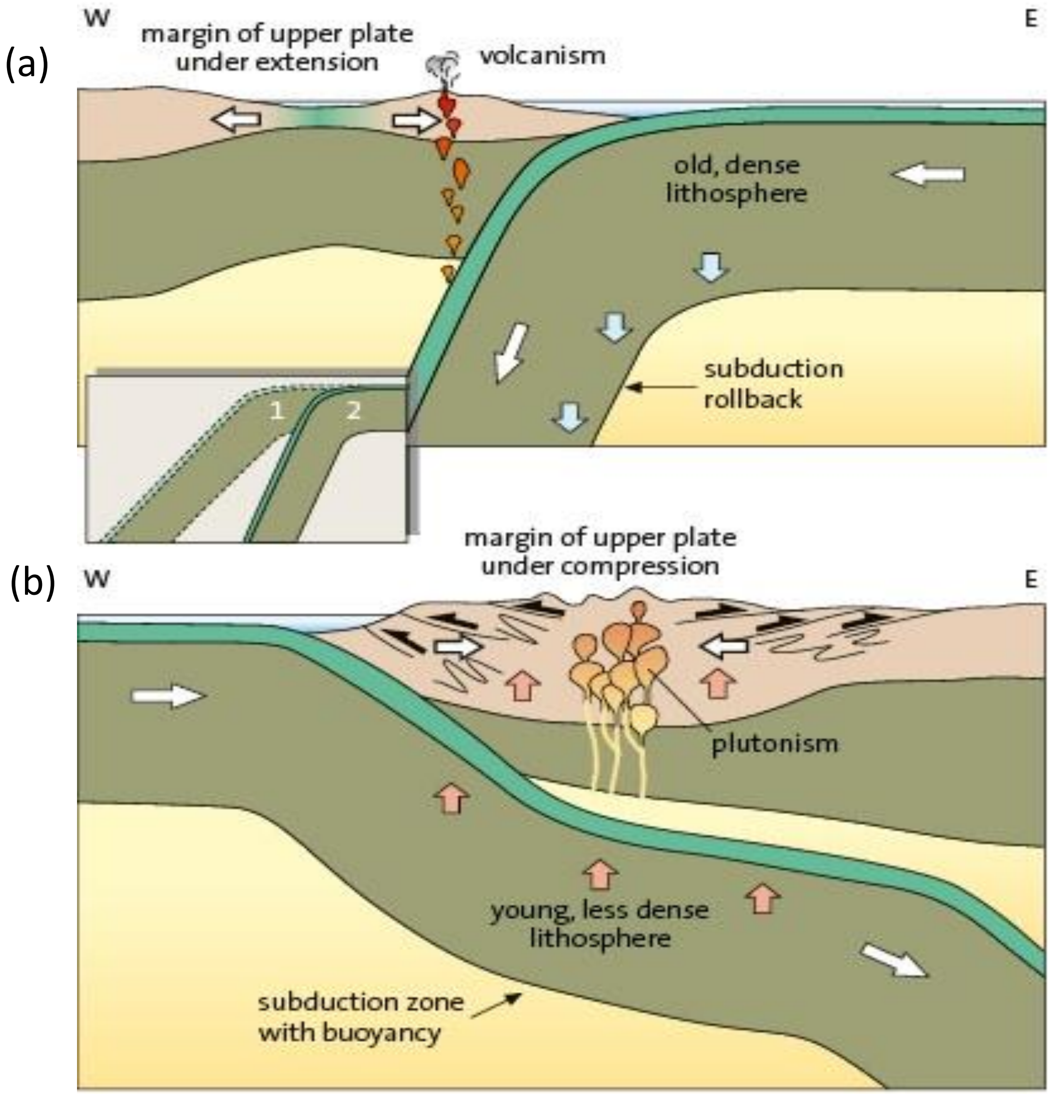

(a) Spontaneous subduction: extensive decoupling, strong slab pull with consequent roll-back of the subduction zone, extensional structures in the upper plate (backarc basin, new oceanic crust formation), deep trenches, high elevation of volcanic arc (i.e., **Marianna-type subduction**).

(b) Forced subduction: shallow subduction and a strong coupling with the upper plate (compressional forces are transferred to the upper plate), back-arc compression, thickening of the upper plate, shallow trenches, high elevation of volcanic arc, larger compressional earthquakes (25-100 km), flow of the asthenosphere restricted to mantle wedge (i.e., **Chilean-type subduction**)

Factors influencing the dip:

- Slab age (if > 30 Myr the slab can subduct spontaneously at high angle)
- High rate of underthrusting enhance uplift
- Absolute motion of the overriding plate
- Slab width (enhances trench suction which favors the uplift of the slab)

- **Forced subduction may evolve from spontaneous subduction as increasingly younger portions of the downgoing plate.**

Mariana-type and Chile-type subduction zones

The transfer of forces at convergent plate boundaries can vary with time

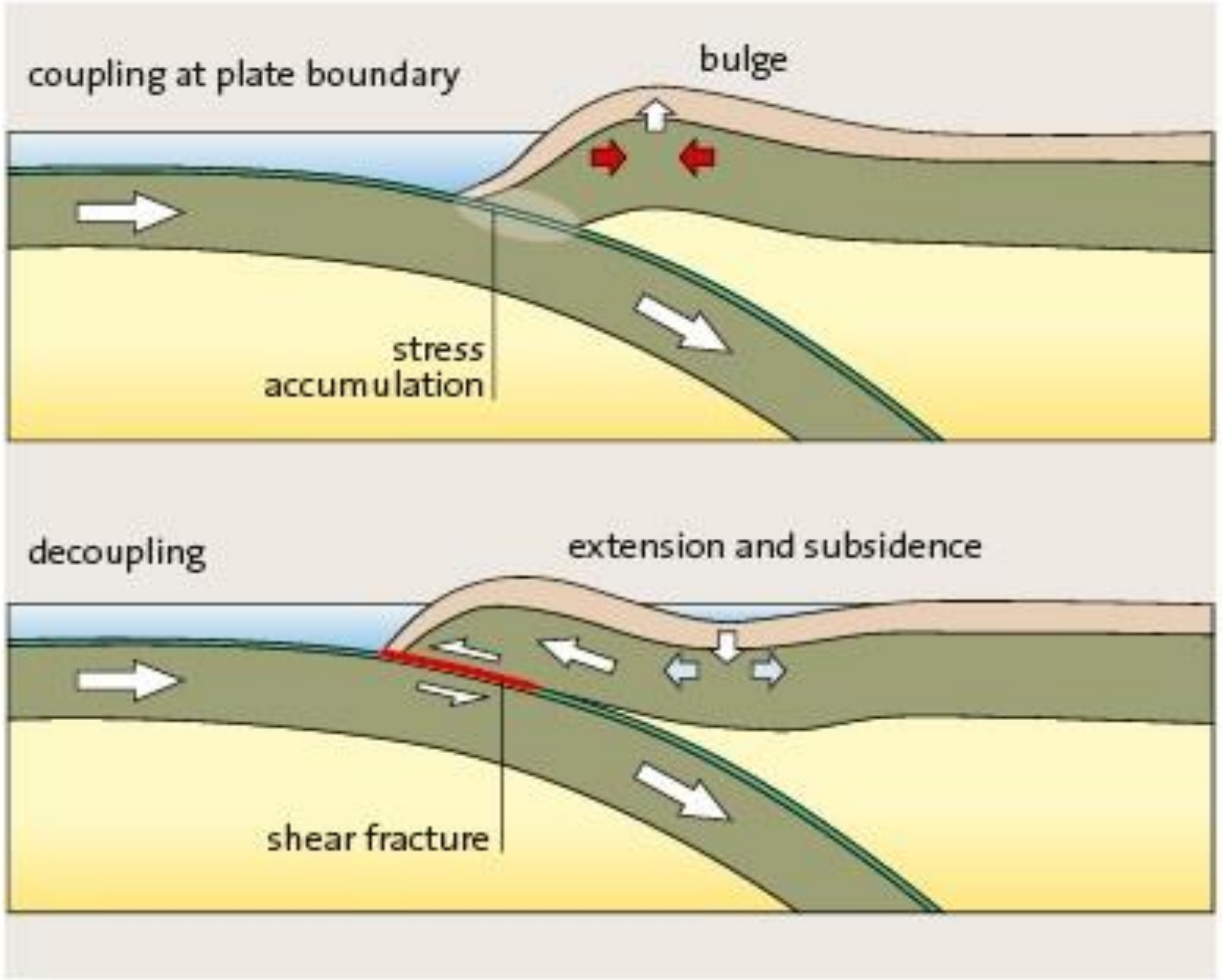

- Phases of compression that reflect coupling of forces between both plates may be followed by extensional phases during which decoupling occurs.
- During periods of plate coupling, the edge of the upper plate is vaulted until there is a spontaneous decoupling because of the high accumulation of energy. As a result, the upper plate abruptly steps forward towards the subducting plate and its margin is accompanied by subsidence.

Stress conditions and seismicity in the subducting slab

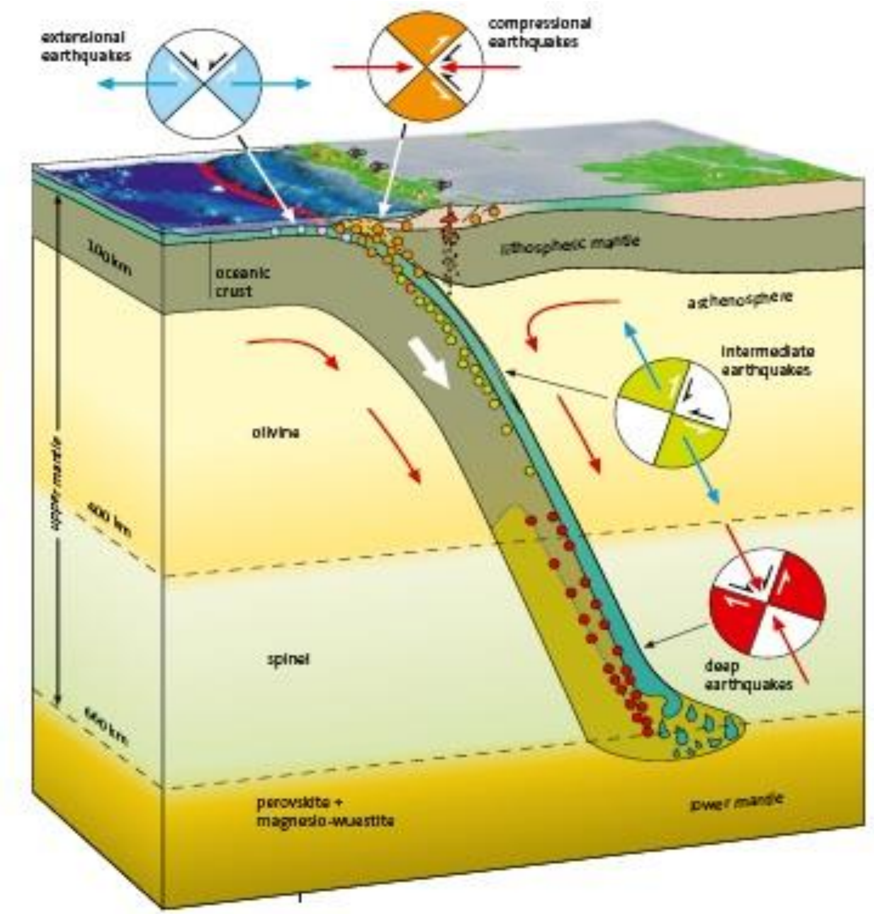

Shallow earthquakes

Depth < 25km: Earthquakes are generated in response to bending of the lithosphere, which puts the upper surface of the plate into tension (normal faults).

Depth >25km <70-100 km (90 % of total seismicity energy): Earthquakes are generated from thrust faulting along the contact between the overriding and underthrusting plates (horizontal compression and friction of between the two plates), e.g., Alaska 1964, Chile 1960 and 2010 (M_0> 9.0), Sumatra 2004. Other earthquakes sources: dewatering of serpentinized mantle and eclogitization.

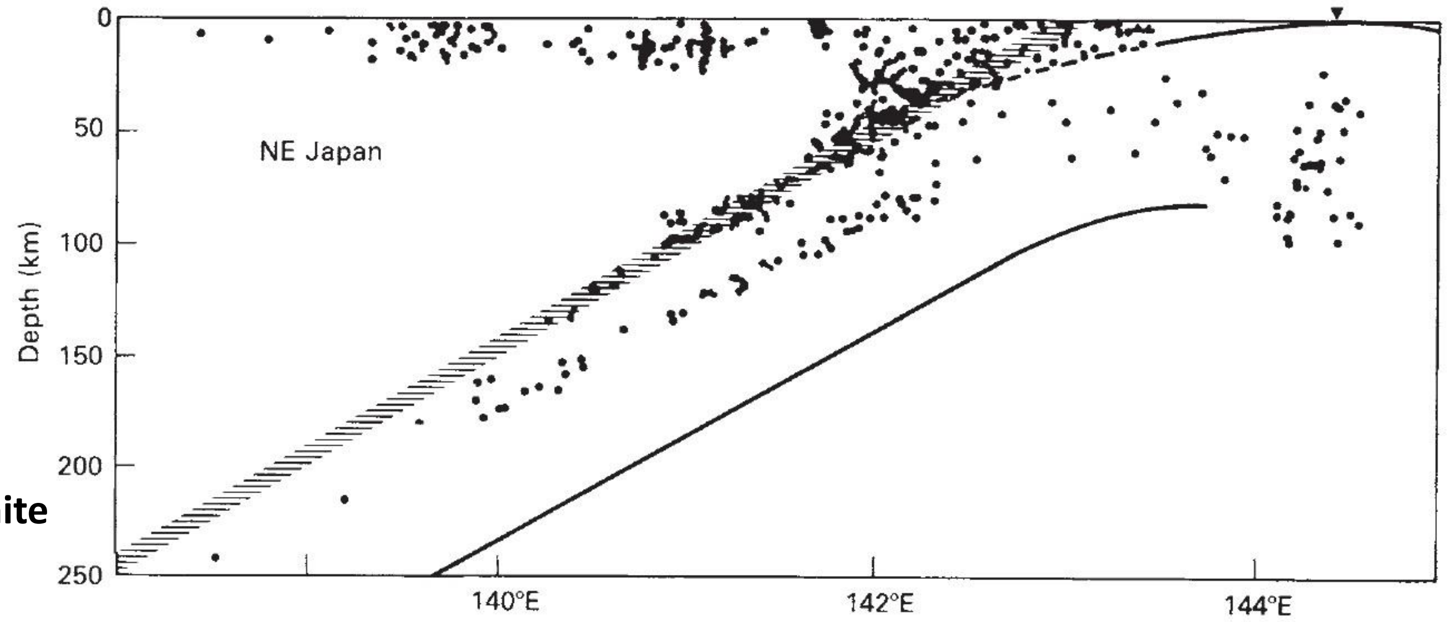

Upper zone: eclogite formation

Lower zone: dehydratation of serpentinite

Stress conditions and seismicity in the subducting slab

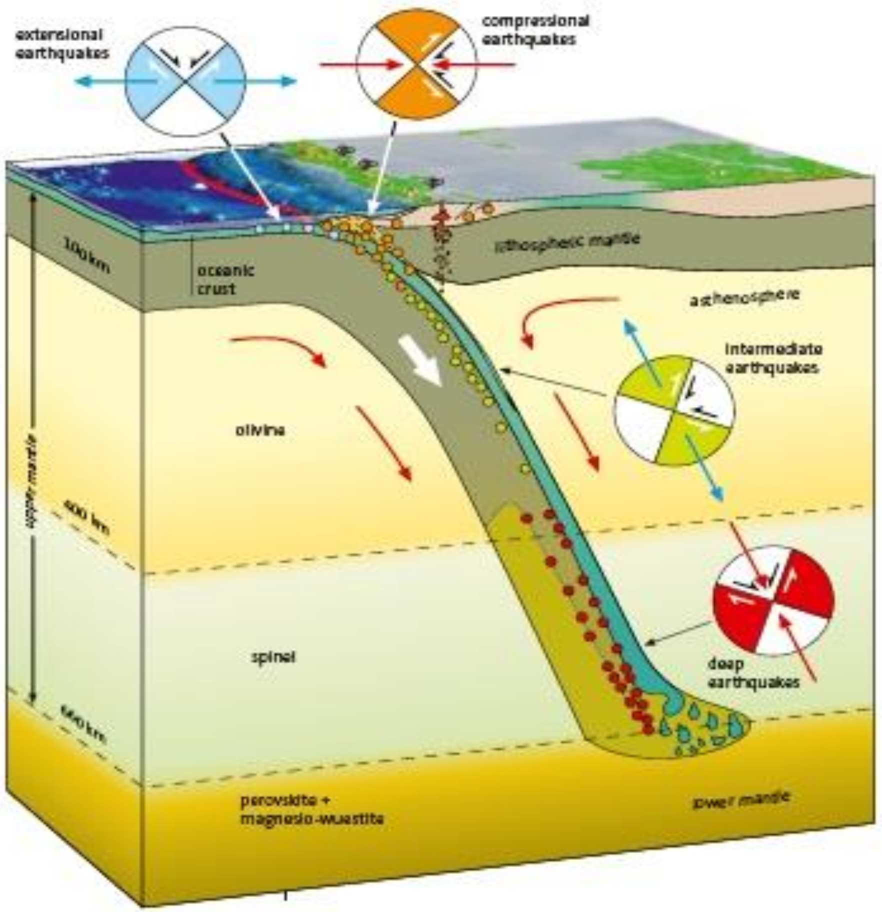

Intermidiate earthquakes (20%)

Depth larger than the thickness of the lithosphere of the overriding plate (> 70-100 km < 350 km): Earthquakes are the result of the internal deformation of the descending slab (tensional stress no resistance from the asthenosphere) and metamorphic reactions involving dehydratation of serpentinized mantle and eclogitization.

Deep earthquakes (8%)

Depth > 350 km: Earthquakes are the result of the high resitance of the mantle to slab penetration (becoming more dense because of mineral phase transitions), which generate compressive stress in the subducting slab.
Olivine-spinel phase transition occurs within the cold subducting slab between 350 and 700 km (olivine is in metastable conditions).

- The phase changes that occur in the slab at a depth of approximately 700 km likely produce fine-grained materials that behave in a superplastic manner and thus cannot generate earthquakes.

Deep stress and seismicity in the subducting slab

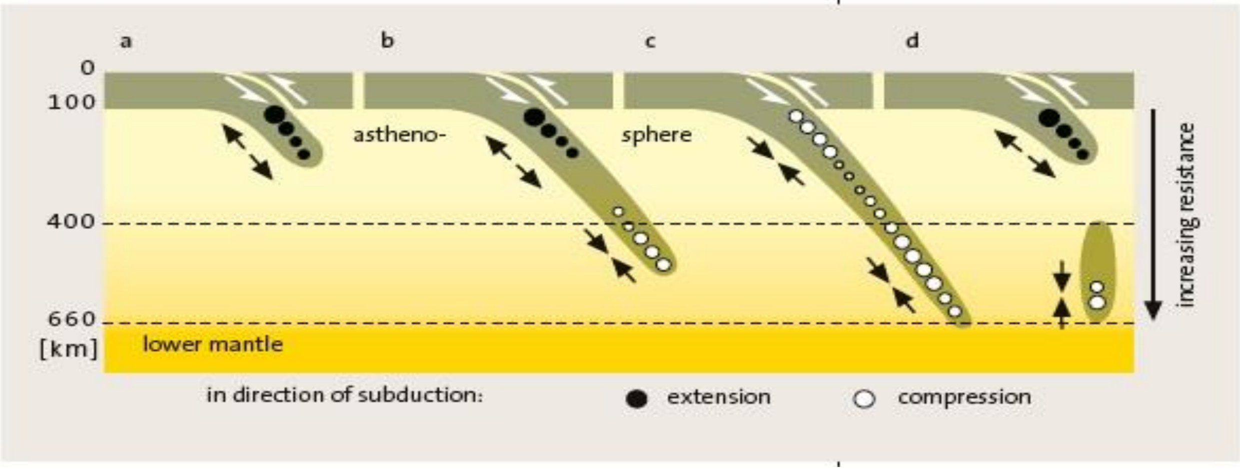

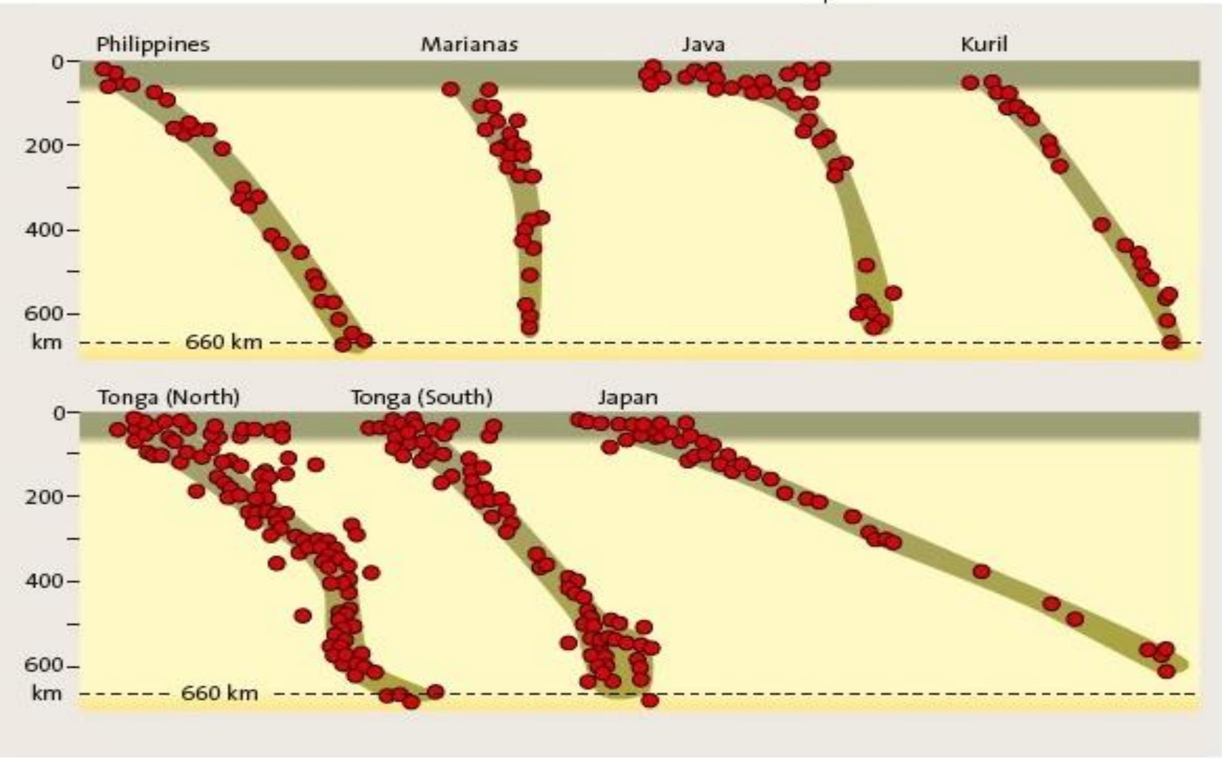

- When the slab reach the bottom of the transition zone, compressive stress is transferred upwards.
- In case of slab-breakoff no stress transfer, the slab remains in state of tensional stress.

Origin of the earthquakes in the subduction zone

- **Origin of shallow earthquakes (25-70 km)**: In compressional conditions, numerous microcracks develop parallel oriented to the direction of maximum compressional stress. This lead to weakening of the rocks, followed by failure and shear planes oblique to the main direction of pressure that join the existing microfractures.
- **Origin of intermidiate earthquakes (70-350 km)**: Dewatering processes with increasing depth of serpentine, which is accompanied by a substantial decrease of volume and consequent microfracturing and weakening of the the rock.
- **Origin of deep earthquakes (> 350 km)**: The mineral phase transition of olivine to spinel (occurring with volume reduction): Small lenses of spinel within the peridotite are aligned perpendicular to the maximum compressional stress and interpreted as “anticracks”, since they are rotated 90° compared with normal microcracks. If enough anticracks are formed, the rock becomes weakened, the anticracks are joined and an instantaneous shear movement of the rock develops, through a pocess called ‘superplasticity’ (favored by high *T* and fine grains).

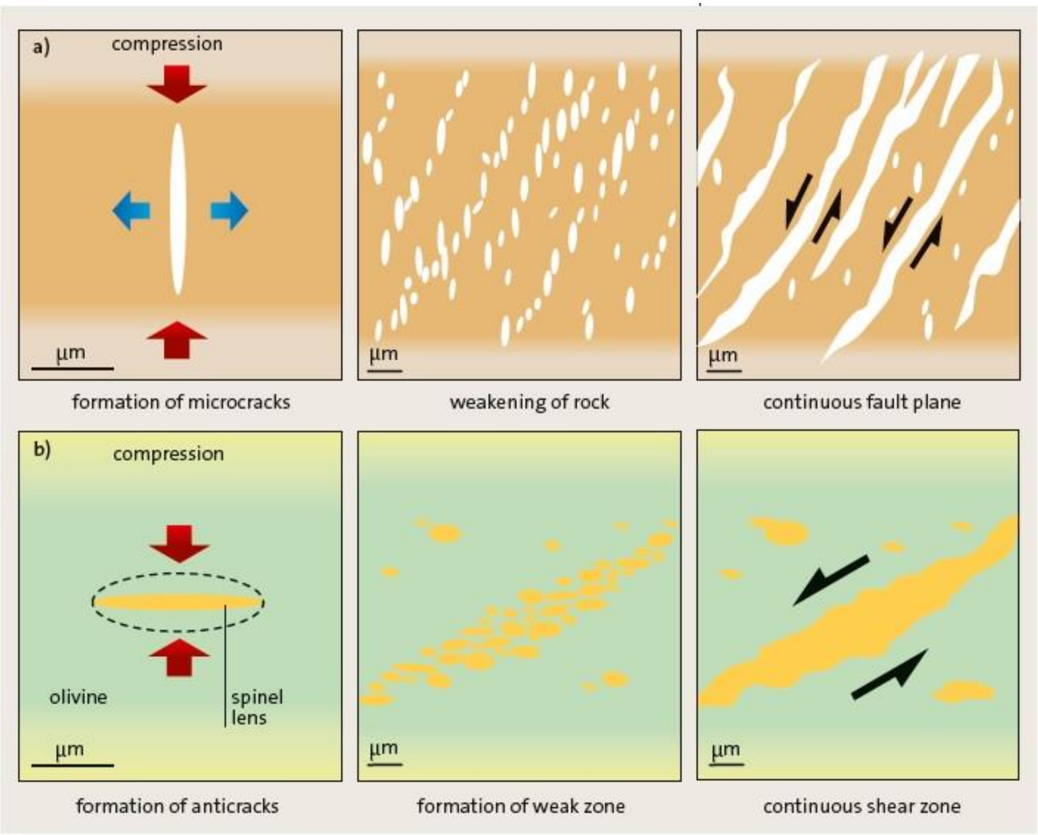

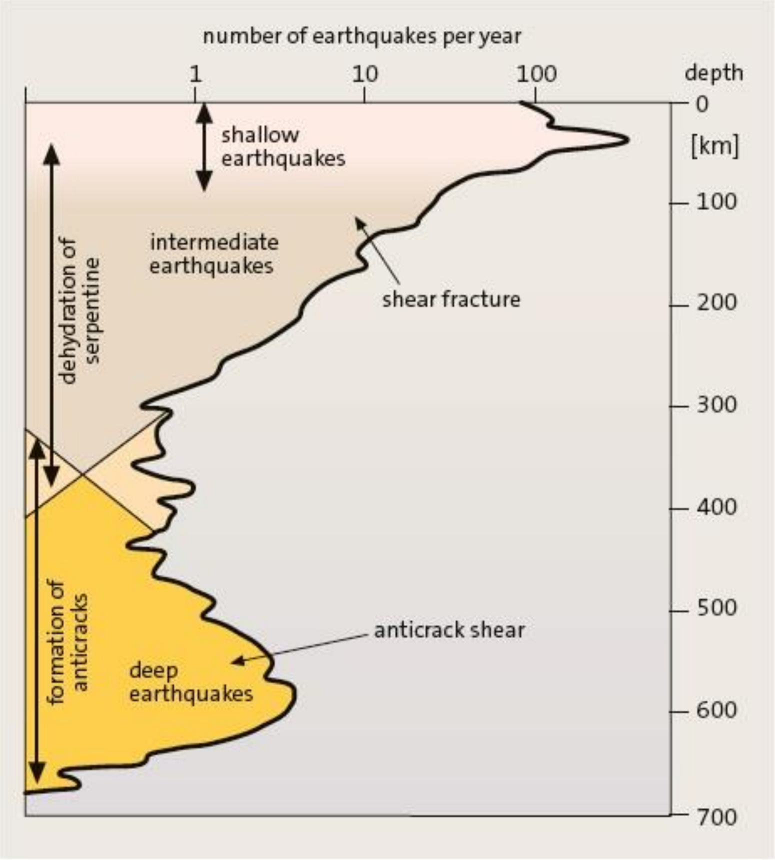

Slab depth penetration

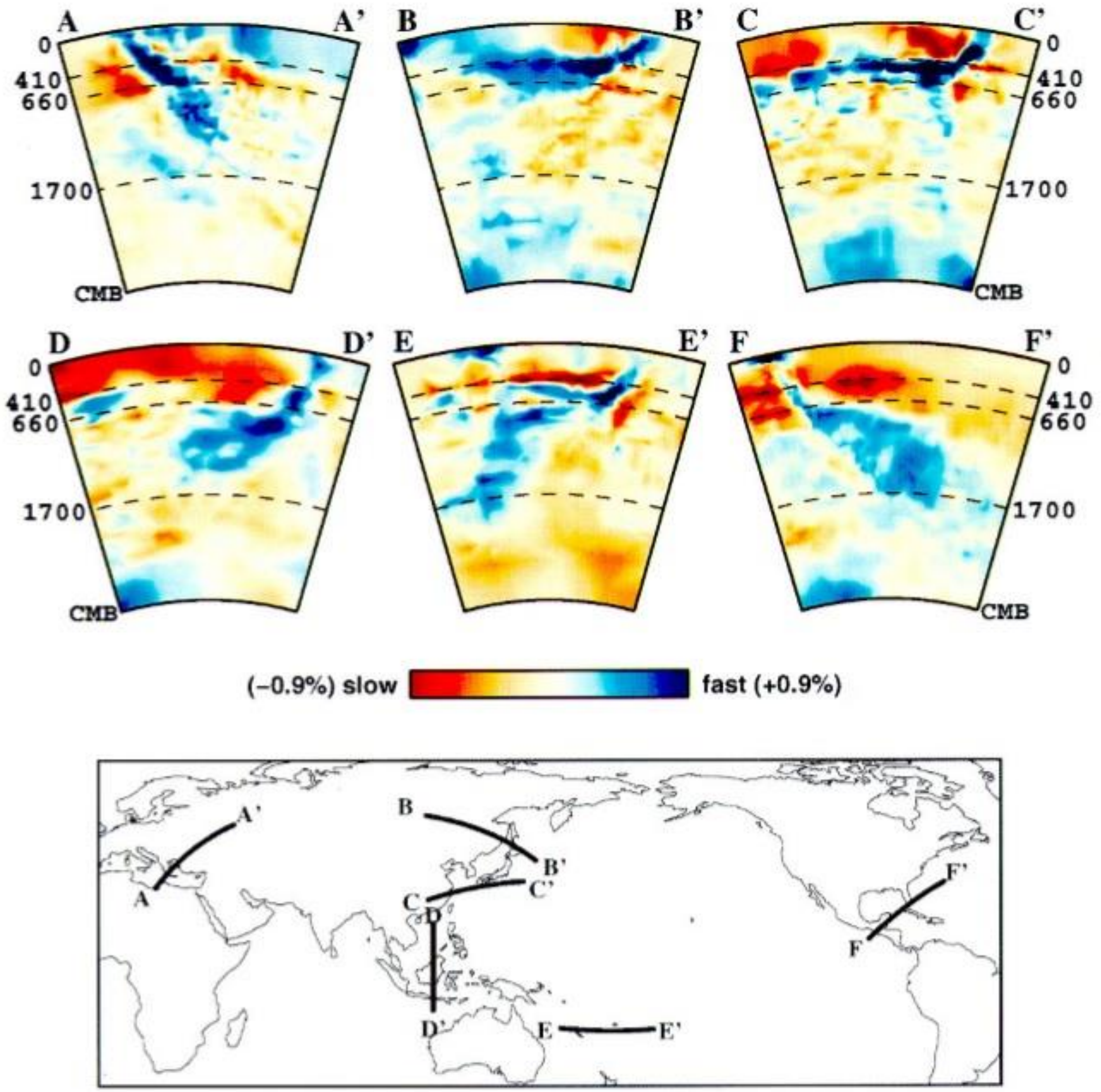

No relationship between age of a subducting slab and depth penetration (transition zone or lower mantle)

Length of Benioff Zone

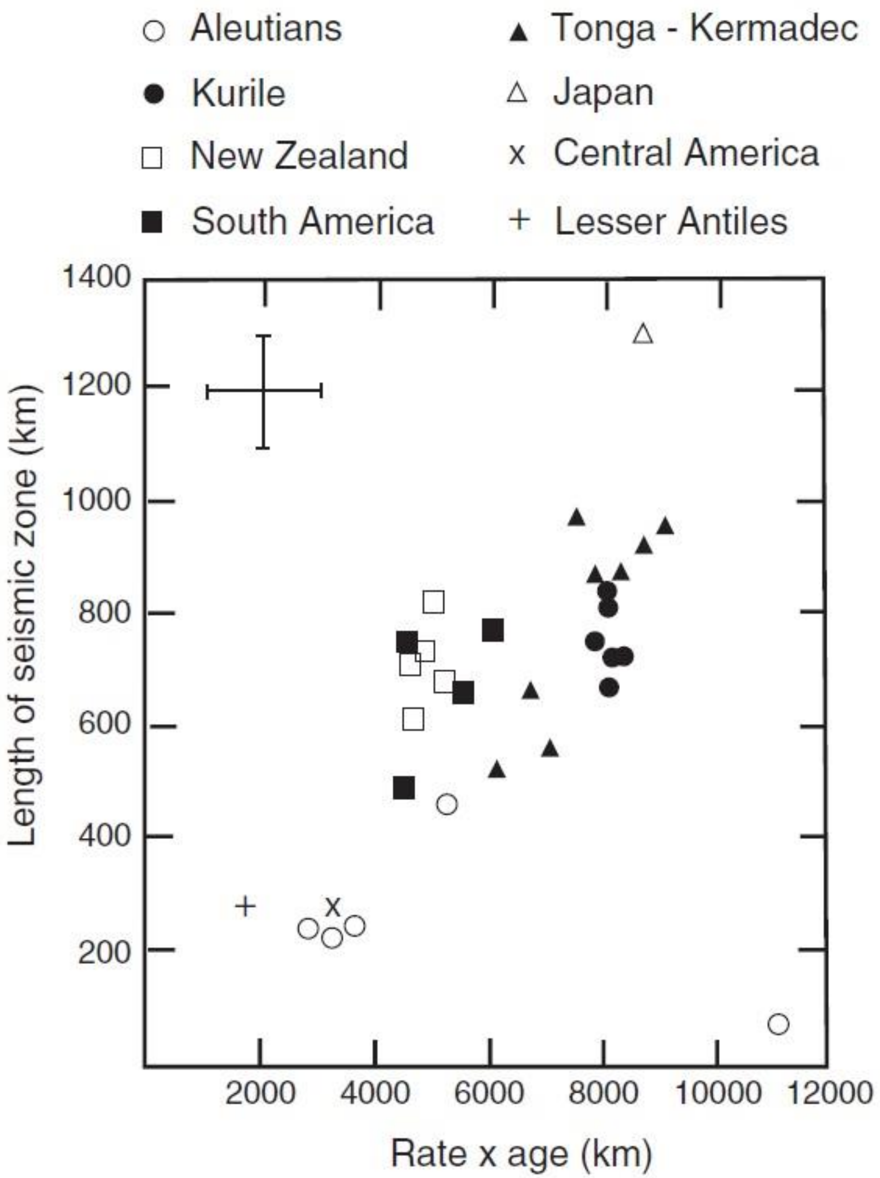

Length of the seismic zone is proportional to the product between the convergence rate and age (the slab should preserve a strong core):

Downward deflection of the lithosphere (length of the seismic zone) proportional to both rate of subduction and age (square of the lithospheric thickness).

Serpentinite in subduction zone systhems

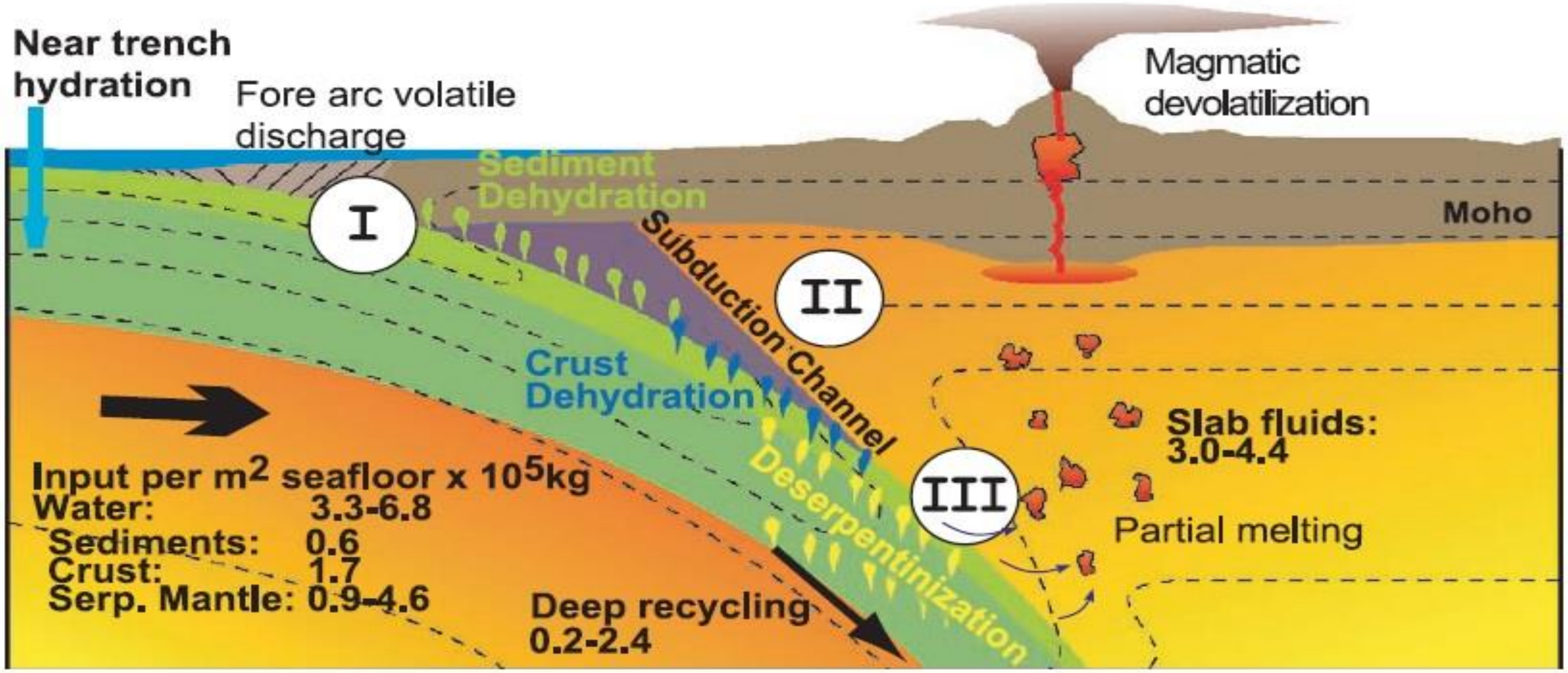

Rupke et al., 2004, EPSL, 223

I shallow fluid release occurs at depths < 20 km from subducting sediments

II Intermediate depth (20– 100 km) water release from sediments and ocean crust

III Deep fluid release (>100 km) from oceanic crust and deserpentinizing mantle triggers arc melting

Physical parameters of the serpentinite

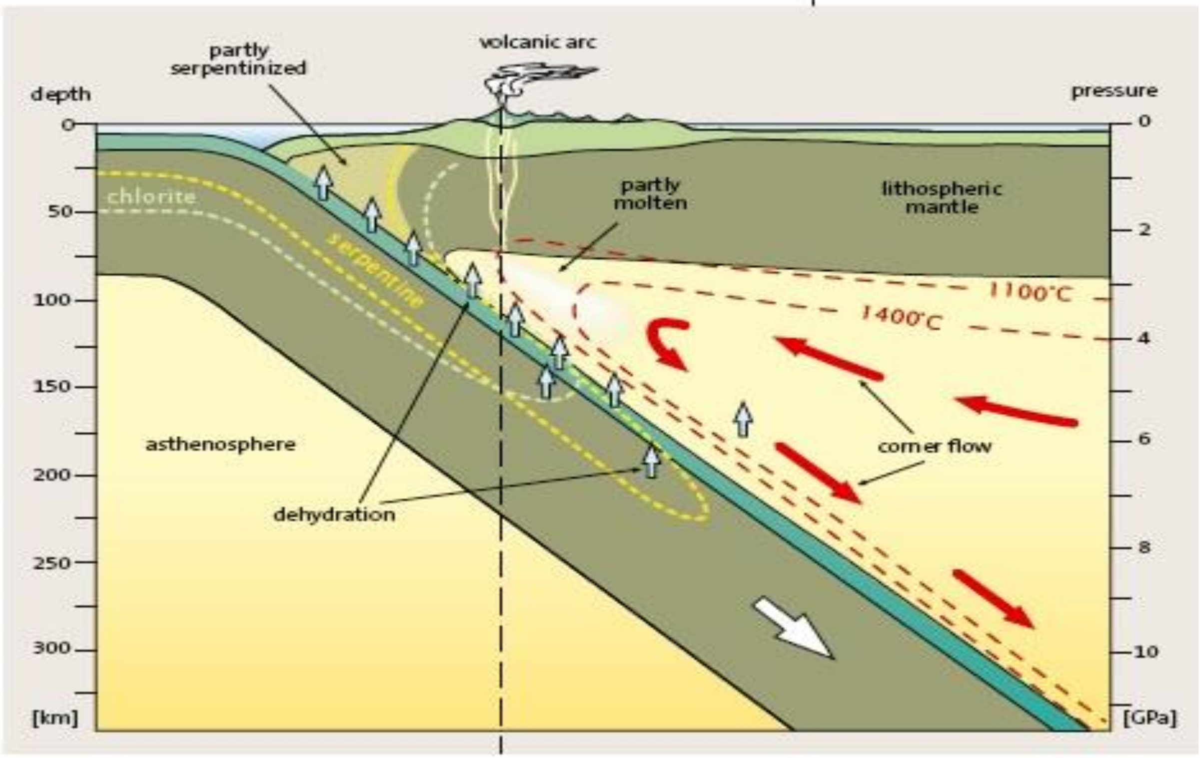

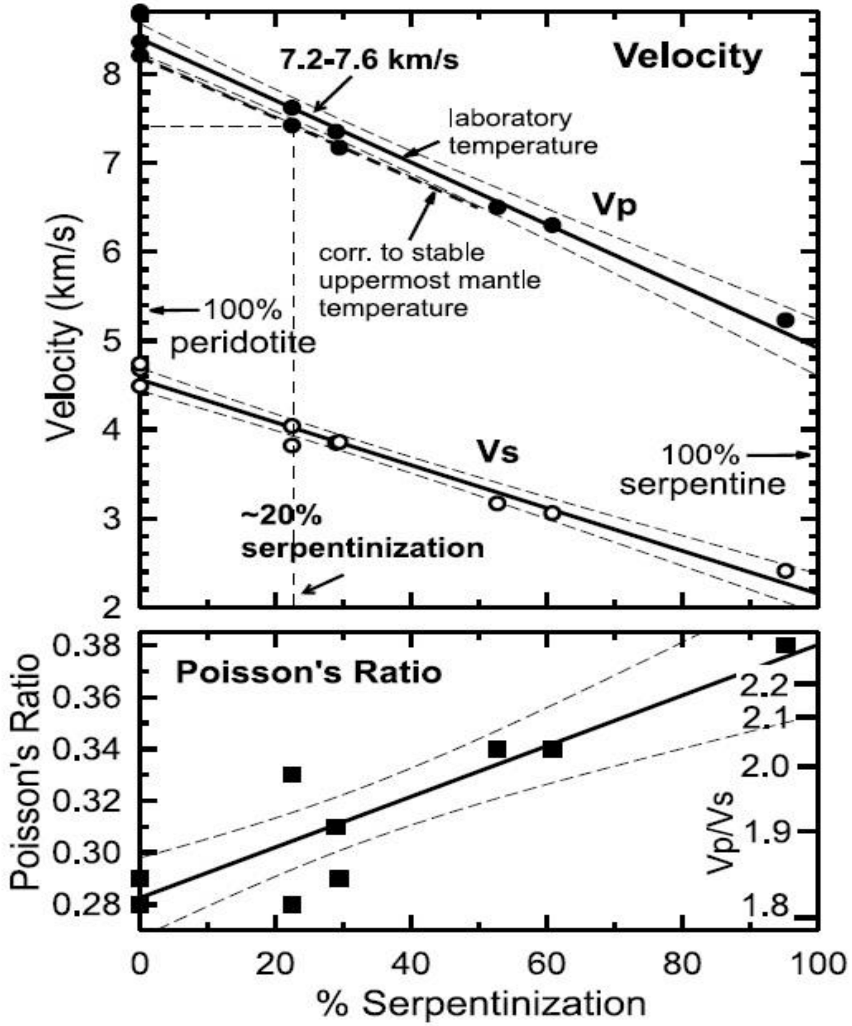

Hyndman and Peacock, 2013, EPSL, 212

Magmatic rocks formed above the subduction zones (9 km^3yr^{-1}) have several percent of water (up to 6 % H_2O)

Serpentine: a magnesium silicate mineral (Mg6[Si4O10(OH)8] with a high water-content 13 weight-%)

- Serpentinite: low Vp and Vs velocity, low density, and high Vp/Vs ratio and σ
- Serpentinization may generate seismic reflectivity, an increase in magnetization, an increase in electrical conductivity, and a reduction in mechanical strength.

Serpentinized forearc mantle

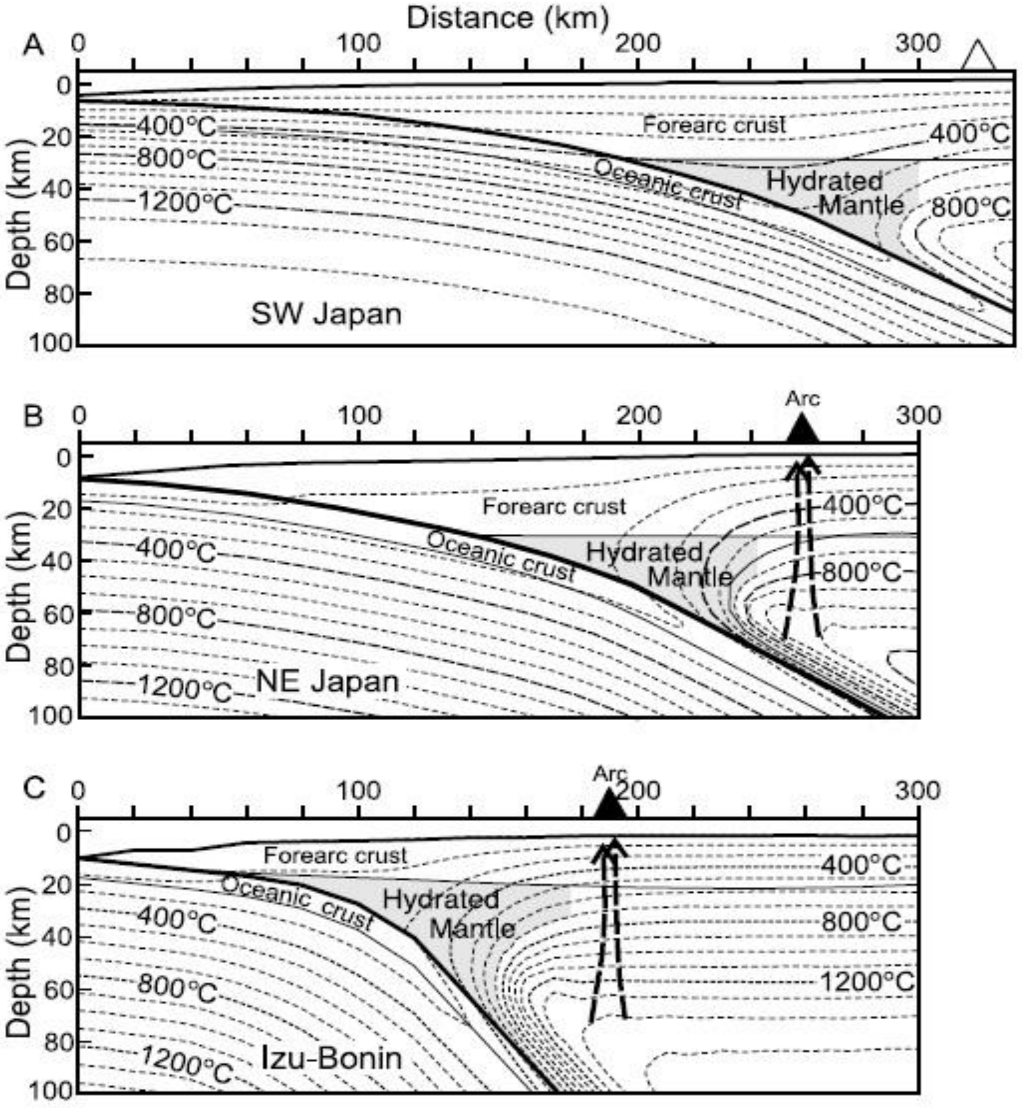

Warm continental subduction zone: Calculated forearc temperatures are 400-600°C. This results in less extended zone of serpentinized forearc mantle, shallow metamorphic transformaiton from blueshist facies to eclogite (50 km).

Cool continental subduction zone: The subducting slab intersects the forearc Moho at 30-50 km depth, the calculated temperatures in the uppermost forearc mantle are 150-250°C.

Cool oceanic subduction zone: Uppermost forearc mantle temperatures are especially low for island arcs with thin forearc crust (10-15 km), where the *T* in the mantle wedge corner are ~100°C. This results in more extended zone of serpentinized forearc mantle, deep metamorphic transformaiton from blueshist facies to eclogite (100 km).

Hyndman and Peacock, 2013, EPSL, 212

Cascadia Subduction Zone

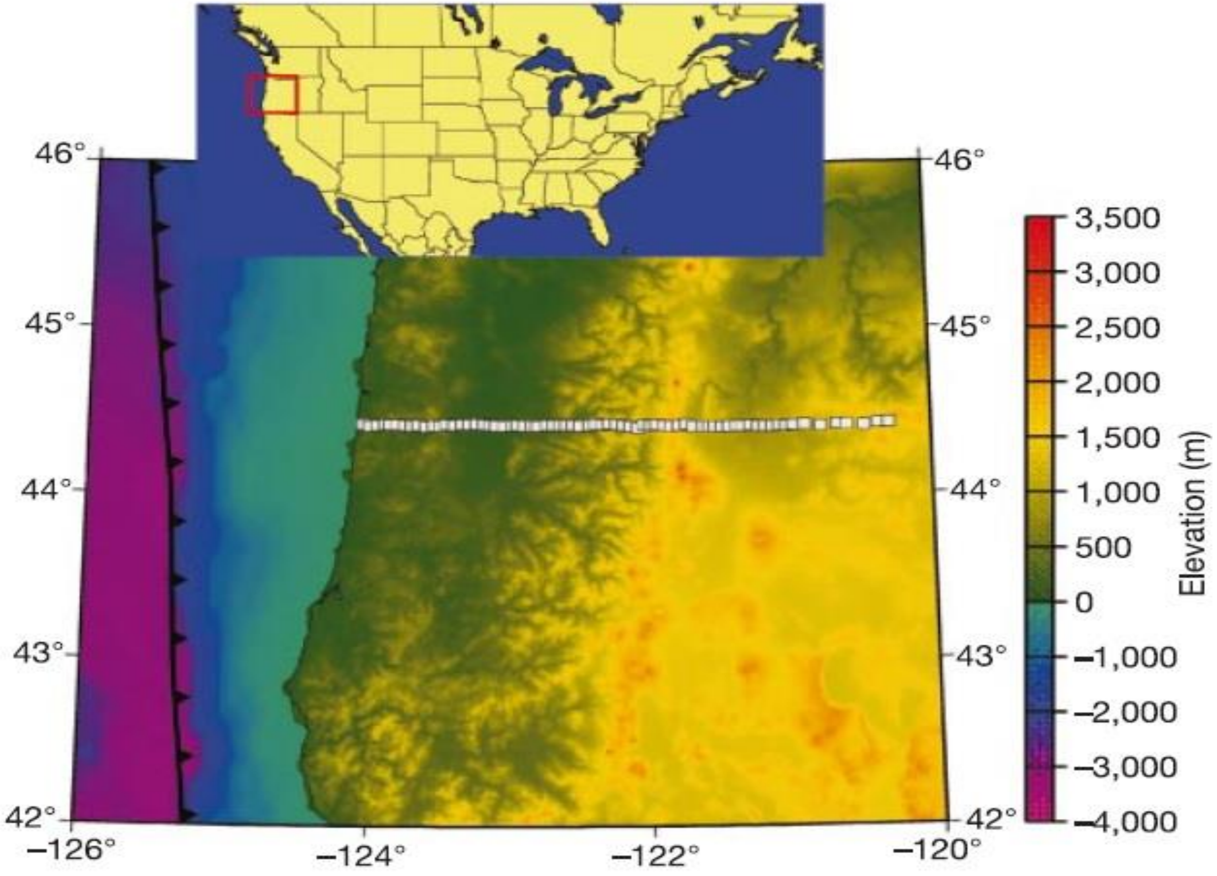

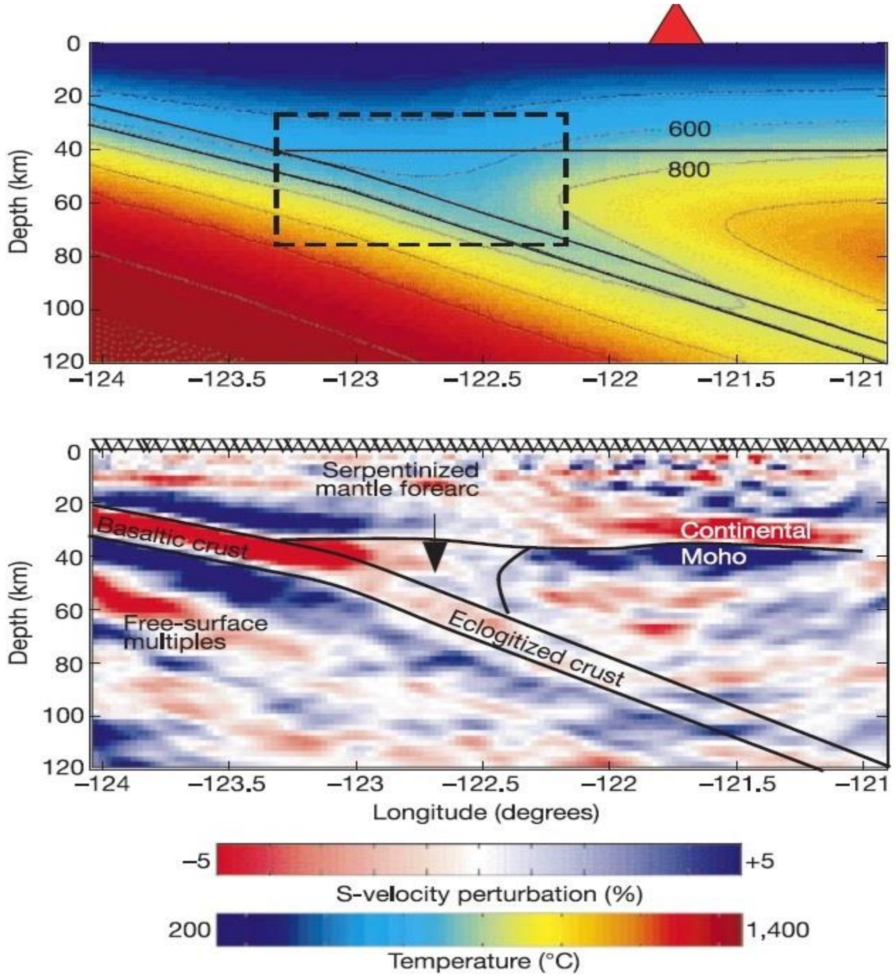

Bostock et al., 2002, Nature, 417

The degree of hydration diminishes eastwards, producing an inverted continental Moho (high-velocity crust on low-velocity mantle), reduced velocity contrast, disappearance of the inverted Moho, and restoration to a normal polarity crust–mantle boundary 40 km west of the arc.

Thermal conditions of a subduction zone systhem

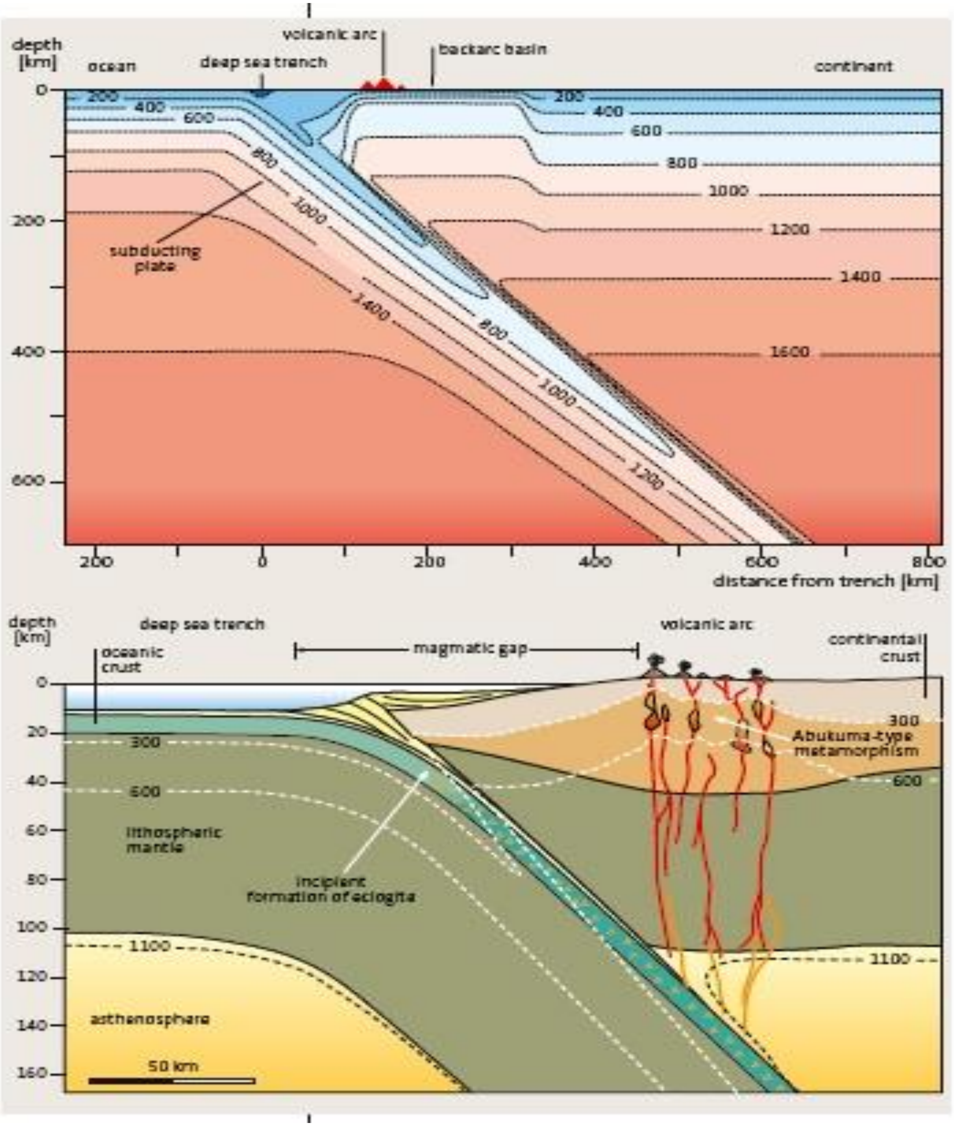

- Rate of subduction.
- Age and thickness of descending slab.
- Frictional heating of the upper and lower slab surfaces.
- Conduction of heat into the slab from the asthenosphere.
- Adiabatic heating associated with slab compression.
- Heat derived from radioactive decay of minerals in the oceanic lithosphere.
- Latent heat associated with phase transitions of minerals (olivine-spinel transition, exothermic; spinel-oxide transitions, endothermic).

Metamorphism in the subduction zones

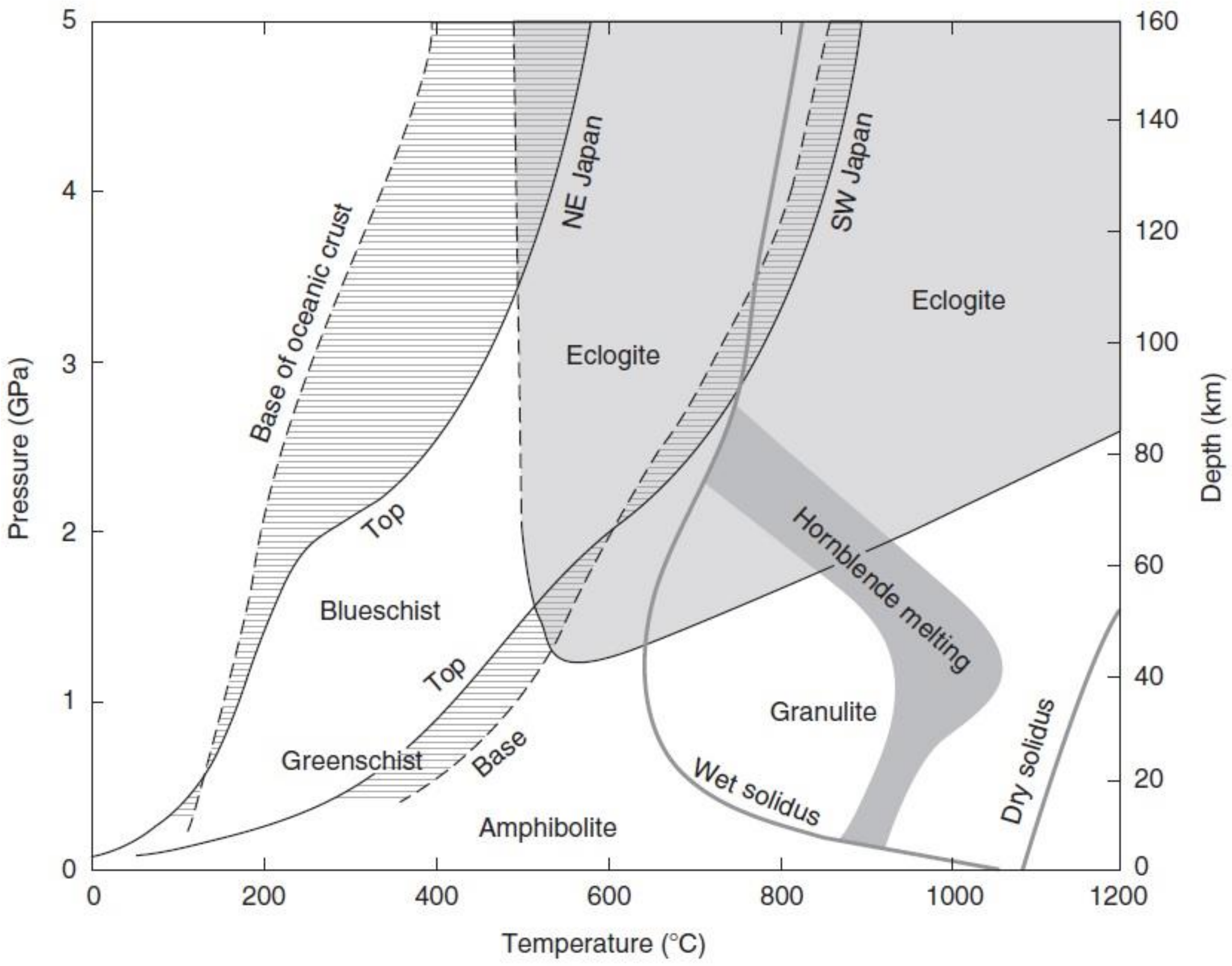

- The most common groups of metamorphic rocks in the subduction zones are blueschist (MP-HP and LT) , greenschist (MP and MT), amphibolite (MP and MT-HT), and the granulite facies (MP-HP and HT), depending on the initial composition of the crust, ambient pressure, temperature and fluid conditions.
- The transition of basalts in amphibolite occurs at *T* >500°C, while at *T* >650°C amphibolite transforms into granulite, which are usually characterized by the presence of anhydrous mineral assemblages (OPX, CPX, and plagioclase).

Uplift of high-pressure metamorphic rocks

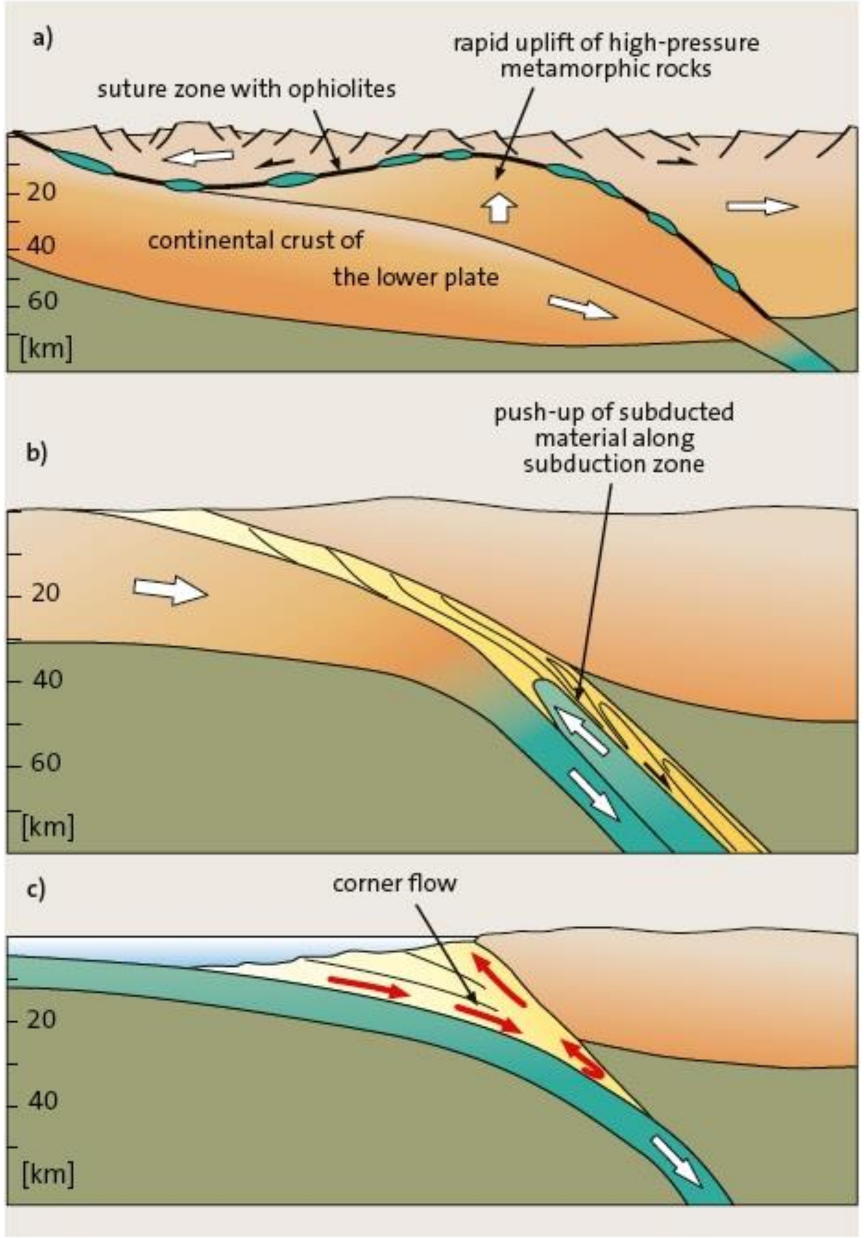

a) Crust that is thickened by underplating during the subduction process is gravitationally unstable, a condition that initiates crustal extension by an orogenic collapse: The rocks are removed by rapid horizontal displacement during orogenic collapse of the orogen (metamorphic core complexes).

b) High-pressure sequences can be pressed in reverse upwards along subduction zones even during continuous subduction and compression.

c) Corner flow can rapidly uplift high-pressure metamorphic rocks: The wedge consists of scraped-off sediments that becomes narrower at depth and thus the subducted and metamorphosed rocks from the lower part of the wedge are returned towards the surface along the frontal part of the upper plate.

Accretionary Prisms

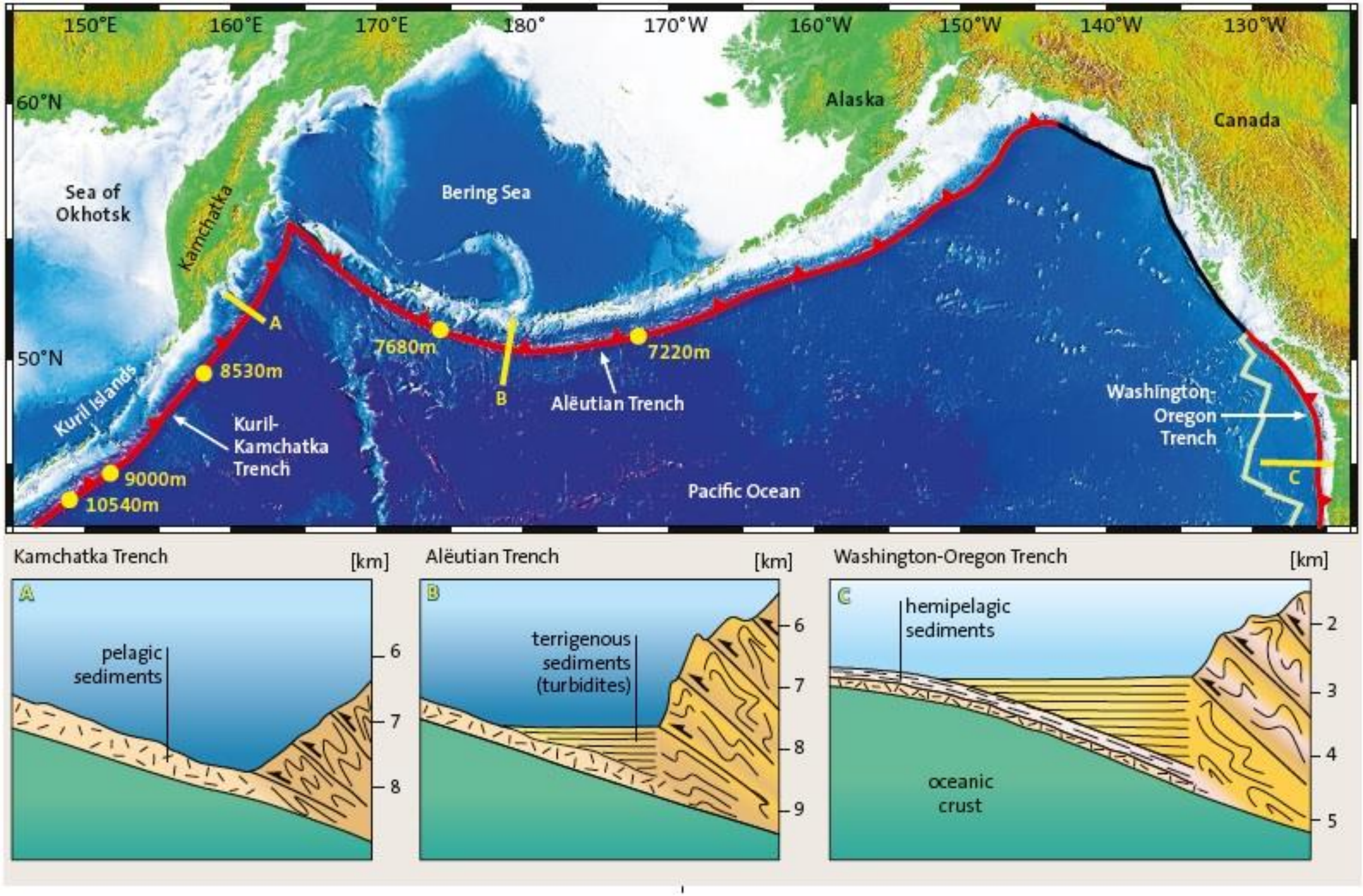

- Most trenches have a mixtures of pelagic and terrigenous deposits as well as sediments and sedimentary rocks transported into the trench on the subducting lower plate.
- The amount of sediment in a trench is related to the balance between the sediment supply and the slow tectonic removal of trench fill.
- Thick trench deposits are generally favored by a low subduction rate and accompanying slow tectonic removal of trench-fill material.

Accretionary Prisms

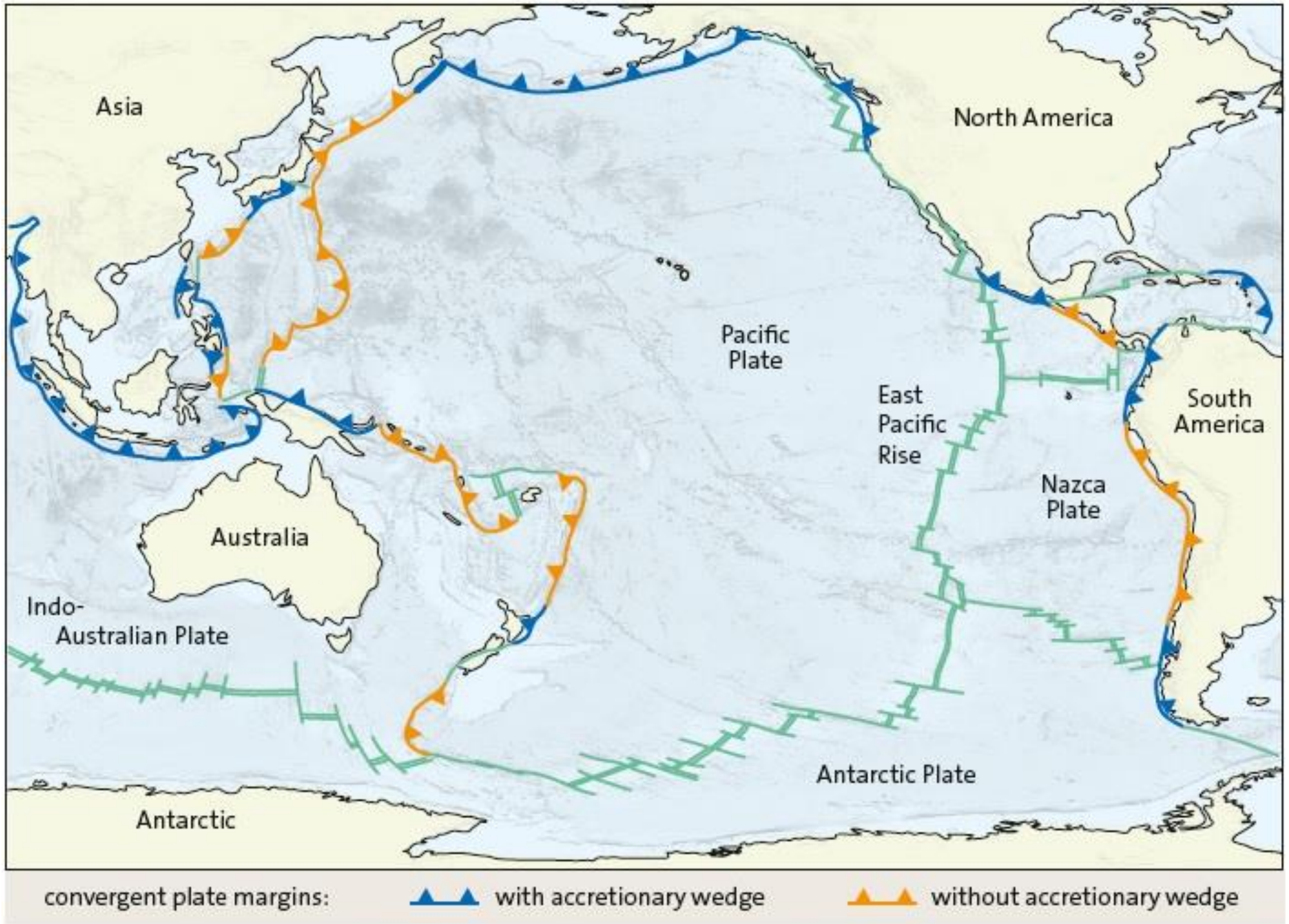

- Sedimentary accretionary wedges occur in many subduction zones including large portions of the Gulf of Oman, Sumatra, SW Japan, and in smaller areas of western North America and the Lesser Antilles.
- Other subduction zones are characterized by subduction erosion, during which rock material is scraped of from the bottom of the upper plate and transported downward with the subducting plate (Tonga Islands, Costa Rica and Chile).

Accretionary Prisms

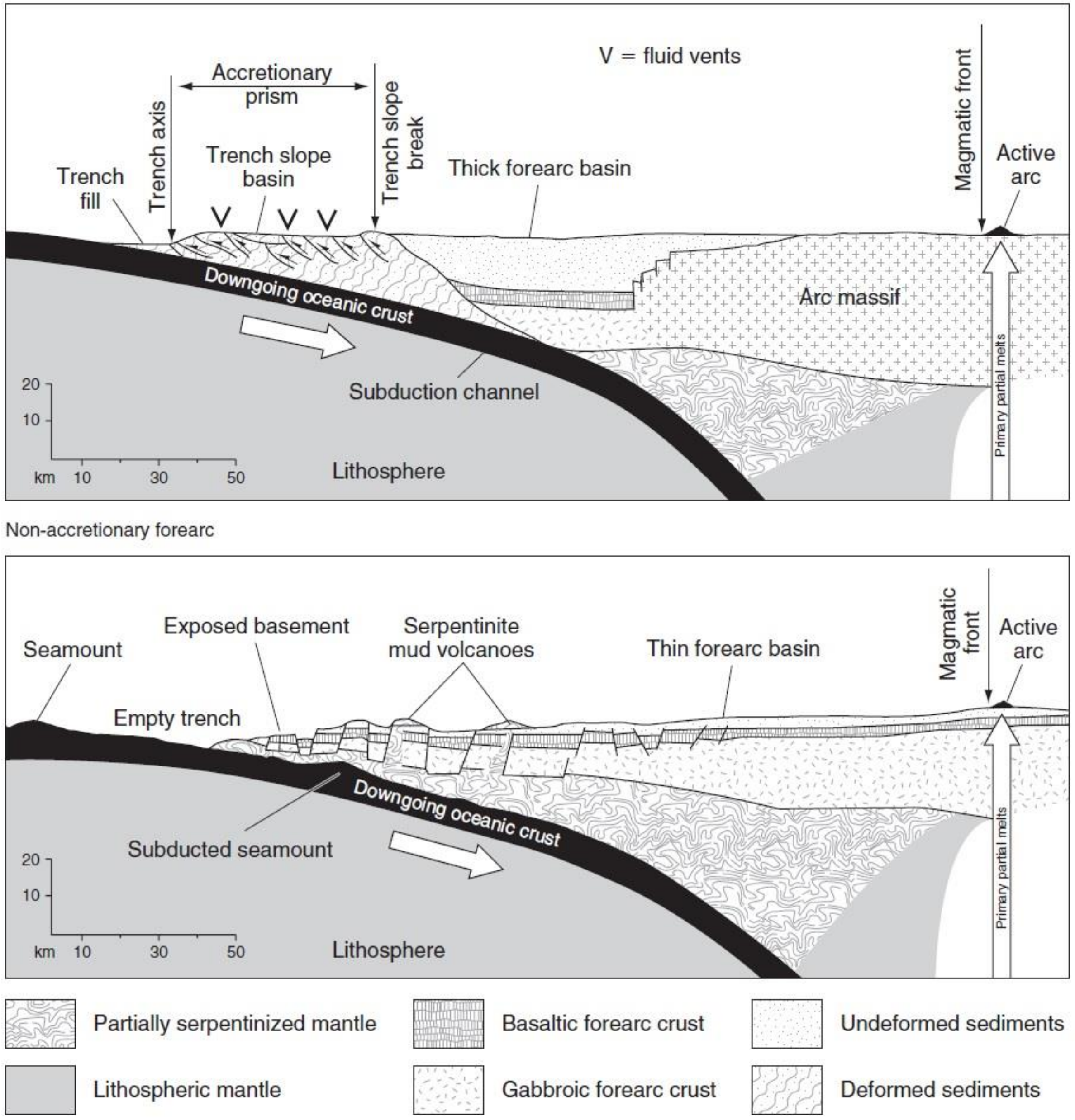

- Accretionary prisms grows from below, developing where trench-fill turbidites (flysch), and some pelagic sediments, are scraped off the descending oceanic plate by the leading edge of the overriding plate, to which they become accreted.
- 80% of pelagic sediments entering the trench is subducted (only when the sedimentary thickness exceeds 400-1000 m it is scraped off).
- Off-scraped material first moves down toward the base of the prism and then moves back toward the surface, creating a chaotic mixture of igneous, sedimentary and metamorphic rock types called a *mélange.*
- Over time, erosion, deformation, and sedimentary recycling result in a long-term circulation of material within the wedge.

Accretionary Prisms

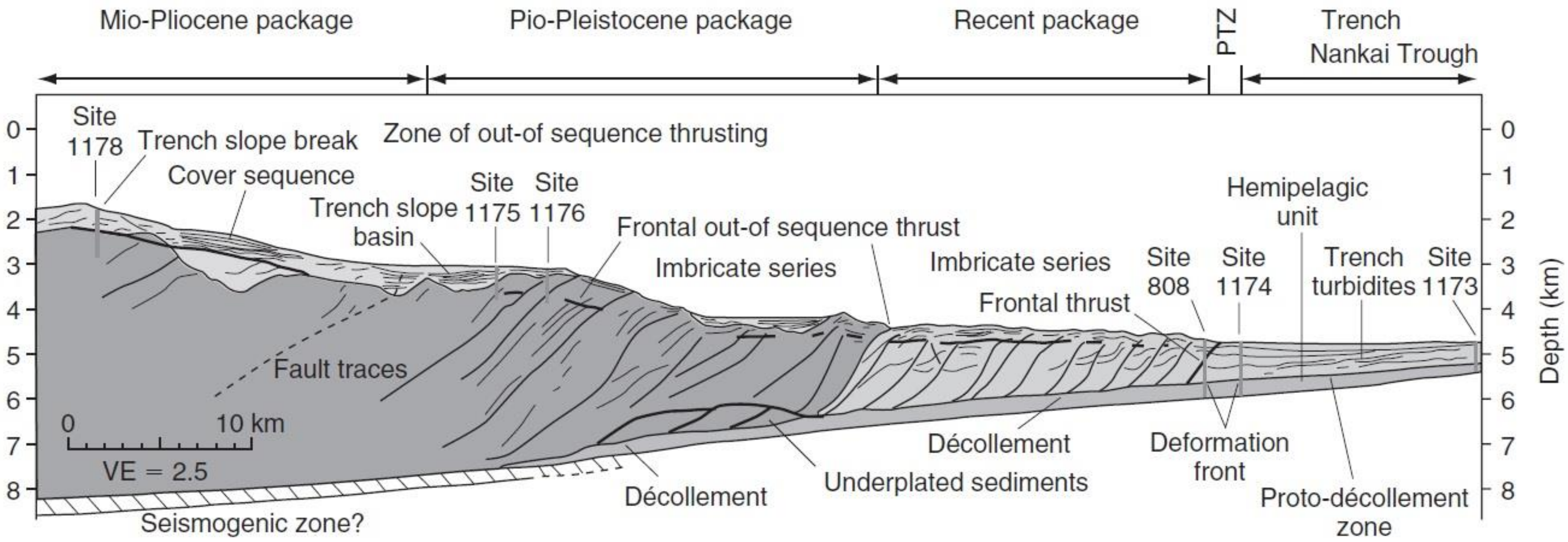

- Beneath the prism, the plate boundary is defined by a 20-30-m-thick, gently dipping fault or shear zone that separates a deformed sedimentary wedge above from a little-deformed section of subducted trench sediment, volcaniclastic rock, and basaltic crust below.
- This boundary, or *décollement*, develops in a weak sedimentary layer (hemipelagic mud) underlying stronger trench turbidites. Above the décollement is a *fold and thrust belt* composed of listric thrust ramps that rise through the stratigraphic section forming imbricated arrays.
- The top of an accretionary prism is defined by a relatively abrupt decrease in slope called the *trench slope break*. Between this break and the island arc, a forearc basin may develop, which is then filled with sediments derived from erosion of the volcanic arc and its substrate.

Accretionary Prisms

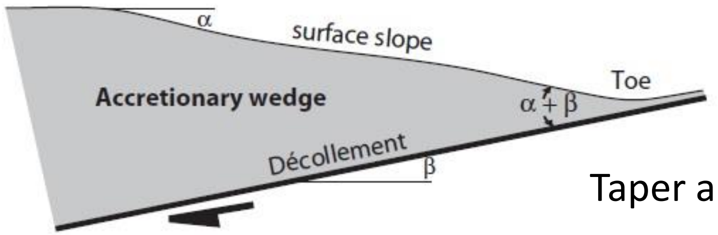

Taper ange: $\alpha+\beta$

λ=Pore fluid factor

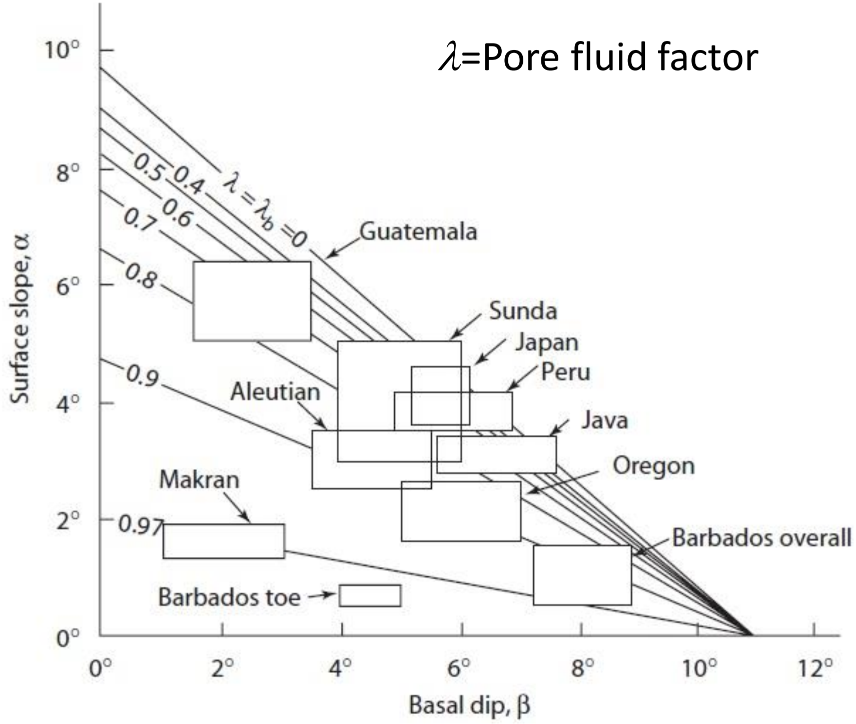

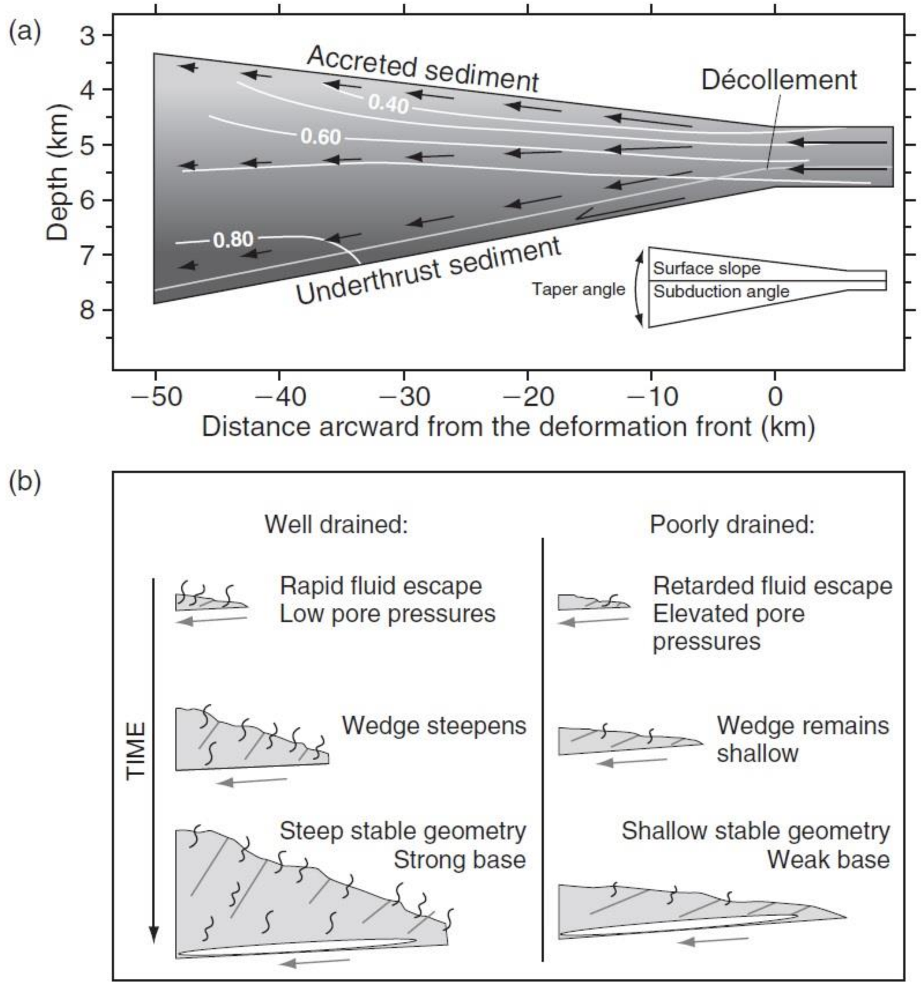

- The overall shape of accretionary prisms in profile approximates that of a tapered wedge, where the upper surface slopes in a direction opposite to that of the underlying décollement.
- The surface slope (α) is determined by the interplay between resistance to sliding on the décollement and the strength of the rock in the thrust wedge, which are strongly influenced by the pore fluid factor (λ), the dip of the basal décollement (β), and the weight of the overlying rock.

Accretionary Prisms

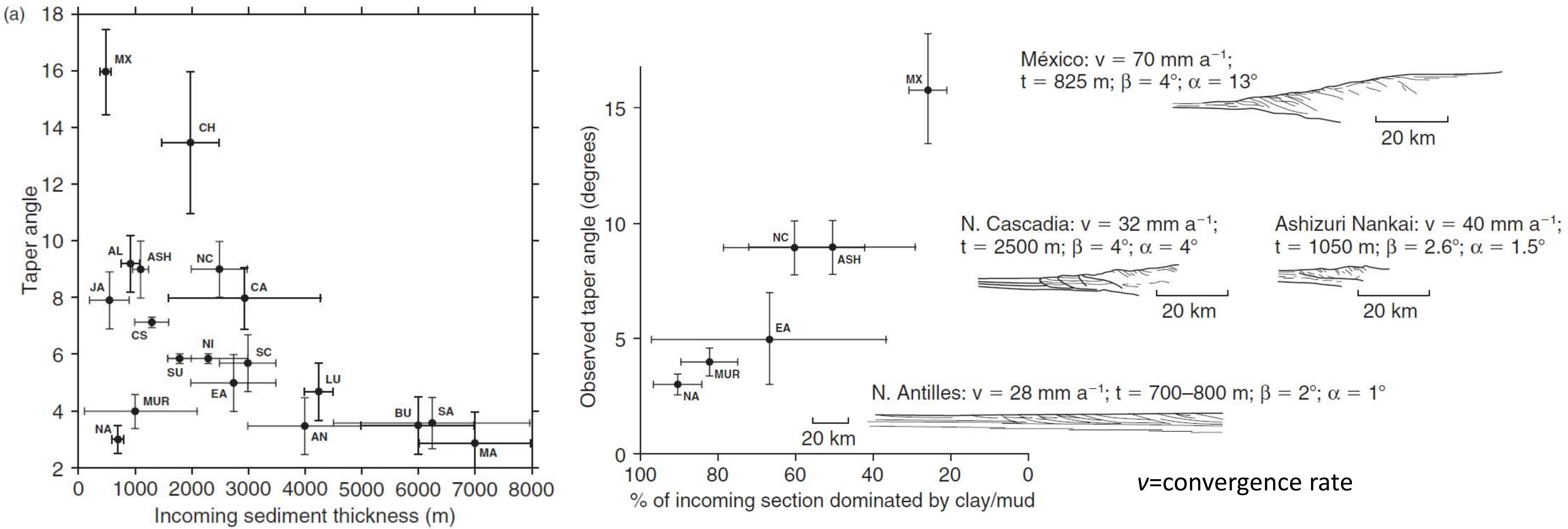

NA, northern Antilles; SA, southern Antilles; MUR, Nankai Muroto; AL, eastern Aleutians (160°W); EA, eastern Aleutians (148–150°W); CA, central Aleutians (172–176°W); NC, north Cascadia; SC, southern Cascadia; ASH, Nankai Ashizuri; MX, Mexico; JA, Java; CS, central Sumatra; SU, Sunda; CH, Chile; NI, Nicobar; AN, Andaman; LU, Luzon; BU, Burma; MA, Makran.

- Thick sedimentary sections produce large prisms that are able to sustain high pore fluid pressures and low stable taper angles.
- Prisms composed mostly of low permeability fine-grained sediments (e.g., northern Antilles), exhibit thin taper angles and those characterized by a high proportion of high permeability turbidites (eg., Cascadia, Chile, and México), have steep taper angles.

Erosion of accretionary prisms

Marianna Subduction Zone

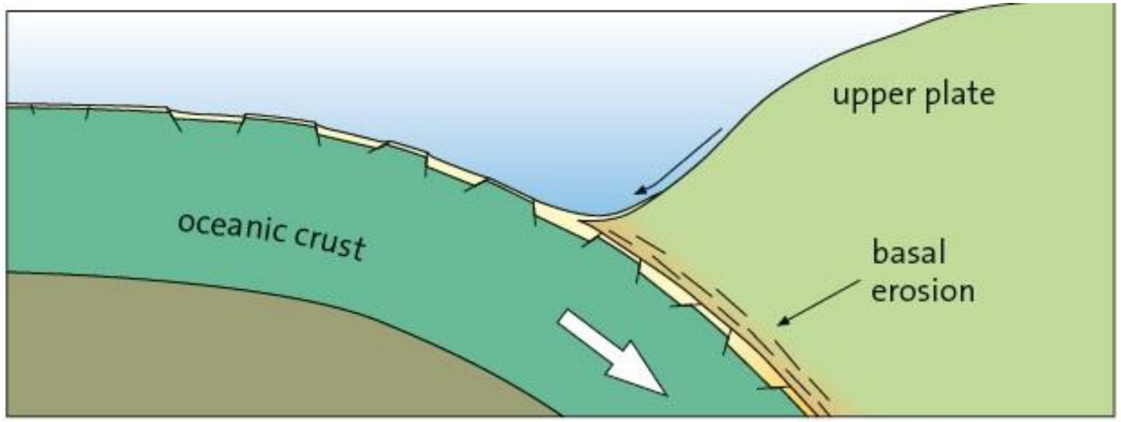

Costa Rica Subduction Zone

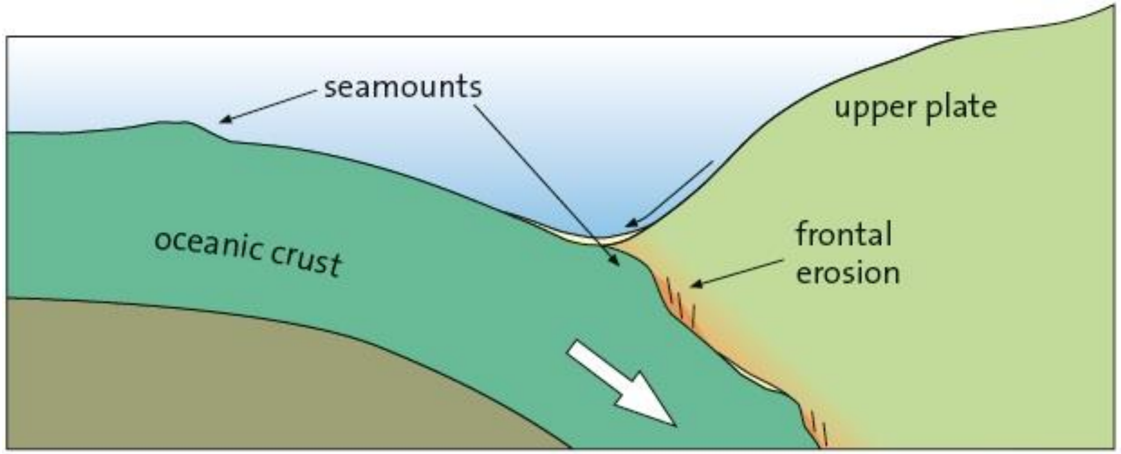

- Subduction erosion is particularly effective when the lower plate has a roughly textured surface and is only covered by a thin sedimentary layer.
- As the lower plate enters the subduction zone and is bent, the upper part of the plate is extended and form a series of horst and graben, favoring the removal of the sediments.
- Seamounts on the subducting plate create a somewhat different kind of subduction erosion: Single seamounts scrape material from the frontal tip of the accretionary wedge along the upper plate and carry it into the subduction zone (frontal erosion).
- Subduction erosion can occur both where the subduction zone angle is relatively low and there is a strong coupling between the two plates (Chile type) and where the subduction angle is high and subduction roll-back occurs (Mariana type).
- Pore fluids in the high-stress zone along the plate boundary decollement actually increase mobility and slippage in this zone by acting as a lubricant.

Erosion of accretionary prisms

Costa Rica Subduction Zone

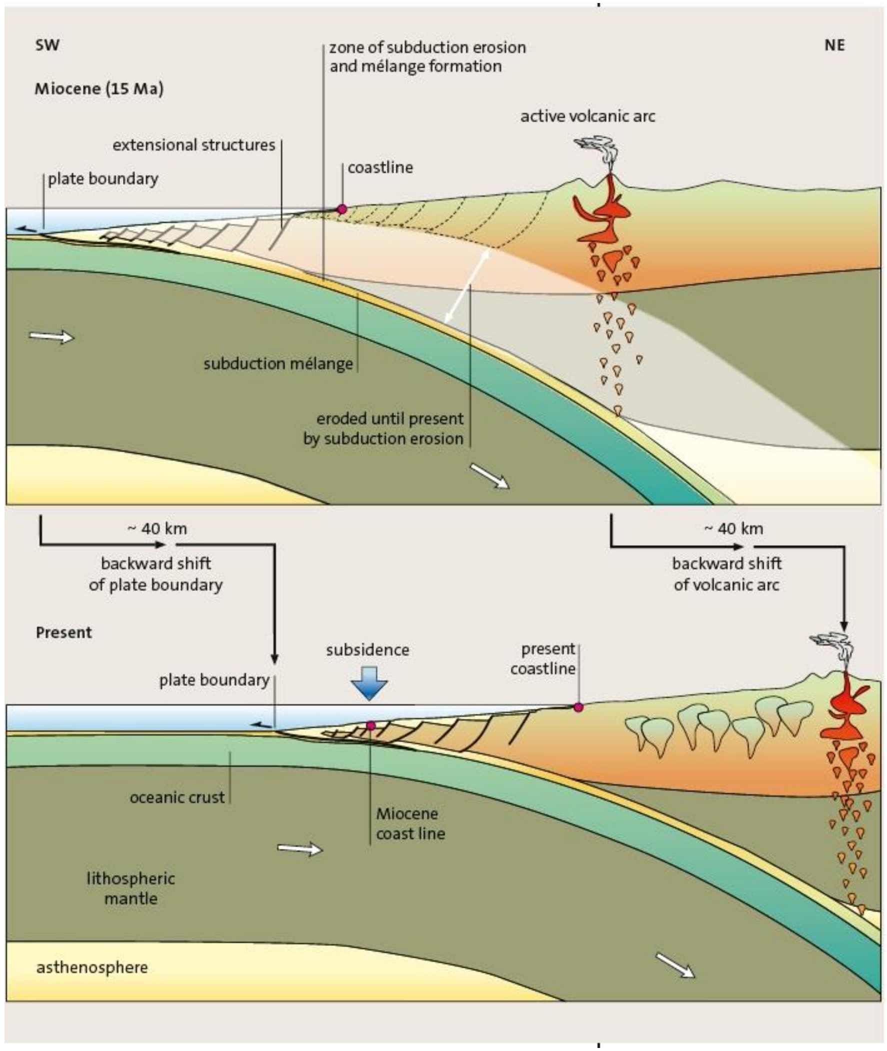

- Erosion of the accretionary prism on the upper plate causes the plate boundary to migrate towards the arc, which itself is moving backward in response to the migrating subduction zone (Costa Rica).
- The Cocos Plate is being subducted beneath the Caribbean Plate with a velocity of about 9 $cmyr^{-1}$. The volcanic front has shifted 40 km backwards (towards the Caribbean plate) during the last 15 million years.

Forearc Basin

- Forearc basins are zones of crustal subsidence that lie between the outer ridge and the volcanic arc, underlain by either thinned continental or normal oceanic crust.
- They are generally dominated by great thicknesses of marine sediment and derived from the adjacent volcanic arc.

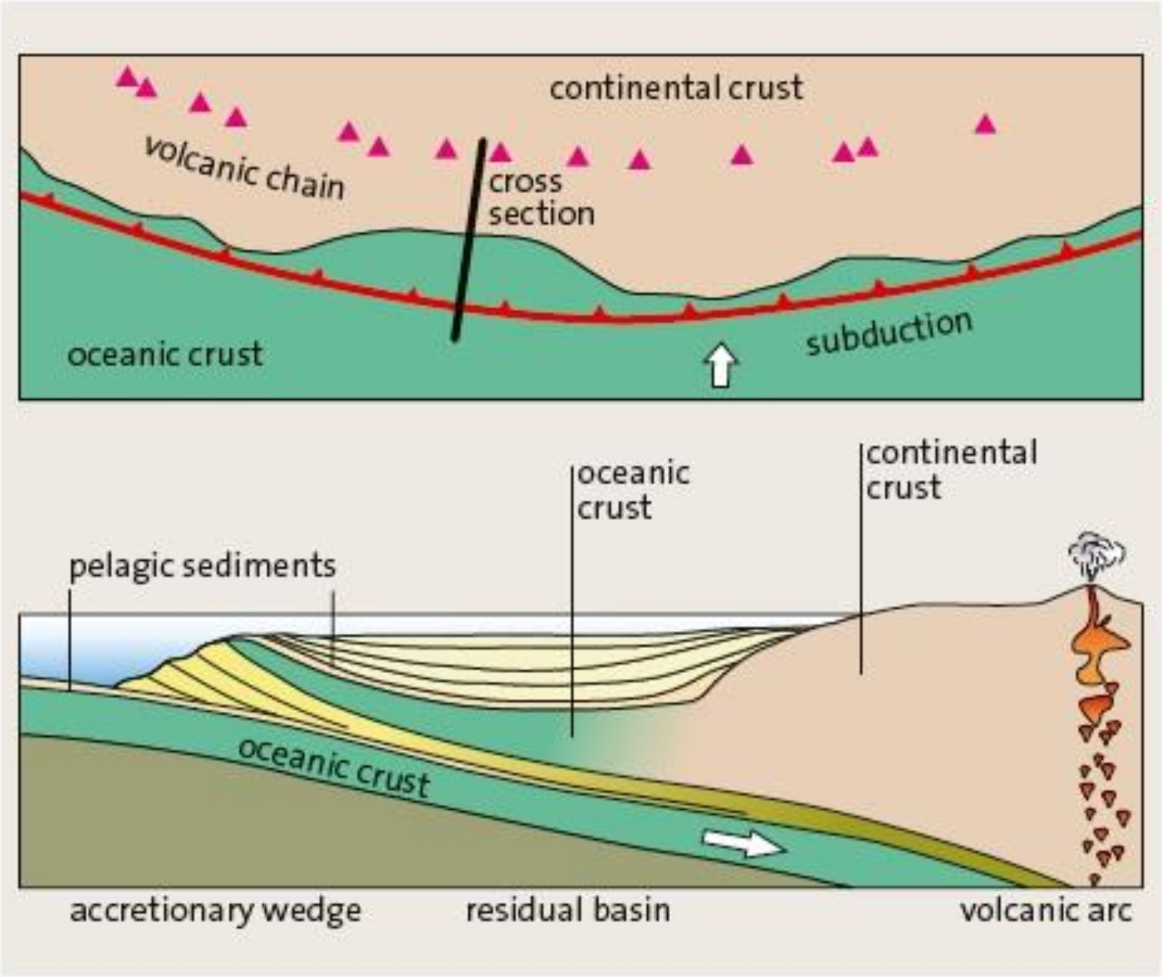

Volcanic Arc

- Volcanic Arc develops 150-200 km from the trench axis
- Depth of the lithospheric slab beneath the volcanic arc is in a range of 65-130 km, depending on the vertical rate of descent of the slab: high descent rate increases the rate of flow in the mantle wedge, causing higher temperature and melting at shallower depth.

Thickness of the arc crust reflects both the age of the systhem and type of the arc

Oceanic Arc: volcanic rocks have 53-55% SIO_2

Marianna volcanic arc (3-4 My): crustal thickness 20 km

Japanese Arc (Neogene): crustal thickness 30-50 km

Continental Arc: volcanic rocks have 63% SIO_2

Andes and Cascades volcanic Arc: crustal thickness up to 60-70 km.

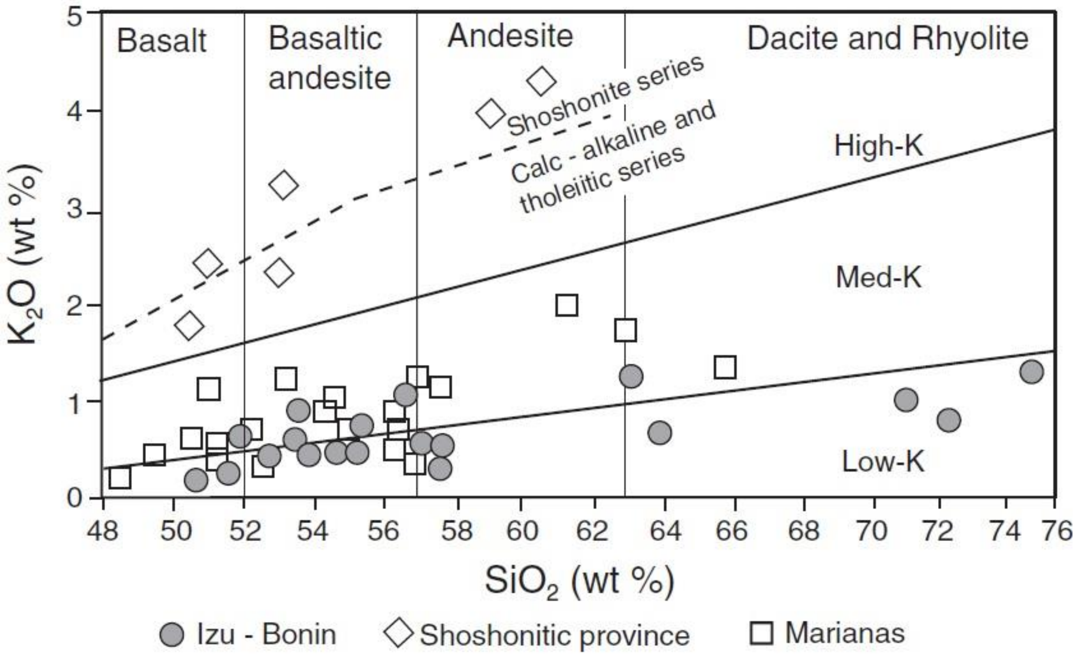

Volcanic Arc

Calc-alkaline basalts

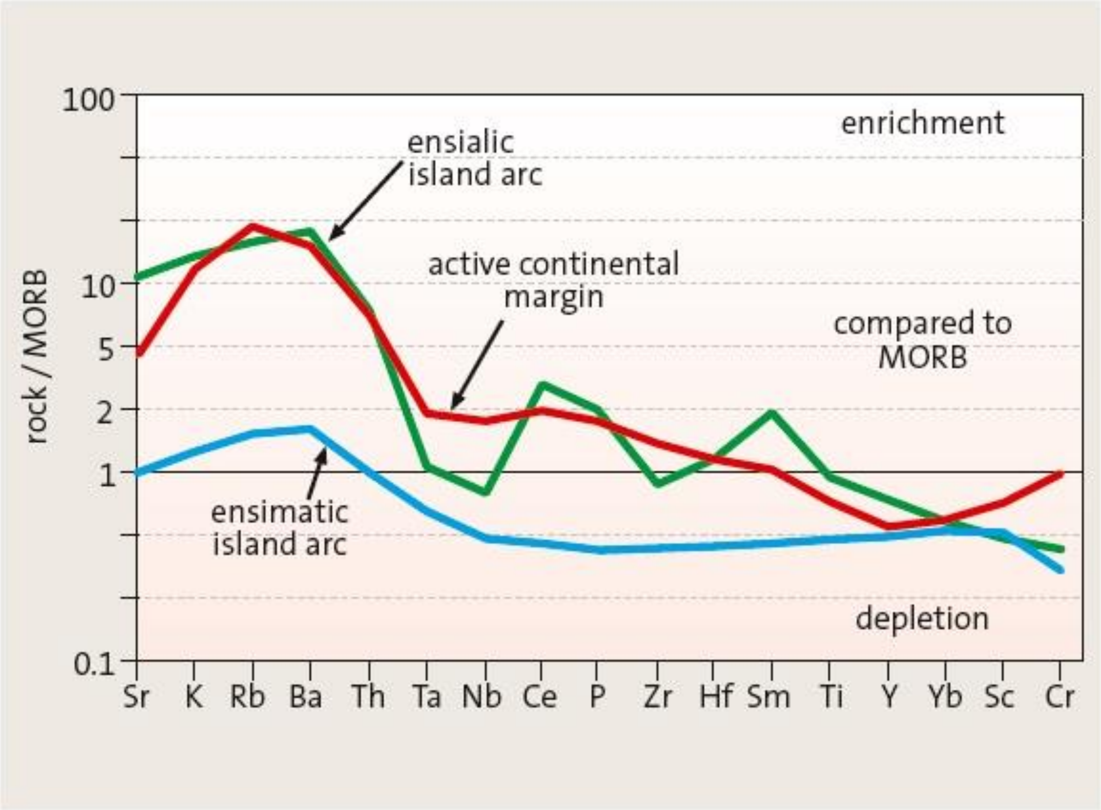

Spatial patterns of volcanic series (Japanise island arc): It reflects decreasing magma generation from the subducted rocks with increasing depth of the subduction zone.

- Low potassium tholeitic series: basaltic lavas
- Calc-alkaline series: andeites moderately enriched in potassium, alluminium (up to 20%) and lithophile elements, such as strontioum, barium, thorium, and uranium and poor in «immobile elements», such as niobium and tantalium.
- Alkaline series: alkaline basalts and high-potassium (i.e., shoshonitic) lavas.

Deviations from the spatial patterns (Marianna arc produces tholeiitic basalts and boninites, derived from melted harzburgites of the lithospheric mantle) are due to variations in the depth and degree of partial melts and other processes (e.g., assimilation, magma mixing)

Backarc Basins

Backarc basins are small basins of either oceanic or continental affinity that form behind the volcanic arc in the overriding plate of a subduction zone.

- Crust composition and accretion rate is similar to that of the oceanic basins (variable spereading velocity: 16 cm yr^{-1} in the backarc basin of Tonga Island to 2-4 cm yr^{-1} in the backarc basin of the Marianna) .
- Crustal accretion, magmatic activity, and thickness of the backarc basins are influenced by processes related to subduction (dynamics of flow of the upper mantle wedge), which cause a main difference in the geochemistry (similar to that of the adjacent volcanic arc, usually including higher water content).
- Sediments deposited in backarc basins consist of arc-derived volcaniclastics and volcanic ashes, sand and mud eroded from the continent, and marine carbonates.
- Magnetic anomalies are present, but not so well developped as in the oceanic basins.

Origin of the back-arc basin, extension induced by:

- Slab roll-back
- Convection of the upper mantle wedge induced by the subducting slab or an increase in the angle of subduction with depth.

Slab geometry parameters

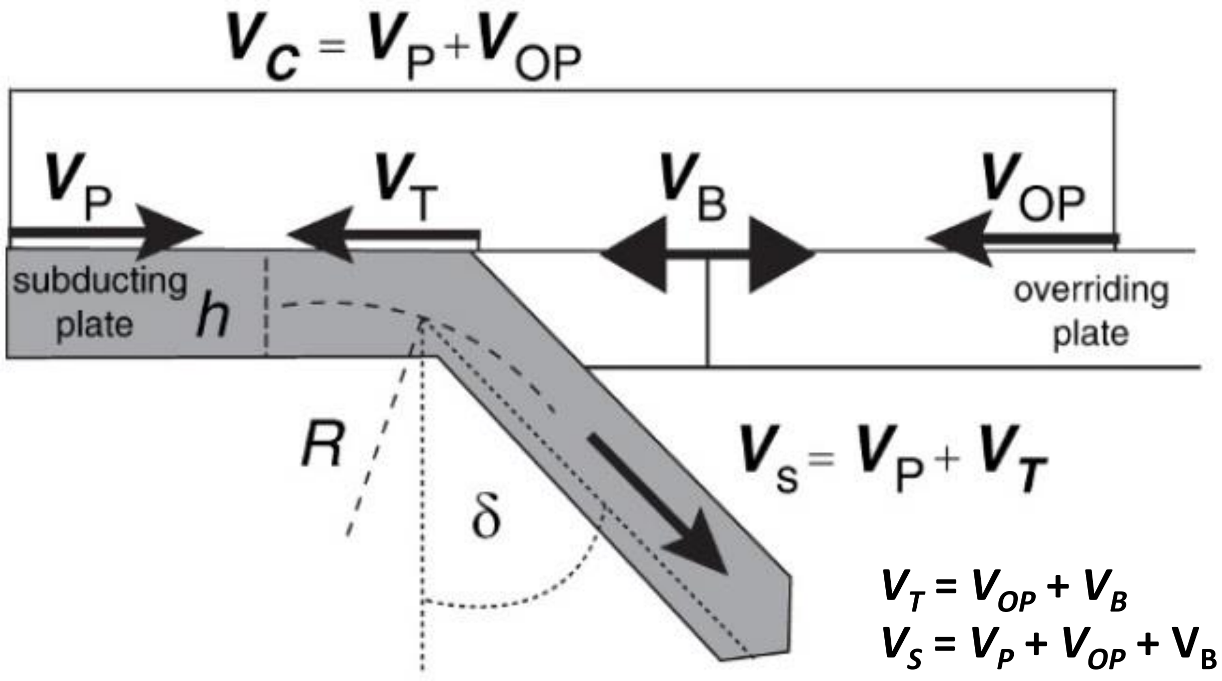

$V_T = V_{OP} + V_B$
$V_S = V_P + V_{OP} + V_B$

V_b= back-arc deformation rate (positive for extension)
V_c= convergence rate
V_{SP} =sinking velocity of the subtracting plate
V_P = plate velocity
V_T = trench velocity (positive for rollback)
V_{OP} = overriding plate *velocity* (positive toward the trench)
h = width of the slab and plate
R = approximate bending radius at the trench
δ = slab dip angle

Becker and Faccenna, 2009

- Any trench migration has important consequences for tectonics such as backarc spreading, but also for large-scale upper mantle dynamics. The migration of the slab inside the mantle induces a toroidal component of flow, with significant effects on back-arc temperatures, volcanism, and the interpretations of seismic anisotropy observations.
- V_T *can* be estimated by subtracting the back-arc deformation rate, V_B from the velocity of the upper plate, V_{OP}, assuming that erosion and accretion at trenches are negligible. Trench migration rates are typically not more than 50% of the convergence rates .
- Trenches are often found to retreat toward the subducting plate with respect to the lower mantle (V_T>O).
- In several regions, e.g. Marianas-Izu Bonin, trenches also appear to advance toward the subducting plates in all reference frames ($V_T < 0$).

- If the sinking rate is larger than the rifting rate, the trench moves away from the upper plate (slab roll-back).
- If the rifting rate at the mid-oceanic ridge exceeds the sinking rate of the subducting slab, then the trench will move towards the upper plate.

Observations subducting plate velocity ($v_{SP\perp}$)

Subducting plates move trenchward ($v_{SP\perp}>0$):

97% for Indo-Atlantic HS [O2005]
89% for Pacific HS [G&G2002]
95% for Pacific HS [W2006]
99% for global HS [G&J1986]
98% for NNR [K2003]
96% for NNR [A&G1991]

maximum $v_{SP\perp}$ range
(all reference frames)
= -8 to 12 cm/yr

Indo-Atlantic HS reference frame

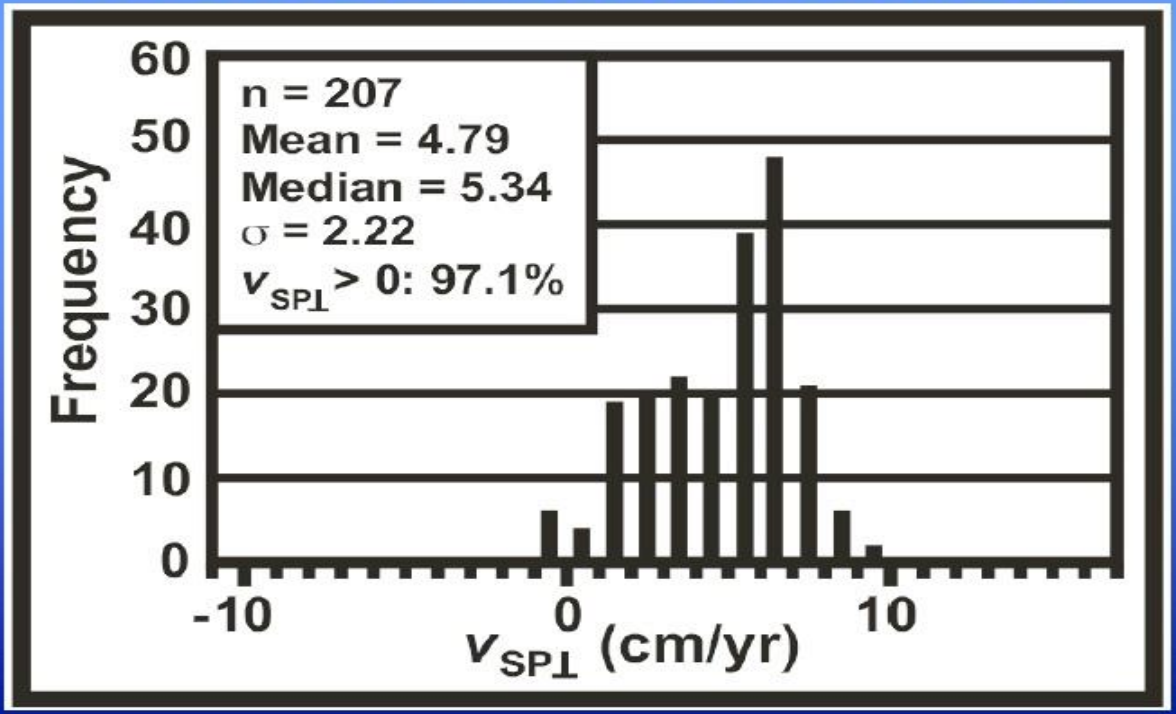

Observations trench velocity ($v_{T\perp}$)

Trenches predominantly retreat ($v_{T\perp}>0$) (i.e. rollback):

73% for Indo-Atlantic HS [O2005]
63% for Pacific HS [G&G2002]
73% for Pacific HS [W2006]
71% for global HS [G&J1986]
62% for NNR [K2003]
67% for NNR [A&G1991]

Indo-Atlantic HS reference frame

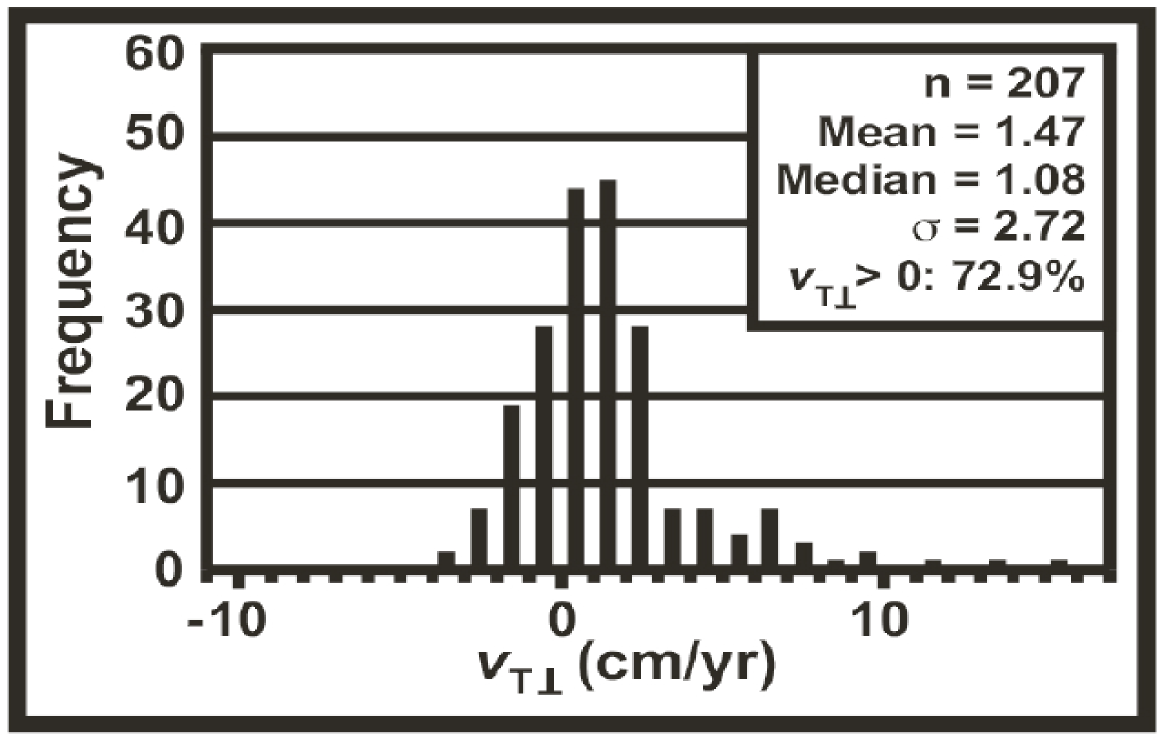

maximum $v_{T\perp}$ range
(all reference frames)
= -6 to 17 cm/yr

Observations subduction partitioning

Subduction rate dominated by $v_{SP\perp}$ ($v_{SP\perp}/v_{S\perp}$>0.5):

81% for Indo-Atlantic HS [O2005]
62% for Pacific HS [G&G2002]
78% for Pacific HS [W2006]
80% for global HS [G&J1986]
79% for NNR [K2003]
79% for NNR [A&G1991]

$v_{SP\perp}/v_{S\perp}$ range = -1 to 2

Indo-Atlantic HS reference frame

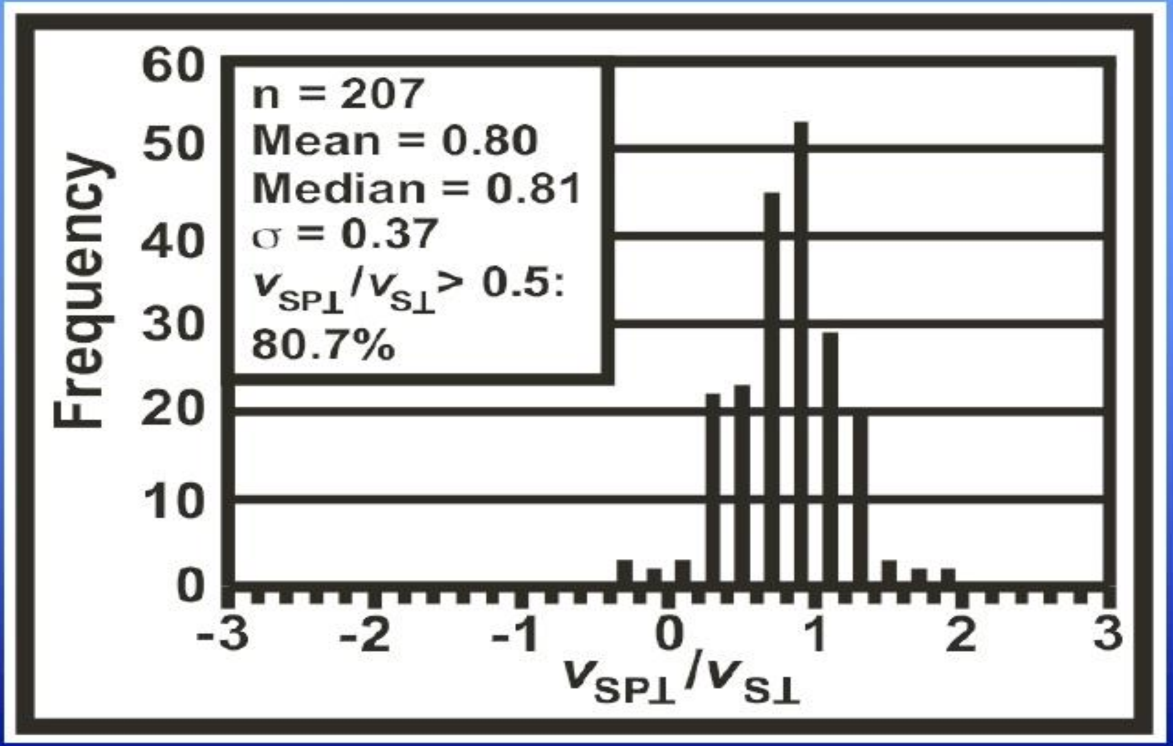

Plate and plate boundary velocities [cm/yr]

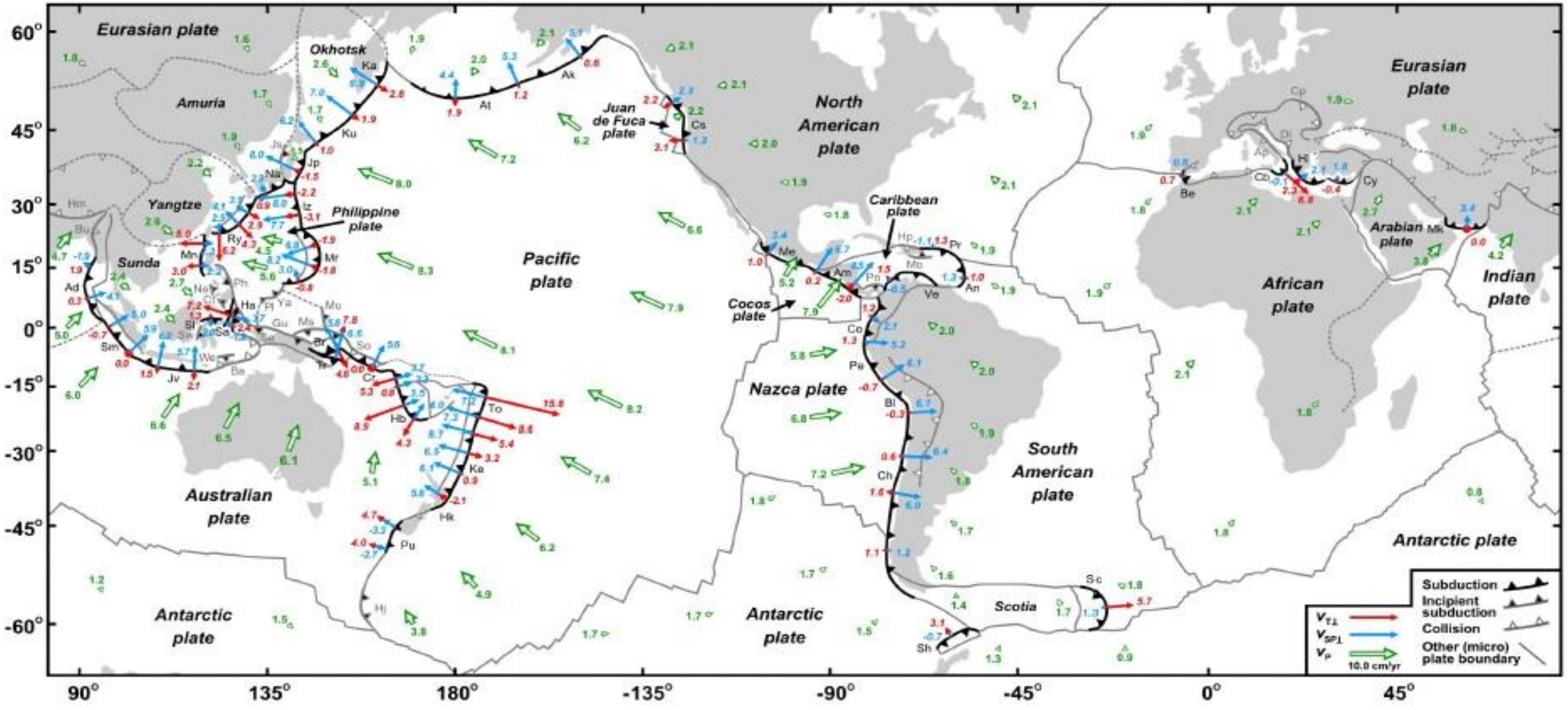

Schellart et al., 2011, JGR

Major subduction zones on Earth, blue vectors: trench-normal subducting plate velocity (v_{SP}), red vectors: trench-normal trench migration velocity (v_T), large white vectors with green outline: plate velocity (v_P) for the major plates and some microplates, calculated in the Indo-Atlantic hot spot reference frame from O'Neill et al. (2005).

Numerical models demonstrated that the trench migration results predominantly from lateral migration of the slab, most likely driven by the negative buoyancy force of the slab itself, rather than from overriding plate motion.

- ❑ Rollback velocities and trench curvature in nature may be controlled by slab width.
- ❑ Narrow slabs (e.g., Scotia arc) show fast rollback, while wide slabs such as in the Chilean roll back slowly.

Subducton partitioning (v_{SP}/v_S) and slab width

- Subduction for narrow slab models (**W = 300–1500 km**) is characterized by rapid trench retreat, slow trenchward plate motion and low partitioning with v_{SP}/v_S = 0.2–0.4, except for the earliest subduction stage (before ~5 Myr). A progressive development of a curved slab and trench that are concave toward the mantle wedge is also observed.
- Subduction for large slab models (**W = 7000 km**) is characterized by overall slow trench migration, rapid trenchward plate motion and high partitioning with v_{SP}/v_S = 0.7–1.2, except for the earliest stage (before ~7 Myr). A progressive development of a curved subduction zone that is overall convex toward the mantle wedge but concave edges are also observed.
- Subduction for an intermediate slab width (**W = 2000–3000 km**) show intermediate behavior.

- ❑ **On a global scale subduction is dominated by trenchward subducting plate motion:** mean partitioning in nature is 0.80, while for 80.7% of the trench segments $v_{SP}/v_S > 0.5$.
- ❑ Partitioning is always high far from slab edges (D_{SE} > 2200 km), with $0.76 \leq v_{SP}/v_S \leq 1.84$. Low partitioning ratios in nature ($v_{SP}/v_S < 0.39$) are only found close to lateral slab edges (D_{SE} < 1000 km).
- ❑ In the numerical models, the lowest partitioning ratios are found for narrow slabs such as W = 300 km with v_{SP}/v_S = 0.28–0.32.

D_{SE}=horizontal distance from the slab edges

<u>In Summary</u>:

- **Slab segments close to lateral slab edges (as well as narrow slabs) experience relatively minor resistance from the ambient mantle to migrate laterally, resulting in relatively fast v_T.**
- **Segments far from lateral slab edges will experience large resistance from the ambient mantle, resulting in relatively slow v_T.**

Subduction kinematics and dynamics

- Data for subducting plate age shows negligible/minor correlation with $v_{SP}\perp$ and $v_T\perp$

- **Data and numerical subduction models show significant correlation between slab width and $v_{SP}\perp$:**

- *Subducting plate velocity scales with $W^{2/3}$*

- **Data and numerical subduction models show significant correlation between slab width and $v_T\perp$:**

- *Trench retreat velocity scales with 1/W*

- **$v_{SP}\perp$ is associated with poloidal flow, while $v_T\perp$ is associated with quasi-toroidal flow.**

- **Slab rollback induces a toroidal flow around the lateral slab edges from the sub-slab region towards the mantle wedge.**

- **The toroidal flow has a strong component of upwelling next to the slab edge, sub-slab region and mantle wedge.**

Physical parameters affecting velocity of trench ($v_T \perp$), subducting plate($v_{SP} \perp$), and overriding plate ($v_{OP}\perp$)

Physical parameters affecting $v_{SP} \perp$

- **% of plate circumference attached to a slab** (*Forsyth and Uyeda,* GJRAS 1975; Gripp and Gordon, GJI 2002)

Physical parameters affecting $v_T \perp$

- **Upper plate velocity** (Jarrard, RG, 1986; Heuret and Lallemand, PEPI, 2005)
- **Trenchward subducting plate velocity** (*Schellart*, EPSL, 2005)

Physical parameters affecting $v_{SP}\perp$ and $v_T\perp$

- **Slab/mantle viscosity ratio** (*Di Giuseppe et al.*, G3, 2008; *Schellart*, G3, 2008; *Stegman et al.*, Tectonophysics 2010)
- **Mantle viscosity stratification** (*Kincaid and Olson*, JGR 1987; *Zhong and Gurnis* Science 1995)

Physical parameters affecting $v_{SP}\perp$, $v_T\perp$ and $v_{OP}\perp$

Subducting plate age (Molnar and Atwater, EPSL 1978; Carlson et al, GRL 1983; Sdrolias & Muller, G3 2006; Capitanio et al, EPSL 2007; Goes et al, Nature 2008):

Old slab → dense → rapid rollback, plate motion and extension

Young slab → light → no rollback, slow plate motion and shortening

- **Slab width** (Dvorkin et al., Tectonophysics 1993; Schellart, JGR 2004; Stegman et al., G3 2006; Schellart et al., Nature 2007, Science 2010)

Slab Geometry

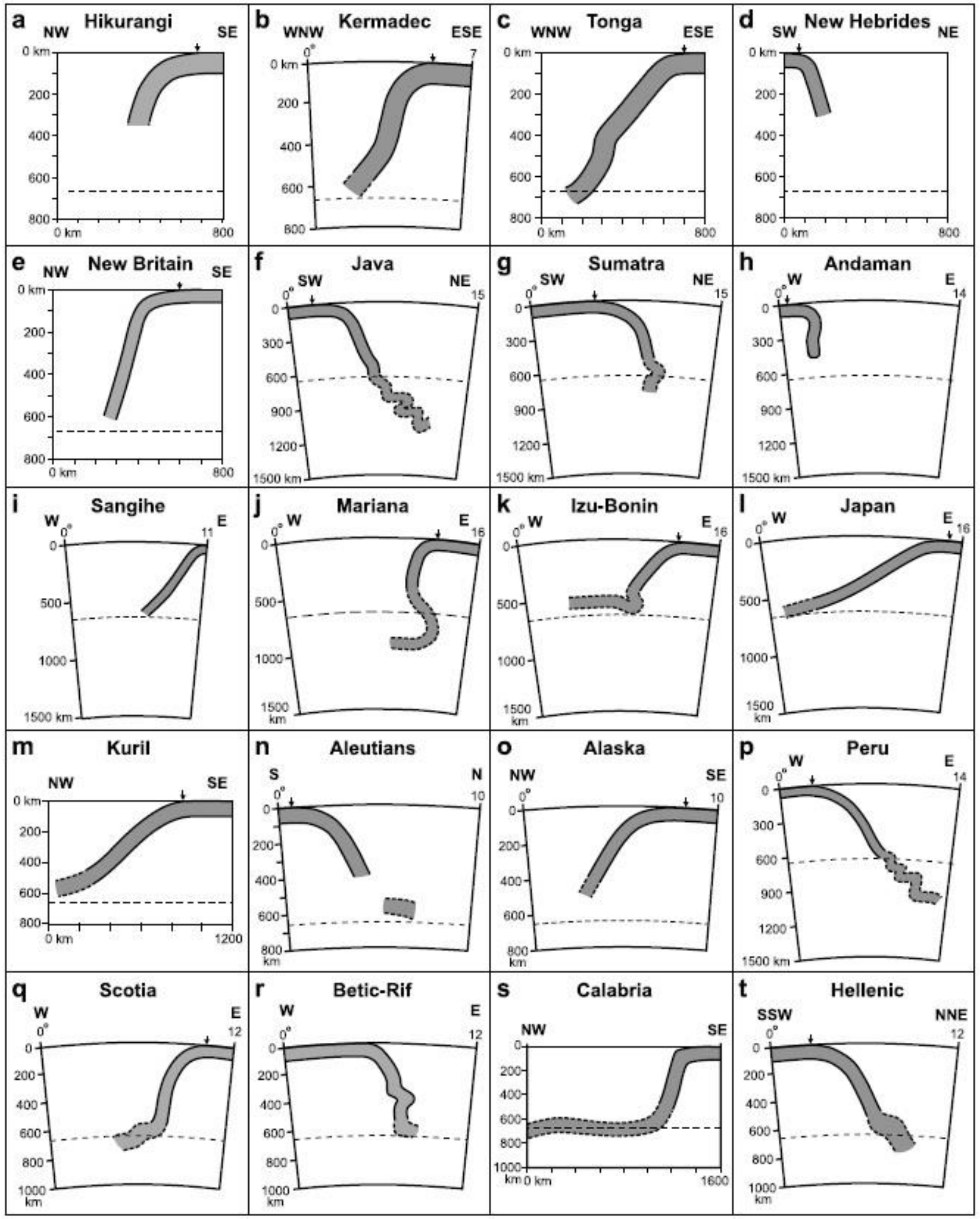

Small arrows indicate the trench location Schellart, 2010, JGR, 115

- All slabs show that in the uppermost 300–500 km, the slab is convex upward.
- Slabs that do not reach the upper-lower mantle discontinuity at 660 km are convex upward throughout (e.g.,Hikurangi, New Hebrides, Andaman, Alaska).
- Those that do reach the discontinuity can be relatively straight below ~400 km depth (e.g., New Britain, Sangihe), or show indications of kinking (e.g., Kermadec, Tonga) or folding (e.g., Java, Sumatra, Mariana, Peru, Betic- Rif) or have a concave upward bend near the transition zone with a horizontally deflected slab geometry (e.g., Calabria, Scotia, Kuril, Japan).
- All slabs also show that their downdip curvature changes considerably with depth.

Subduction Styles

Subduction occurs via several different styles, characterized by a distinct type of slab geometry, generated by the associated subduction kinematics, in agreement with two controlling factors: **flexural stiffness** and **slab buoyancy**.

Subduction styles observed in analogue and numerical experiments: slabs retreating and plate advancing

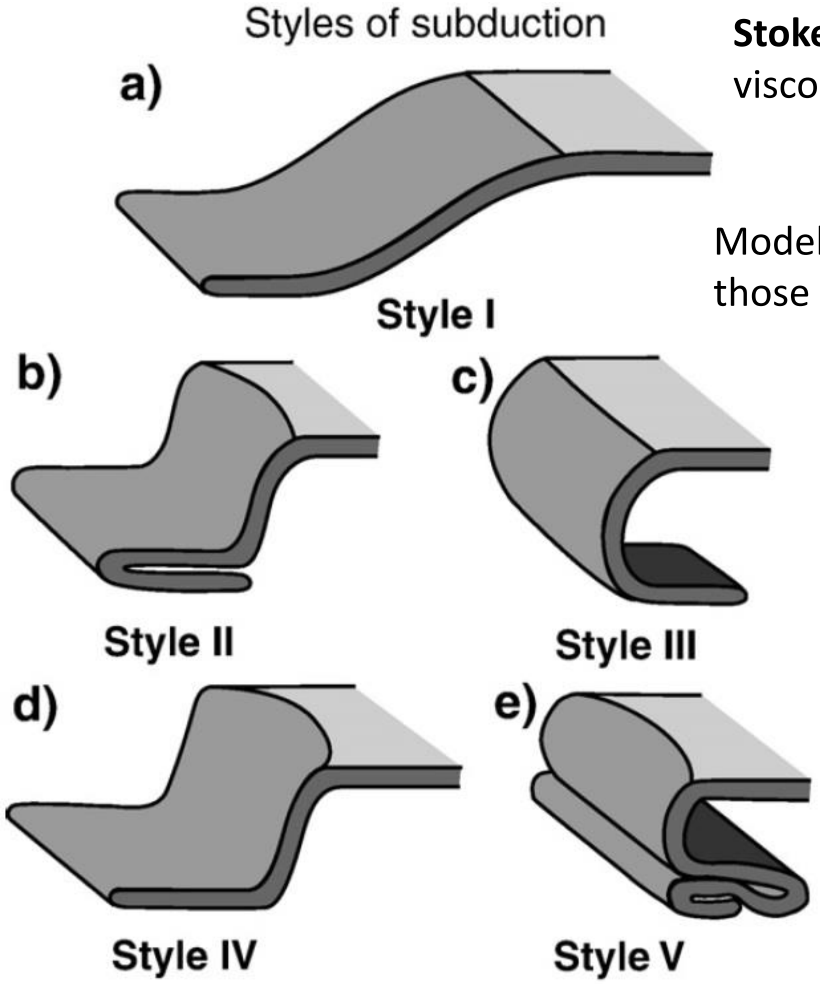

Stokes buoyancy (B_S,s^{-1}) is the ratio of volumetric potential energy ($\Delta\rho g h_{plate}$) to the upper mantle viscosity (η_{UM}):

$$B_S = \frac{\Delta\rho g h_{\text{plate}}}{\eta_{\text{um}}}$$

Models which accommodate subduction entirely through slab rollback and a retreating trench are those with $B_S > 10^{-11}$, while moldels in which plate advance is favored are those with $B_S < 10^{-11}$).

Flexural stiffness (D_{vis}, Nms) is similar to the elastic equivalent (flexural rigidity), depending on the cube of the plate thickness:

$$D_{\text{vis}} = \frac{\eta_{\text{plate}} h^3_{\text{plate}}}{3}$$

Effective flexural stiffness (D_{vis}*): $D^*_{\text{vis}} = \frac{D_{\text{vis}}}{\frac{1}{3}\eta_{\text{um}} H^3} = \frac{\eta_{\text{plate}}}{\eta_{\text{um}}}\left(\frac{h_{\text{plate}}}{H}\right)^3$

H=mantle thickness

Plate strength is described qualitatively as “strong” or “weak”, considering that a value of η_{plate}/η_{um}~500 usually discriminates between the two.

- **The transition between strong slabs (Regimes I–III) and weak slabs (Regimes IV–V) is (D_{vis}*~0.5).**
- **The models in certain strong slab regimes exhibit advancing trenches.**
- **The models in the weak slab regimes exhibit features such as highly curved trench geometry.**
- **Slab piles occur in Earth as a result of weak slabs interacting with a partially stratified mantle.**
- **Slabs that are weak can be easily perturbed by a number of processes that occur in the Earth.**

Stegman et al., 2010, Tectonophysics, 483

Subduction with variations in slab buoyancy

Subduction of the continental island and of continental margin

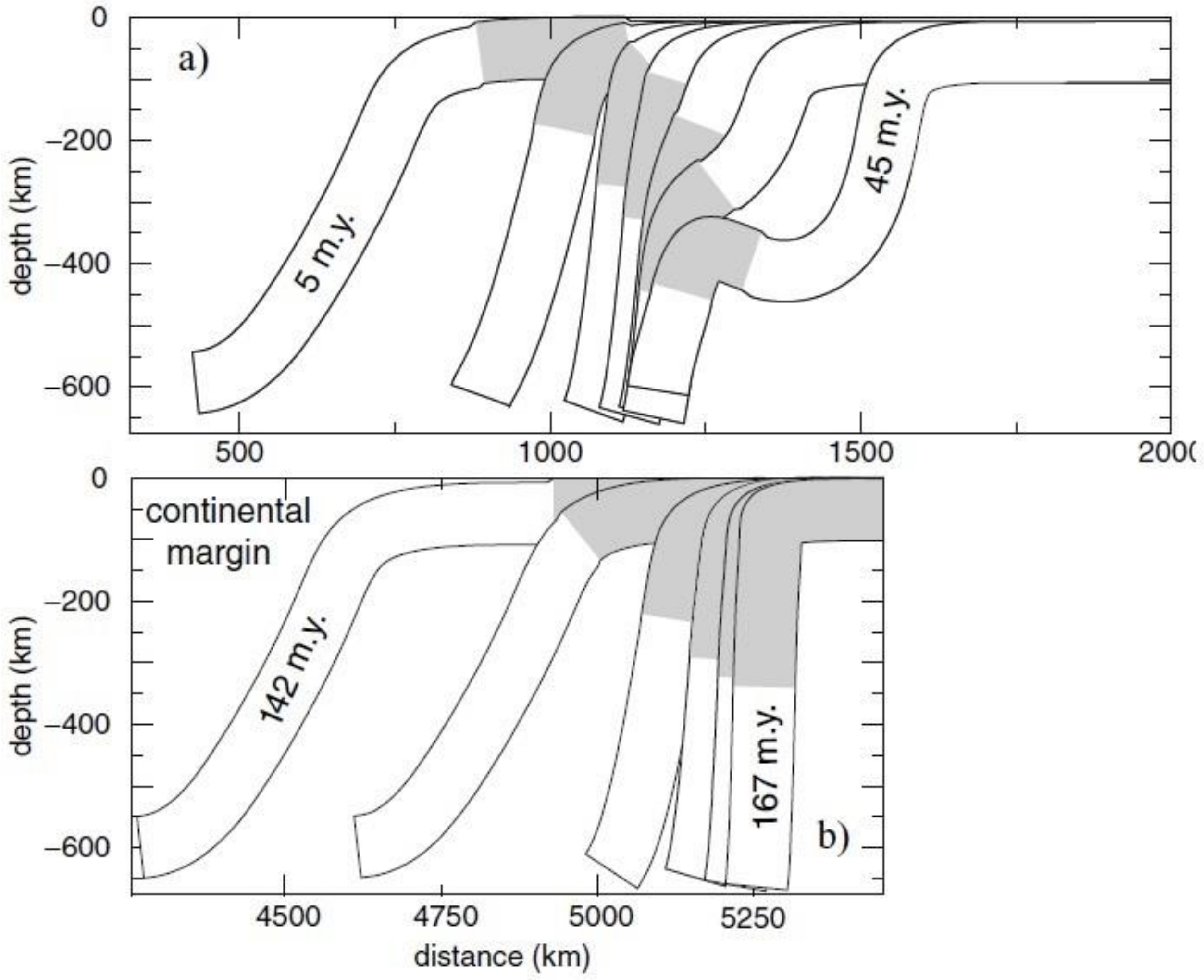

Royden and Husson, 2009

- Flattening of the shallow slab occurs when dense lithosphere follows buoyant lithosphere into the trench because the dense slab at shallow depth sinks more rapidly than the buoyant material at larger depth.
- There is a strong correlation between slab dip and trench migration rate: For narrow, highly buoyant slab segments, the dip of the slab may become inverted at depth, with a local depth-minimum coinciding with the buoyant slab segment.
- Rapid cessation of subduction is due to the creation of a shortcut for mantle flow that is critical in enabling rapid steepening of the slab into its final, stationary position.
- When subduction terminates, the viscous stresses on the slab disappear and the stresses on the slab arise only from its buoyancy.
- In these conditions, the extensional stress within the subducted slab is greatest at the former ocean-continent transition and increases upwards to the point where the density of the slab is less than the density of the surrounding mantle. This may induce possible slab detachment at this site.

Continental collision due to convergent plate boundaries in the Western Mediterrenean

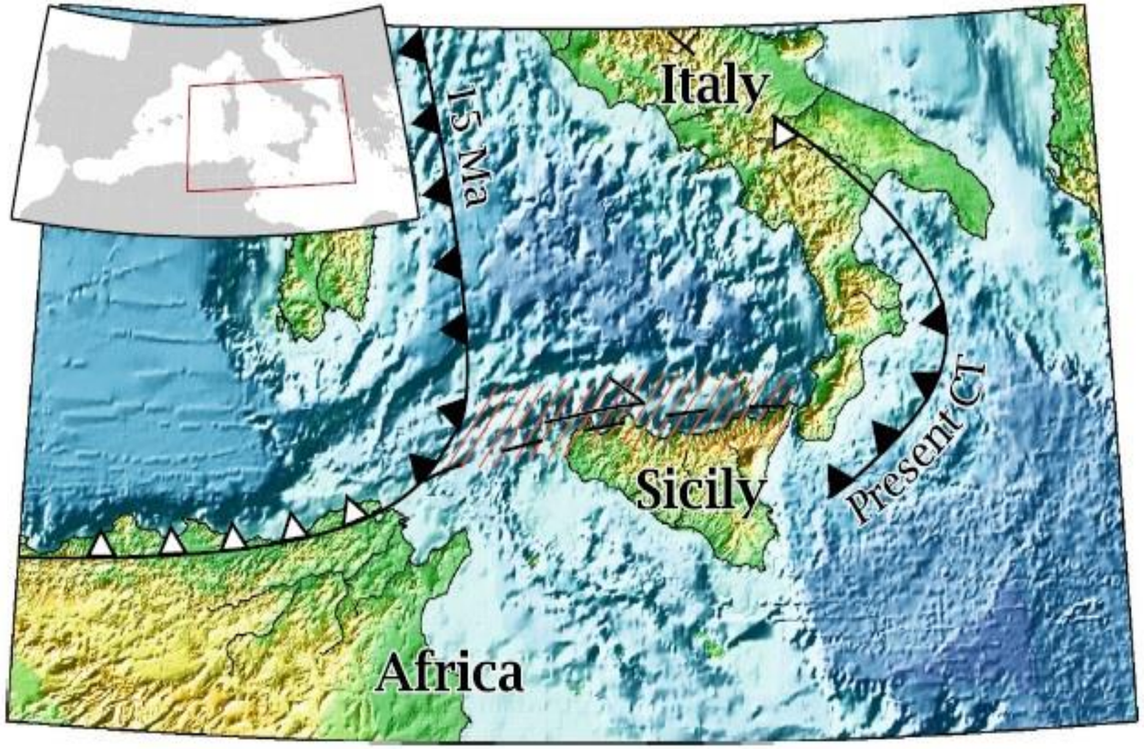

White dents = detachment of subducted slab
black dents = continuous slabs.

- In the Late Oligocene arc migration started from a location along the eastern margin of Iberia and southern France. The migrating trench system made contact with the north African continental margin in the Langhian (~15 Ma).
- In a second episode of extension starting at about 10 Ma, the extension continued with an eastward shift of activity, towards the Tyrrhenian realm.

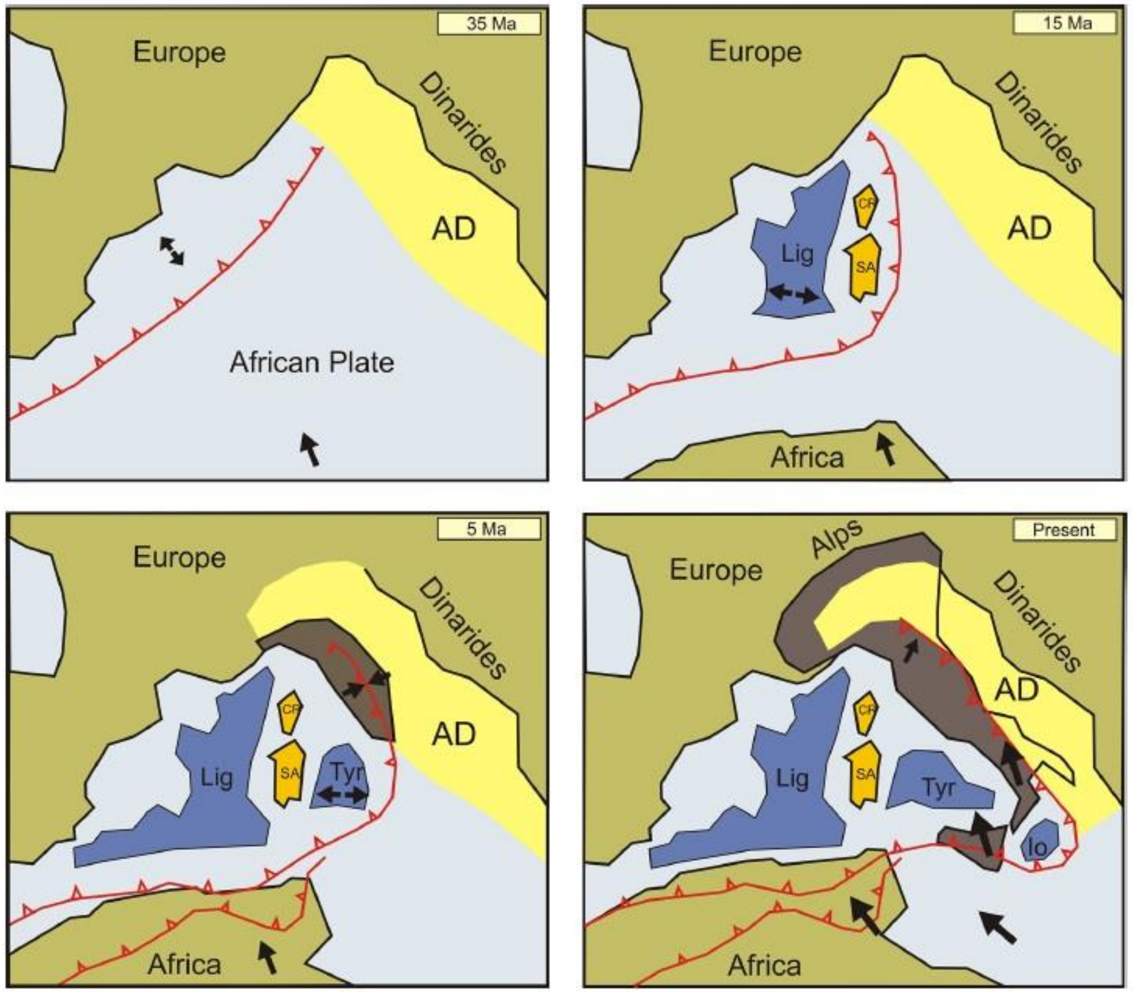

Lig – Ligurian Sea, CR – Corsica, SA – Sardinia, Tyr – Tyrrhenian Sea, Io – Ionian Sea, AD – Adriatic Sea.

Koulakov et al., 2015, Solid Earth, 6,

Mediterranean Tectonics

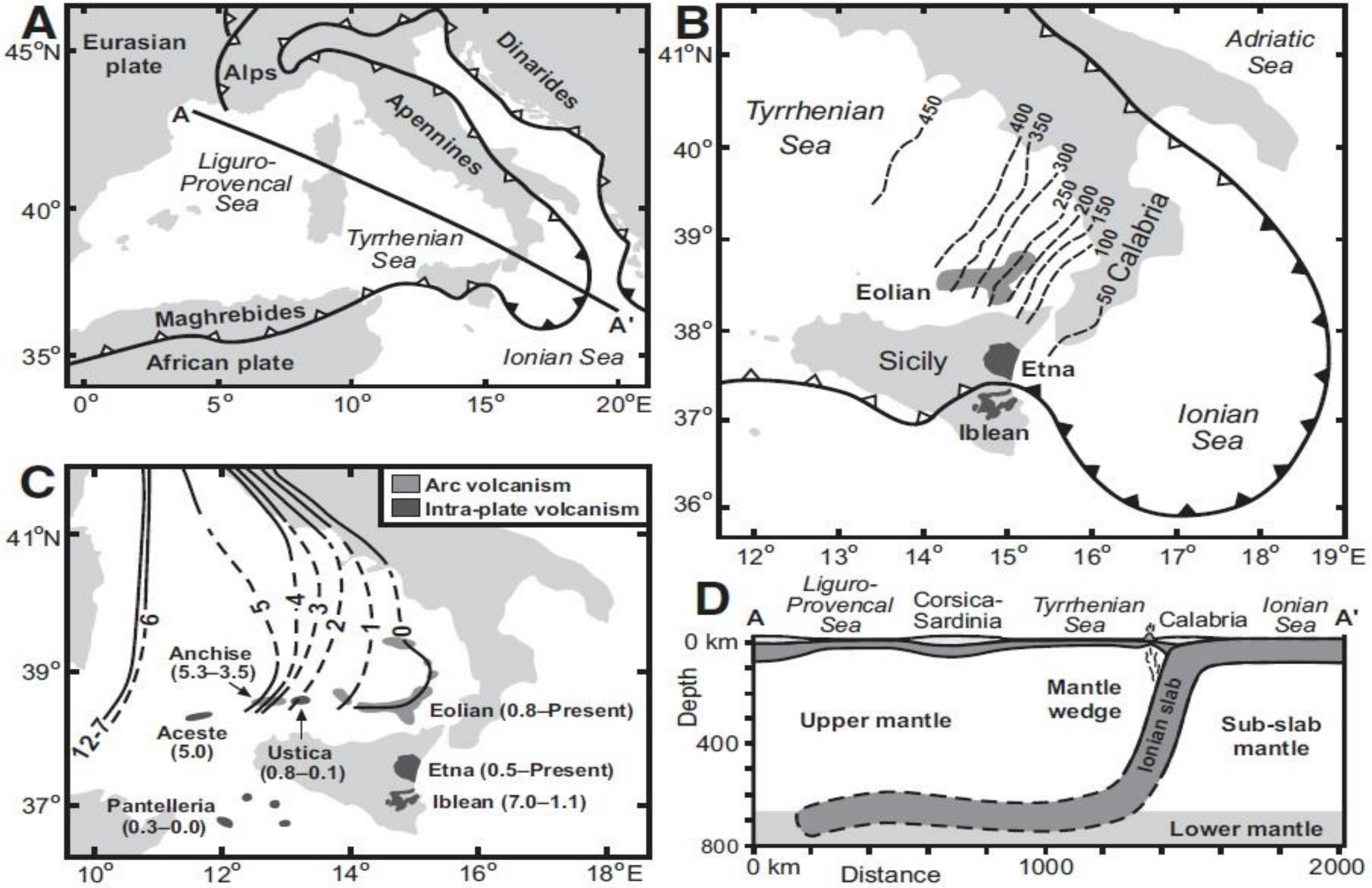

Schellart, 2010, GSA

- Reconstruction of the southern Apennines suggests a Late Miocene subduction rate of ~30–50 mm/year or perhaps higher.
- In Pliocene time, the southern Apennine trench encountered the continental Adriatic lithosphere and subduction ended by Quaternary time.
- Then, there was a rapid termination of subduction in the latter stages of continental margin subduction, which can be ascribed to slab break-off (e.g., slab delamination, slab tearing).
- The subduction remained limited to a narrow area (Ionian slab), whose east-directed fast rollback caused the opening of the Tyrrhenian and migration of magmatic arc with progressive time.

Slab subduction and back-arc basin in the Tyrrhenian domain

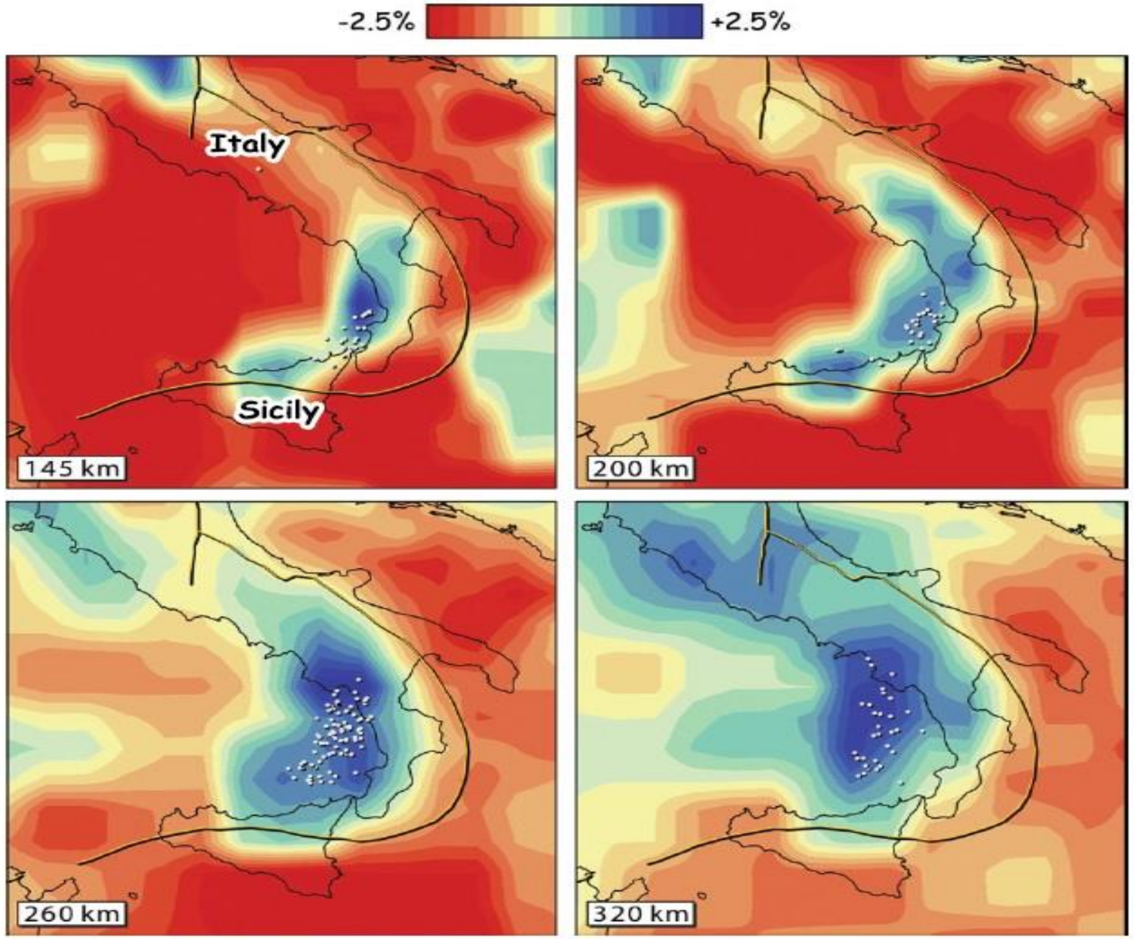

Bijwaard and Spakman, 2000, JGR

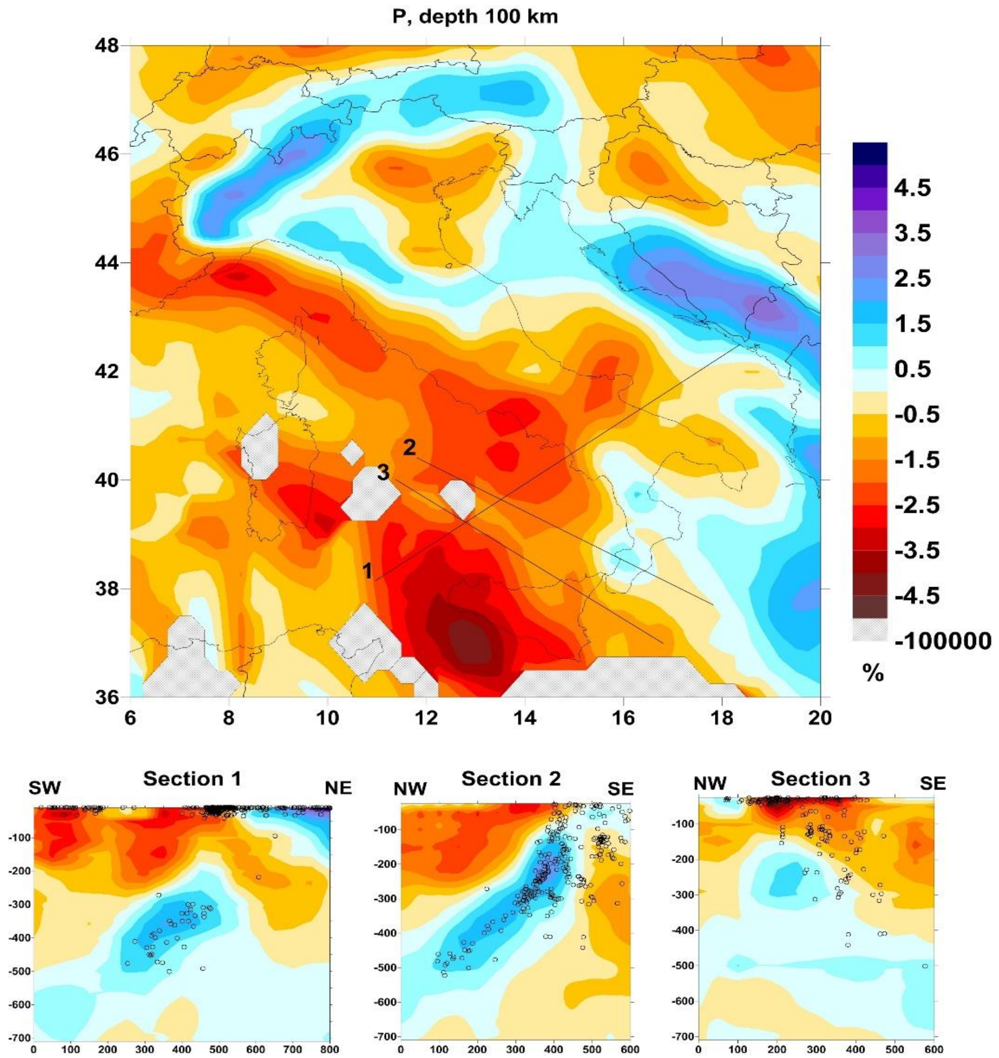

Koulakov et al., 2009, GJI

- The seismic velocity distribution shows evidence for the absence of high velocity slab material, and hence for slab detachment, below the north African margin and the central Apennines in the ~100–300 km depth range.

Slab Geometry in 3D

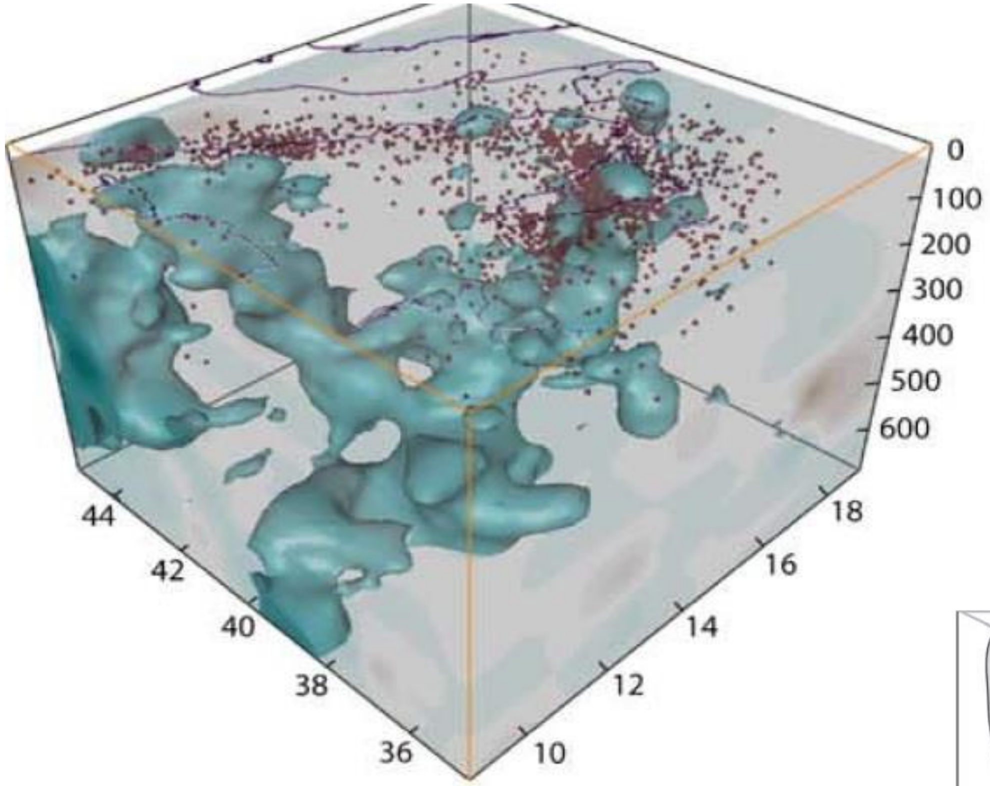

- Seismic tomography results show gaps within the subducting lithosphere, which are interpreted as deep subvertical tear faults.
- The development of such tear faults is consistent with proposed kinematic reconstructions, in which different rates of subduction rollback affected different parts of the subduction zone.
- There is a possible link between the development of tear faults and the occurrence of regional magmatic activity with transitional geochemical signatures between arc type and intraplate oceanic island basalts (OIB) type, associated with slab tearing and slab breakoff.

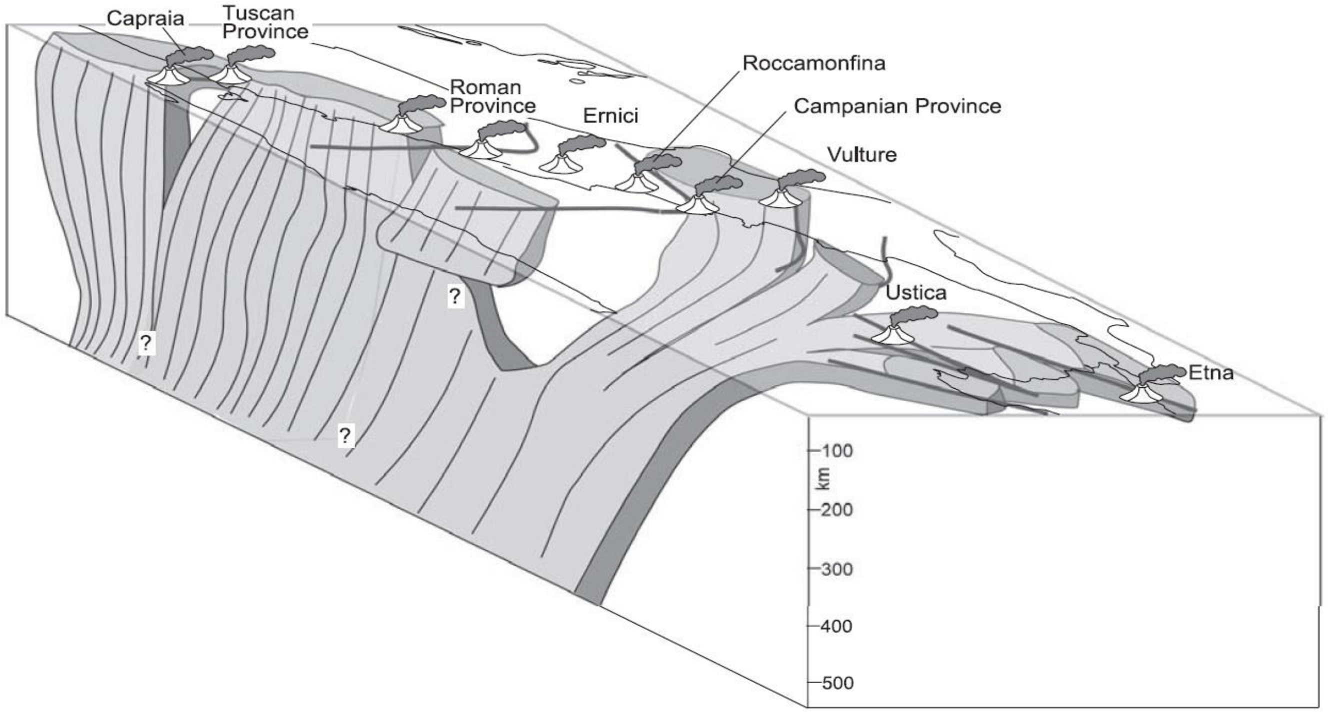

Rosenbaum et al., 2008, Tectonics, 27

Slab geometry interpretation: formation of a Subduction-Transform-Edge-Propagator (STEP) fault

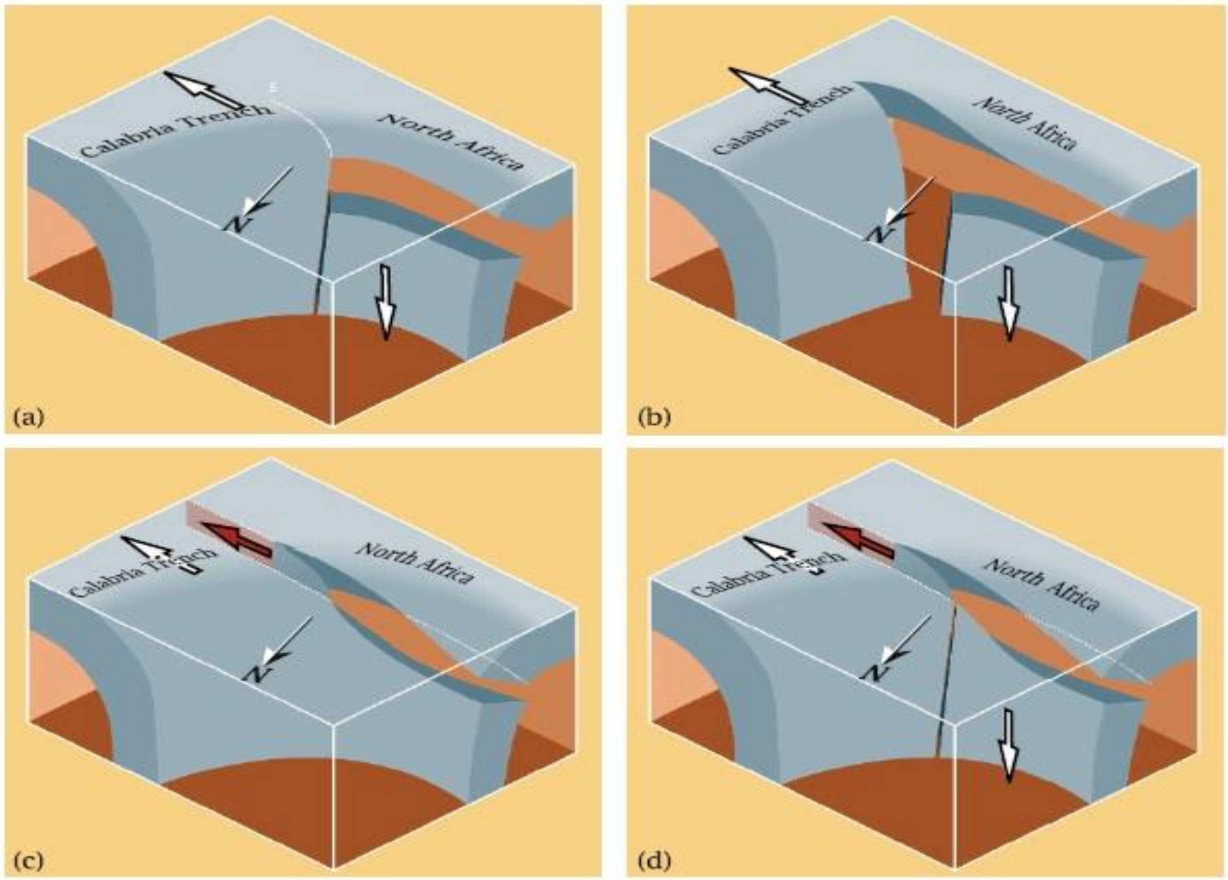

Wortel et al., 2009

Plate boundary evolved through:
(1) Continental collision ("soft", in the north African case); (2) Slab detachment; (3) Formation of a vertical tear, which laterally separates the detached part of the slab from the adjacent still continuous part of the subducted slab; (4) Formation of a STEP fault and retreat of the continuous segment of the slab; (5) Back-arc extension.

- The STEP is formed by the action of the slab pull acting on the continuous slab, around the edge of which the mantle material flows and accommodates the roll back.
- Another possibility for the STEP formation is the rotation of the detachment fault in the subducted slab towards an approximately vertical orientation (case c-d)

Kinematics of the Tyrrhenian

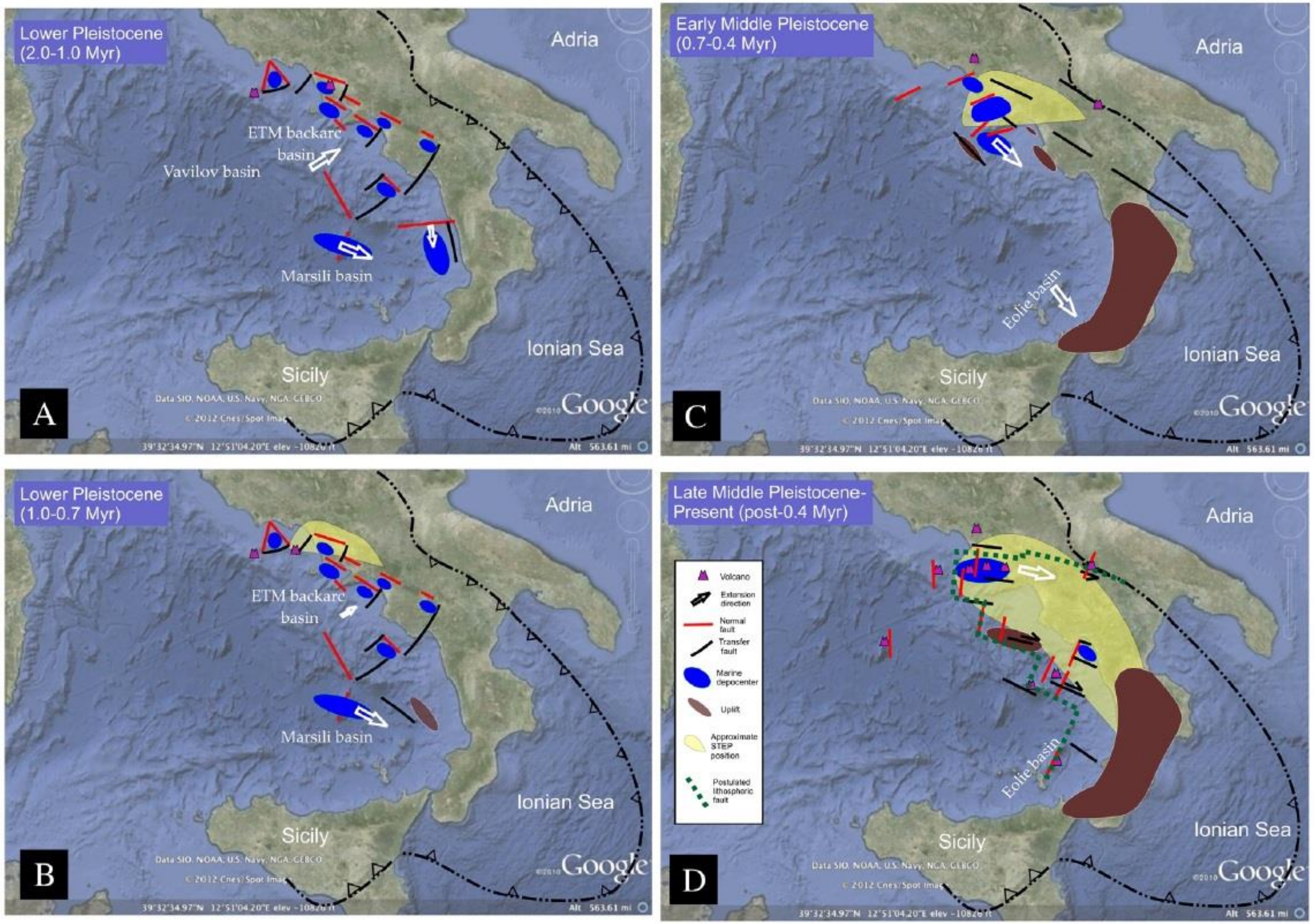

Milia et al., 2017, Tectonophysics, 710-711

- During the Lower Pleistocene (2.0–1.0 Myr) extensional tectonics affected the entire Eastern Tyrrhenian Margin (ETM) and the western flank of the Apennines, creating several basins: three contemporaneous extension directions (NE–SW in the Campania margin, NW–SE in the Marsili basin and N–S in the Calabrian Margin) .
- In the late Lower Pleistocene (1.0–0.7 Myr), extensional faults continued their activity in the Campania Margin, Marsili basin, and western flank of the Apennines, with a higher speed of the Marsili basin opening compared to that of the ETM.
- In the Early Middle Pleistocene (0.7–0.4-Myr) an abrupt change of direction of extension (from NE-SW to NW-SE) in the ETM occurred, accompanied by uplift of Calabria and volcanic activity (tearing propagation).
- In the Late Middle Pleistocene to Present (>0.4 Myr) extensional basins (Southern Gaeta Bay, Campana Plain-Campi Flegrei and Sapri basins) formed, with intense volcanism and eastwards migration of the extension was recorded. NNE-trending normal faults developed in the ETM and Apennines.

Upper plate and slab features developed during the evolution of the STEP fault

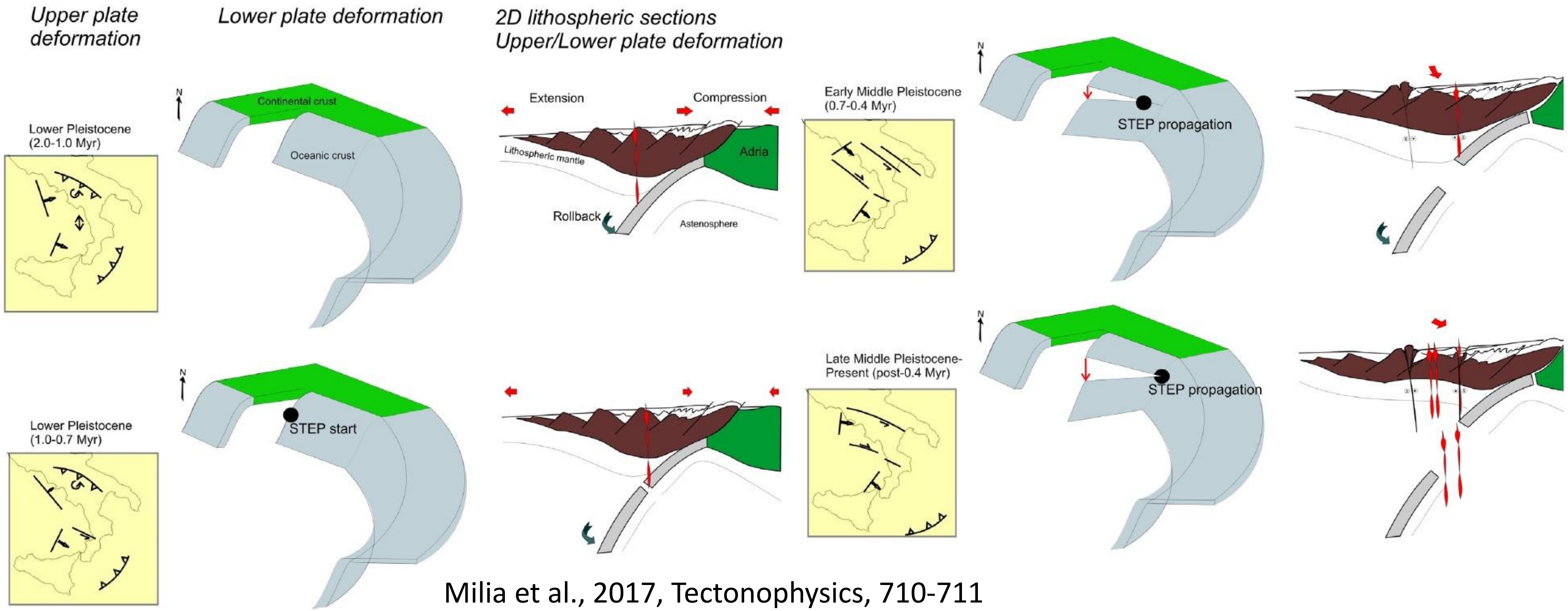

Milia et al., 2017, Tectonophysics, 710-711

- During the Lower Pleistocene (2.0–1.0 Myr) the upper plate extension is directed perpendicular to the Apenninic trench (ENE) contemporaneously, in the southern part, the extension is directed perpendicular to the Ionian trench (SE). The difference in the extension orientation may reflect the different velocity in the rollback of the continental and oceanic slab sectors.
- Through the late Lower Pleistocene (1.0–0.7 Myr) the reduction in the extension value along the Campania Margin and the increase in the extension value of the Marsili basin, induce the formation of a transfer fault zone in the Calabria Margin (maybe as a response in the upper plate of the STEP fault nucleation and rollback of the slab).
- The Early Middle Pleistocene phase (0.7–0.4 Myr) there was (1) an abrupt change in the extension direction (from NE to SE), associated to the formation of rapidly evolving half graben localized in the Northern Campania Margin; (2) end of the NE-directed thrust propagation in the Apennines and rapid uplift of Calabria (due to the toroidal flow around the Ionian slab).
- The Late Middle Pleistocene-Present (post-0.4 Myr) period records a minor reorientation (E-SE) of the direction of extension in the ETM (enlargement of the gap effect of the continuum propagation of the STEP fault).

Dynamic topography induced by subduction: the Calabrian Arc

Elevation distribution of the marine terraces in northeastern Sicily and Calabria

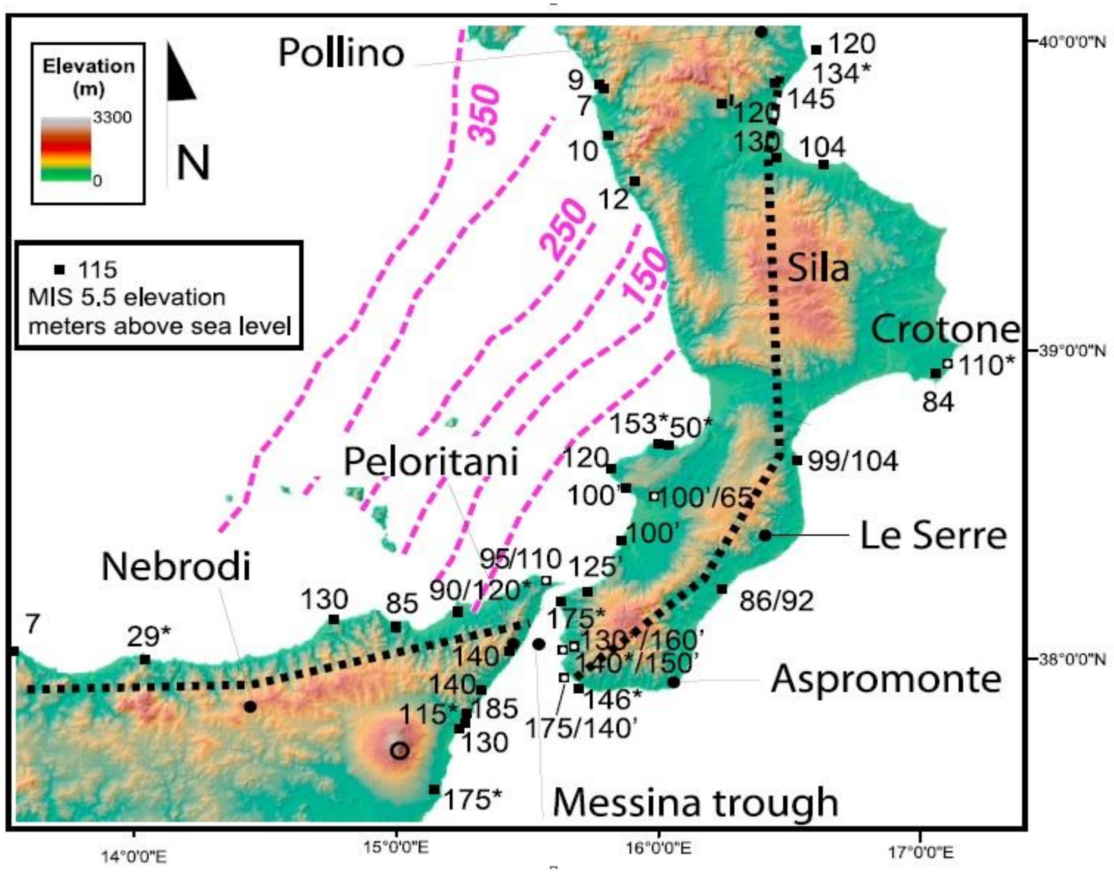

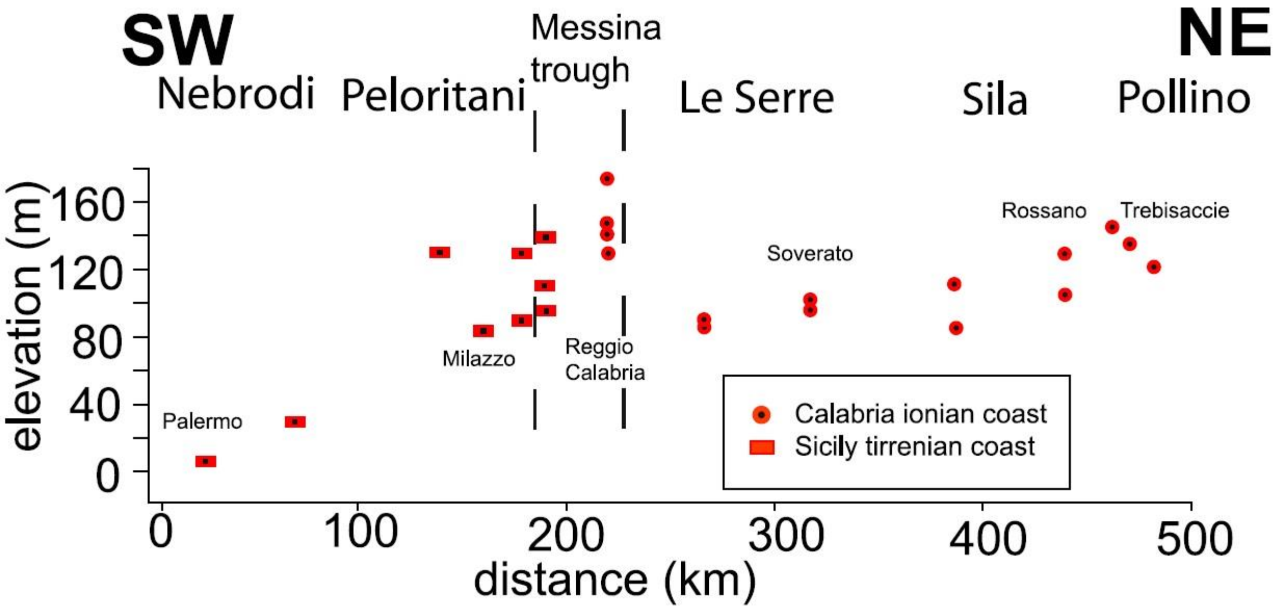

Faccenna et al., 2011, Tectonics, 30

- The Calabrian subducting slab presently consists of an approximately 200 km wide and ~600 km deep Wadati-Benioff zone dipping toward the northwest at about 70°.
- Minimum values of uplift correspond to the active portion of the slab, whereas maximum values of uplift correspond to the Messina region.

Dynamic topography induced by subduction: the Calabrian Arc

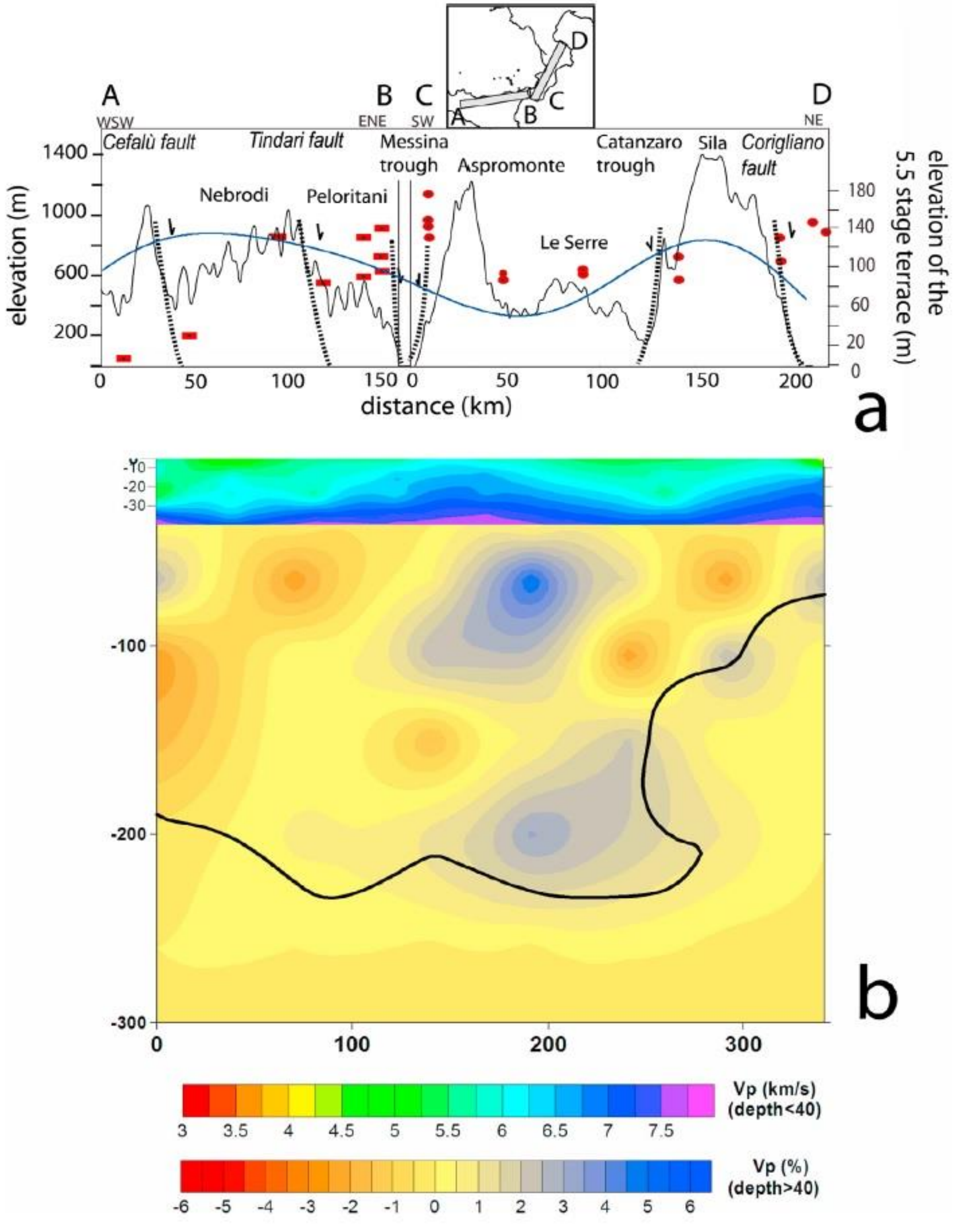

Faccenna et al., 2011, Tectonics, 30

- The topography of the Calabrian Arc is dominated by the superposition of short-wavelength features, related to local faulting and regional-scale (≥100 km) wavelength features.
- Long-wavelength topography shows two maxima corresponding to the Nebrodi Mts. and the Sila-Pollino massif, which bound a relatively depressed region, corresponding to the area overlying the active Wadati-Benioff zone.
- Trench rollback is generally associated with topographic sinking of the upper plate, as retrograde slab motion pulls the upper plate down.
- Detachment or breaking of subducting slabs are efficient sources of rapid upper plate uplift, which would be related to the lithospheric response to unloading.
- The average differential elevation between the two flanking bulges and the central depressed region ranges between about 500 and 800 m.
- The uplift rate deduced from terraces elevation is of the order of 0.8–1 mm/yr and the onset of uplift is in the lower Pleistocene. The uplift is increased by about 30% to the north and southwest of Le Serre, at least during the last 125 kyr.
- Mount Etna volcanism is positioned on top of a highly uplifted and still uplifting region indicating, together with Etna's volcanism itself, upwelling on the slab's edge.

Dynamic topography induced by subduction: the Calabrian Arc

Instantaneous mantle flow generated by the subduction of an isolated slab adapted to the case of Calabria

P-wave velocities at a depth of 150 km

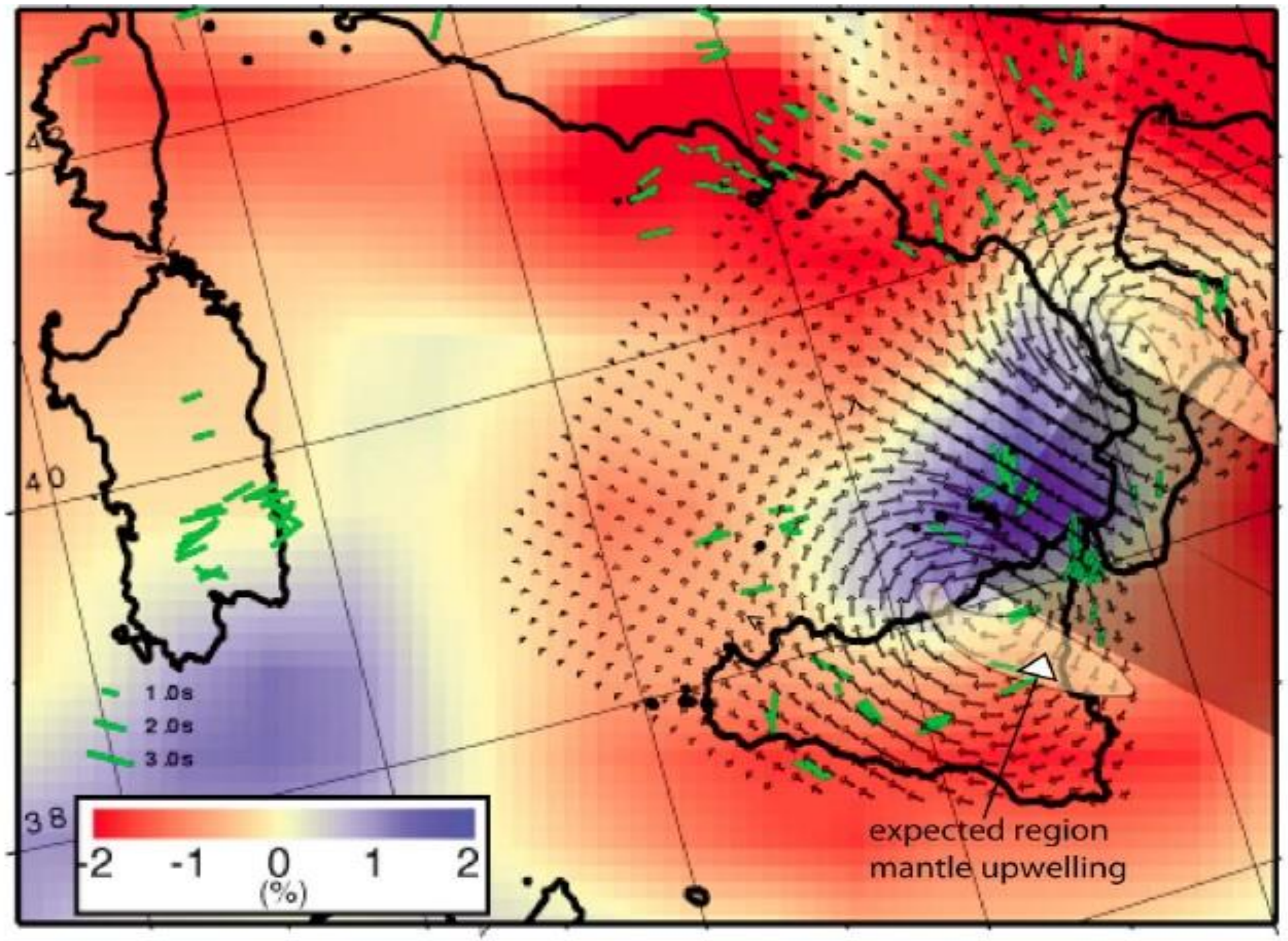

Faccenna et al., 2011, Tectonics, 30

In green are shown the results from SKS splitting data

Different models have been proposed to explain uplift and deformation process in Calabria, among the others:

(1) Unloading due to slab break off.

(2) Dynamic topography related to circulation around a narrow, retreating, subducting slab.

- Rebound after unloading due to slab brak-off could have indeed produced uplift of the upper plate. However, slab mantle viscous coupling is expected to produce subsidence rather then uplift during the fall of the detached portion of the slab.
- The deformation history of Calabria and the Etna's volcanism could have been originated dynamically by the action of a complex 3D mantle flow around the slab edge.

Toroidal flow around the Ionian slab caused by slab retreatment

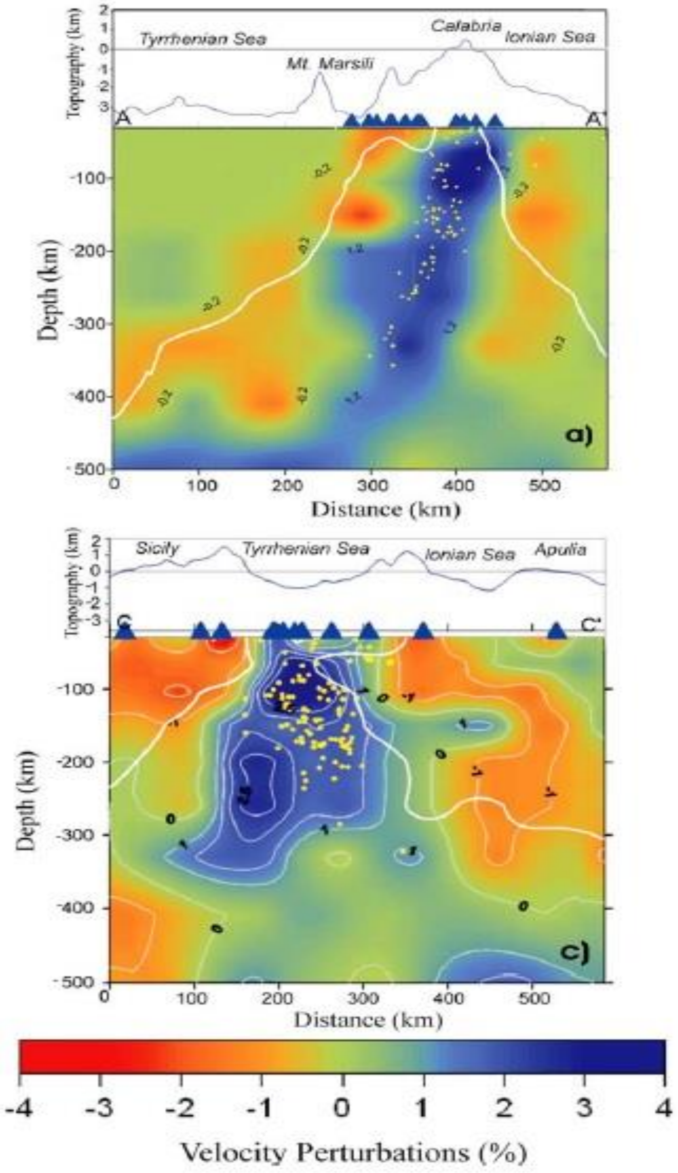

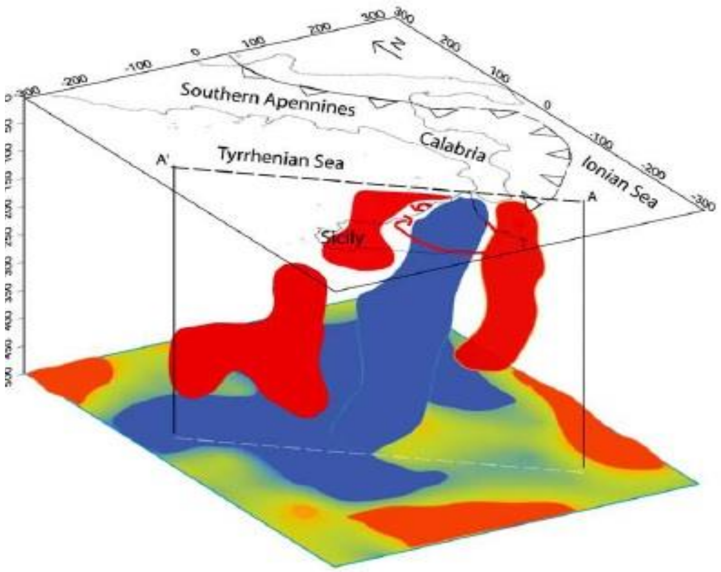

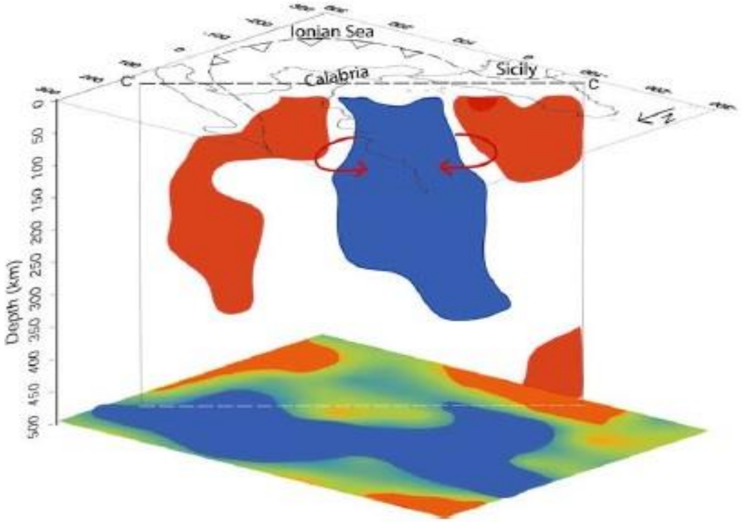

- Toroidal motion is mostly enhanced during retrograde slab motion, or by its steepening as mantle material beneath the slab is displaced toward its front, flowing laterally around the edges and producing two symmetrical vortex-like structures.
- This induces a (1) pronounced upper mantle upwelling at the slab edges, resulting from the continuous interplay between poloidal and toroidal fluxes, and (2) uplift of the overriding plate and also volcanism induced by decompression melting.

Montuori et al., 2007, JGR, 112

From stretching to mantle exhumation: the Vavilov backarc basin

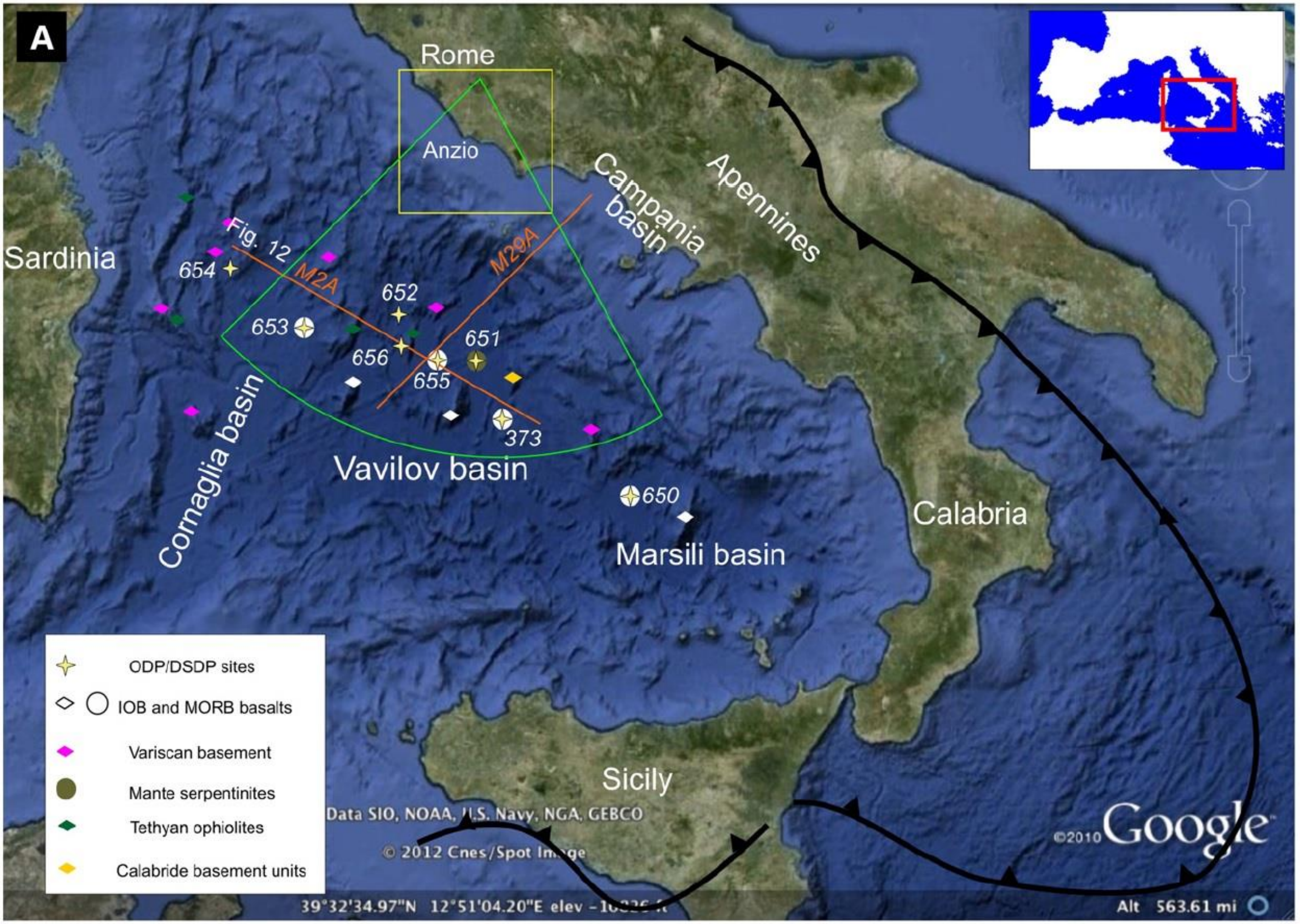

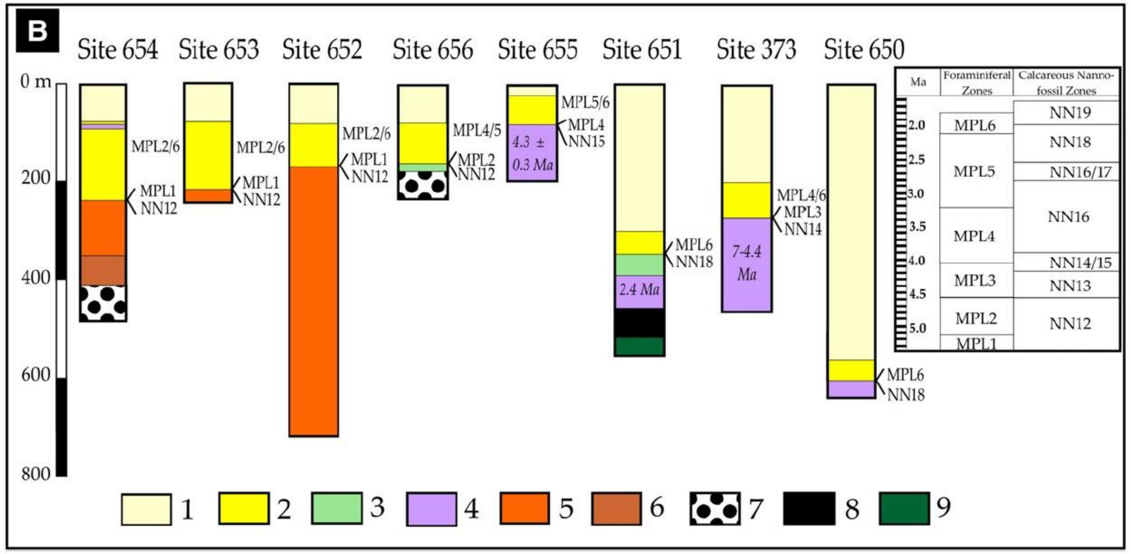

Stratigraphic logs of the DSDP and ODP sites. 1) Pleistocene deposits; 2) Pliocene deposits; 3) dolostones; 4) basalts; 5) Messinian deposits; 6) Tortonian deposits; 7) conglomerates; 8) breccias; 9) serpentinized peridotites.

Milia et al., 2017, Tectonophysics, 710-711

The Tyrrhenian Basin can be divided into northern and southern sectors:

- The northern Tyrrhenian Sea started to form in the lower Miocene as a polyphase rift, displaying a trend of faults convergent toward the North and is characterized by a relatively low value of stretching (crustal thickness between 25 and 20 km).
- The Southern Tyrrhenian Sea is a middle Miocene–Quaternary polyphase rift with several fault trends, which includes the Vavilov basin and is characterized by thin crust (from 15 to 10 km) and lithosphere (~30 km), high heat flow values (> 100 mWm^{-2}) and a large positive Bouger gravity anomaly.

From stretching to mantle exhumation: the Vavilov backarc basin

Structural map of the Latium margin and thickness map of Pliocene-Quaternary deposits

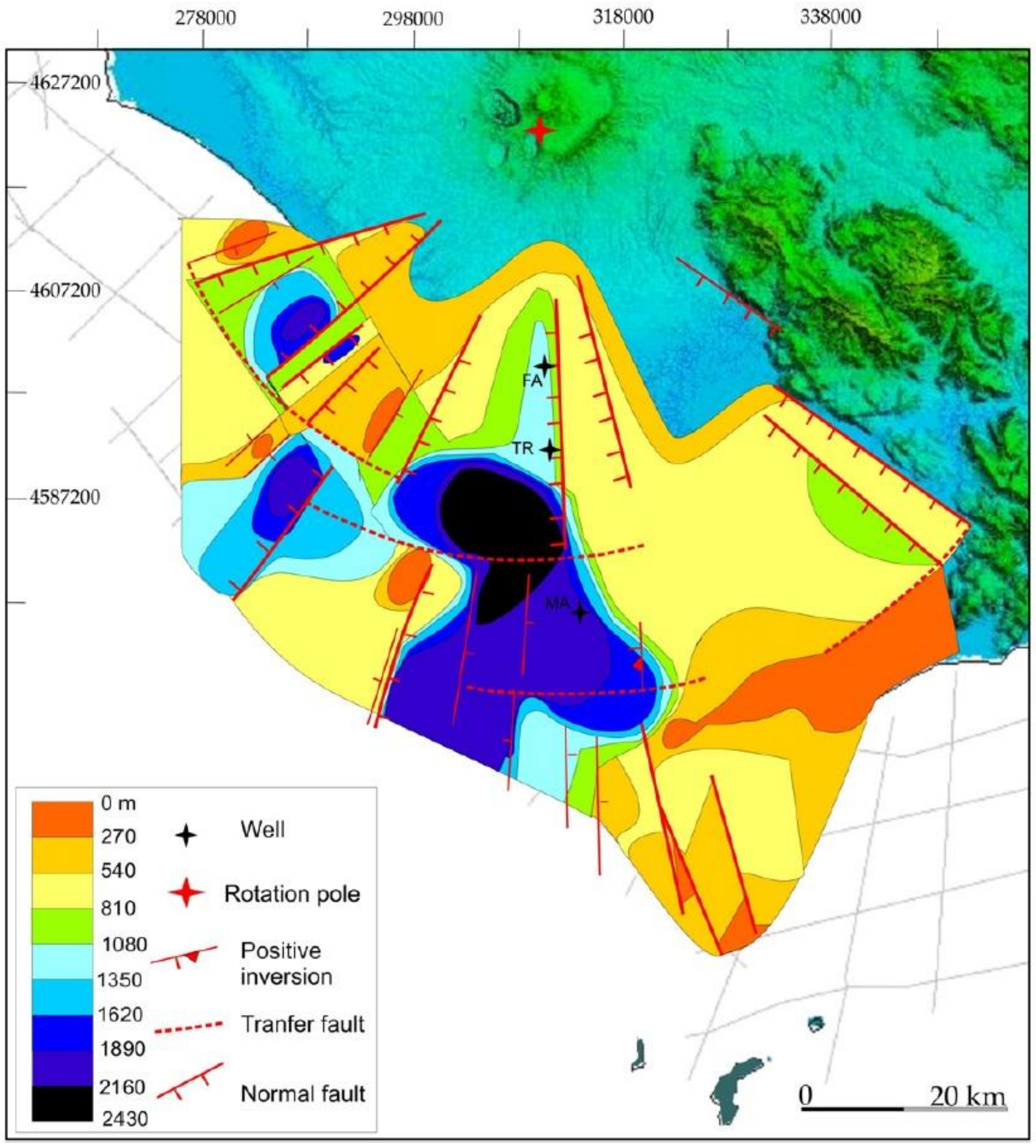

- Three main depocentres: a western basin (~10 km-wide and up to 2000 m thick), a central basin (~20 km-wide and up to-2400 m thick), and an eastern basin (Pontina Plain, up to 1000 m thick).
- The normal faults trend from ENE-WSW to N-S to NW-SE and converge toward a rotation pole located in correspondence of Alban Hills volcano.
- Positive inversion structures indicate that some of the pre-existing faults are successively inverted.

Milia et al., 2017, Tectonophysics, 710-711

FA= Fiume Astura, MA= Martina, TC = Tre Cancelli. Thickness values are estimated merging well and seismic reflection data.

From stretching to mantle exhumation: the Vavilov backarc basin

Eastwards time migration of extension in the Vavilov basin.

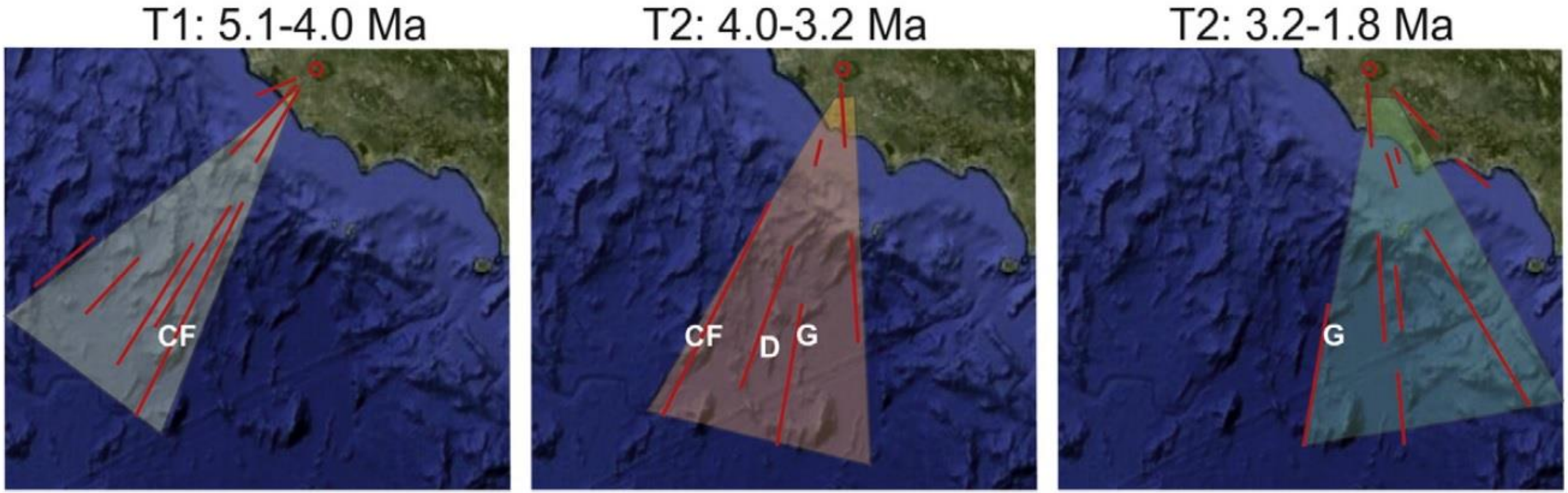

CF = Central Fault, D = De Marchi Seamount, G = Gortani Ridge

Milia et al., 2017, Tectonophysics, 710-711

- The Vavilov rift zone shows a converging pattern of normal faults bounding submarine ridges, from west to east.
- The convergent pattern of normal faults is coherent with a single Euler pole, located in Latium, during the entire basin history.

From stretching to mantle exhumation: the Vavilov backarc basin

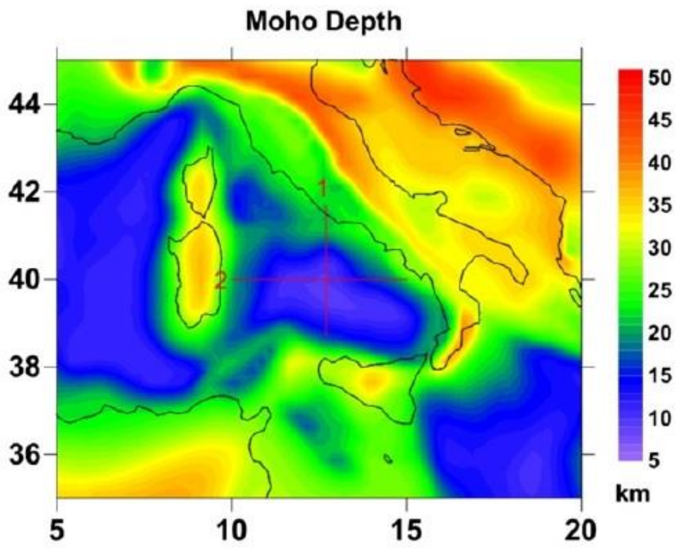

- In the apex region of the Vavilov basin the crust has a thickness of 20–25 km and two crustal layers with distinct seismic velocities typical of extended continental crust.
- The crust thins and decreases its average velocity toward the bathyal part of the basin quite abruptly (decrease: ~10 km and ~0.3 km/s over a horizontal distance of less than 100 km).
- In the bathyal region, the crust of the basin is quite homogeneous, being characterized by a uniform thickness of ~7 km and low seismic velocities (*Vp* ~6 km/s) comparable to strong serpentinized peridotite.

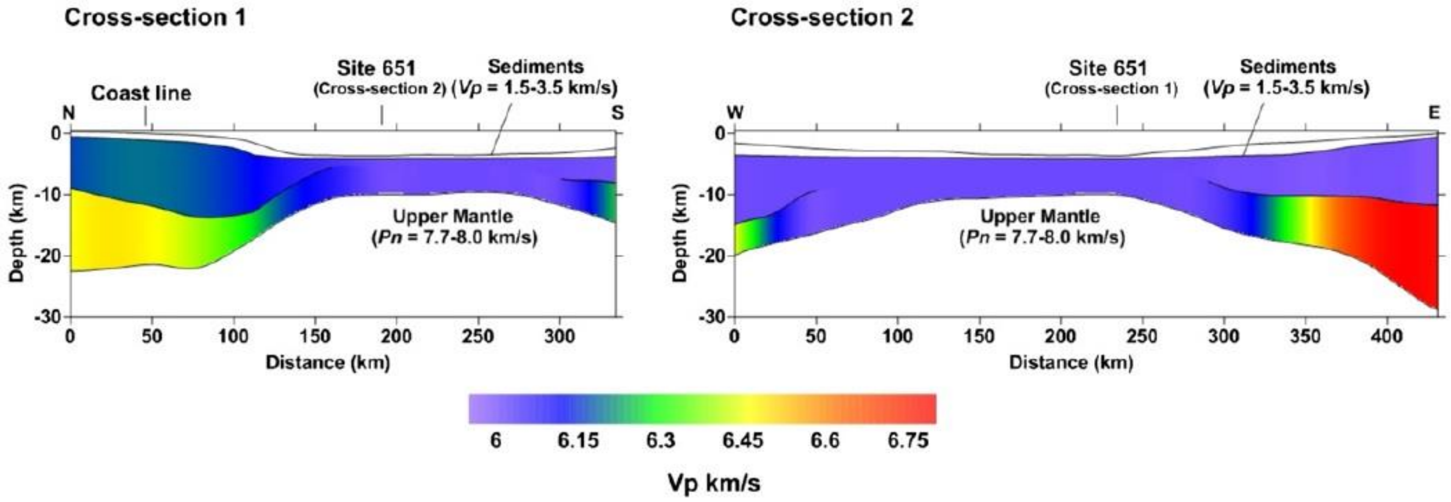

Milia et al., 2017, Tectonophysics, 710-711

Difference in the crustal thickness variations between the distal (smooth) and apex (sharp) region can be due to a change in the crustal strength during the rifting:

- The higher extension rate in the central part of the basin has caused larger *T* in this area than in the apex during the opening phase. Consequently, the crustal brittle-ductile transition has migrated at shallower depth in the bathyal region.

From stretching to mantle exhumation: the Vavilov backarc basin

Mantle rocks have been exhumed along a downward concave fault plane

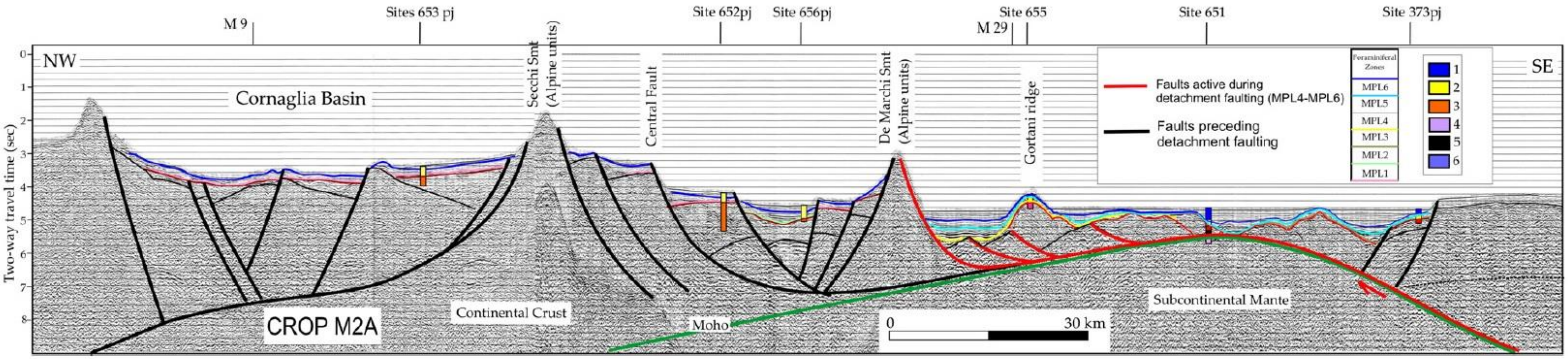

CROP seismic profile M2A and interpretation. 1) Pleistocene deposits; 2) Pliocene deposits; 3) Messinian deposits 4) basalts; 5) breccias; 6) serpentinized peridotites. For profile location see Fig. 1. See text for explanation.

Milia et al., 2017, Tectonophysics, 710-711

From stretching to mantle exhumation: the Vavilov backarc basin

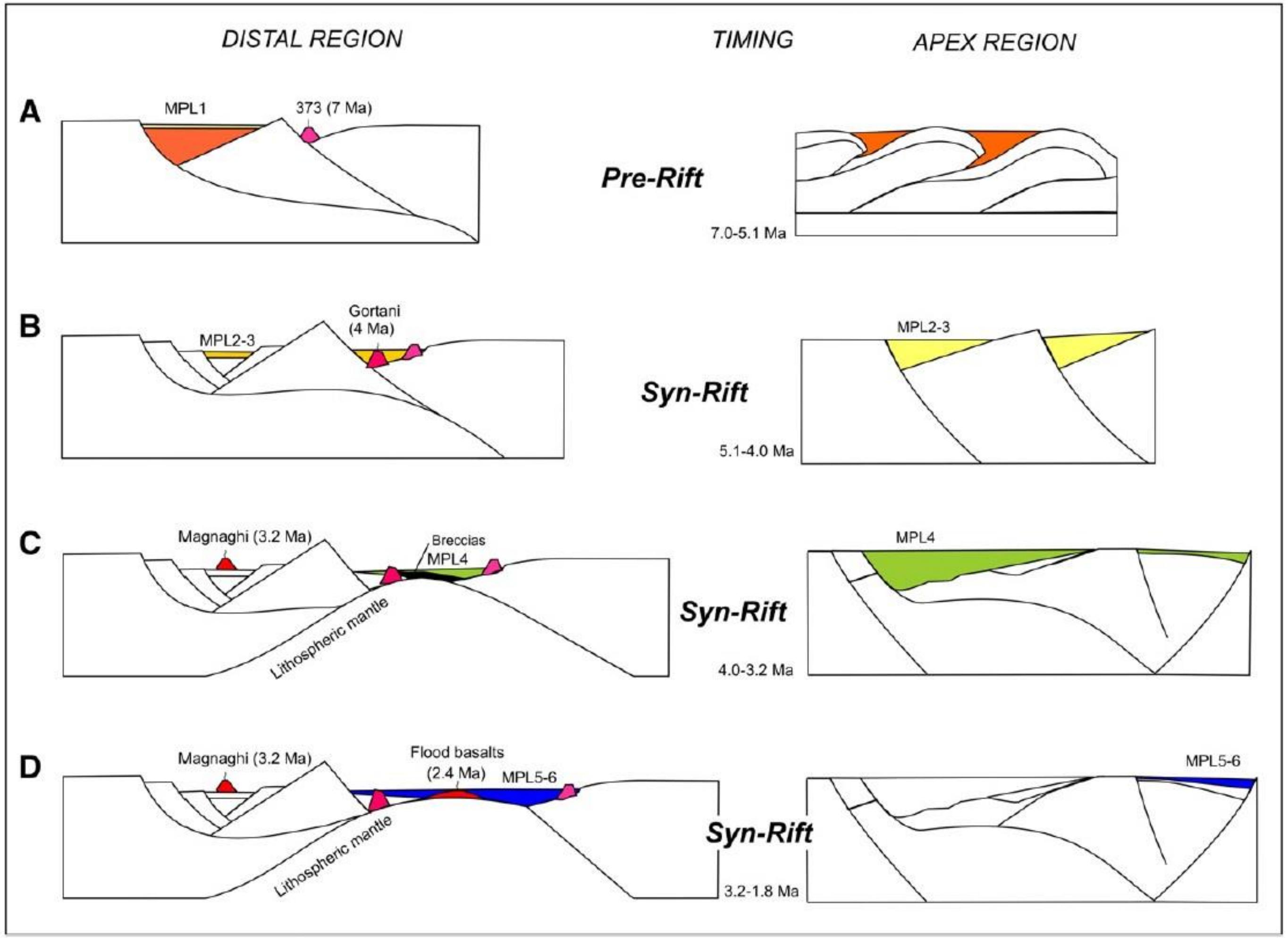

Downward concave fault geometry

Upward concave fault geometry

Milia et al., 2017, Tectonophysics, 710-711

The kinematics of the Vavilov region records the complete evolution of a rift from stretching to mantle exhumation:

- The age of the sedimentary infill documents that the Vavilov basin started to open in the Lower Pliocene (5.1–4.0 Myr) coherently from the apex to distal regions by a pure shear mode, characterized by distributed high-angle normal faulting and asymmetric/symmetric rift basins.
- Rifting lasted 5.1–4 Myr and after a detachment basin evolved from 4 to 1.8 Myr. The extension switched during the upper Pliocene to a simple shear mode, associated to detachment faults.
- A supradetachement basin formed in the apex rift zone, which is characterized by strong subsidence and thick sub-horizontal deposits.
- In contrast, thin deposits are present in the distal zone, due to the increase of the distance from the sediment source area (Apennines).
- The final stage of opening of the Vavilov basin developed by a simple shear mode in the Upper Pliocene. The activity of detachments caused the maximum thinning and exhumation of serpentinized peridotites of the mantle in the distal zone and metamorphic basement rocks in the proximal one.

Gibraltar Arc

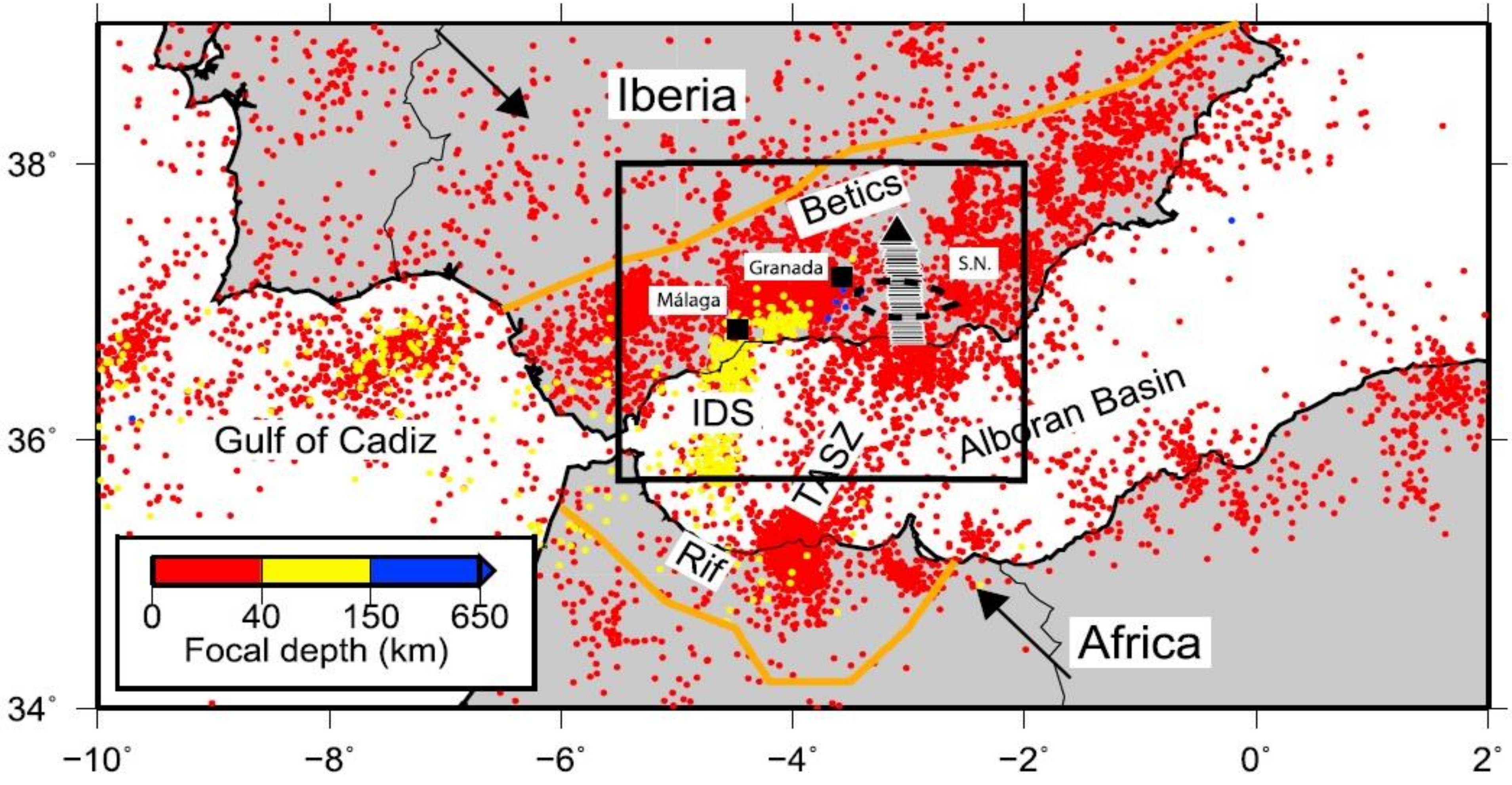

Heit et al., 2017 Geophys. Res. Lett., 44

Slab Subduction beneath Gibraltar Arc

S wave receiver functions (SRFs)

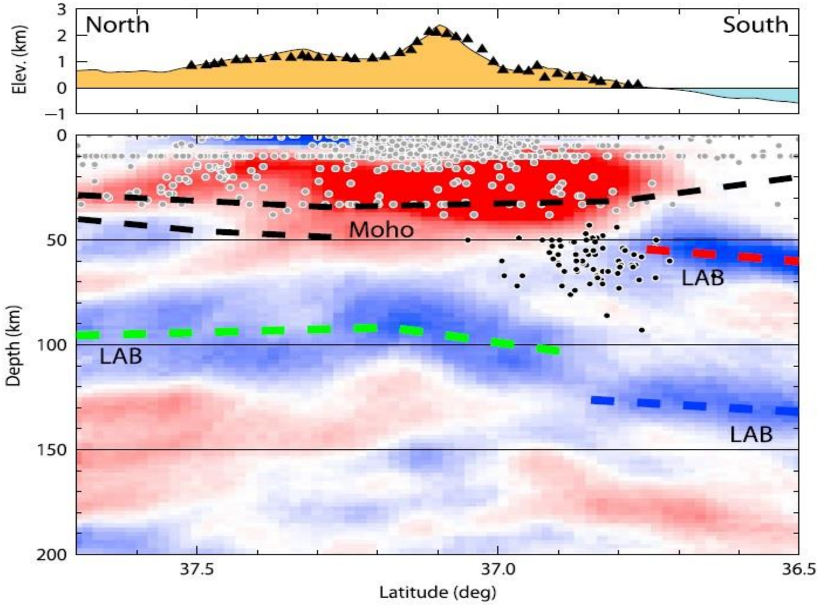

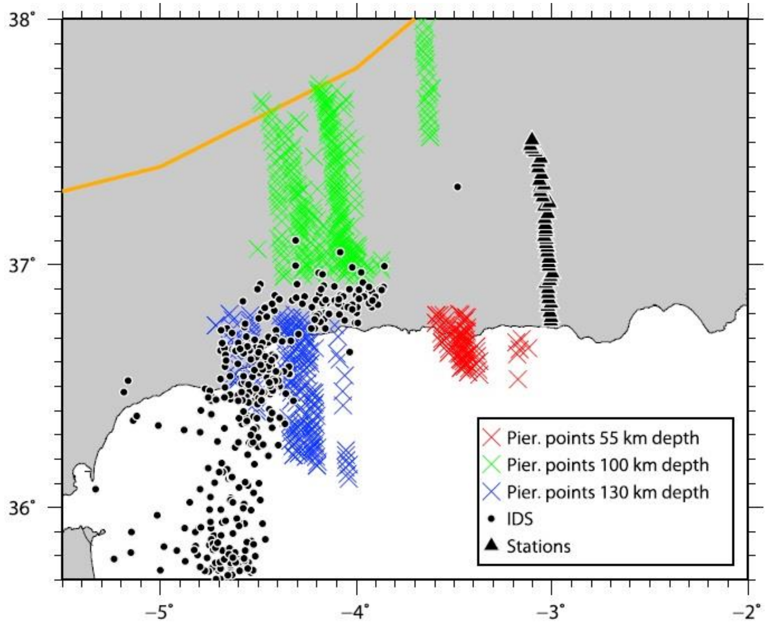

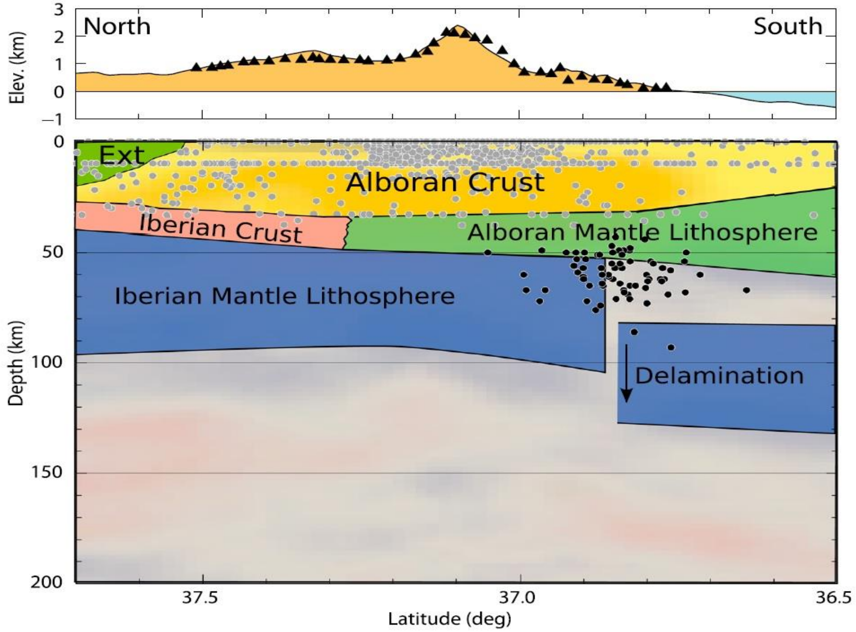

Heit et al., 2017 Geophys. Res. Lett., 44

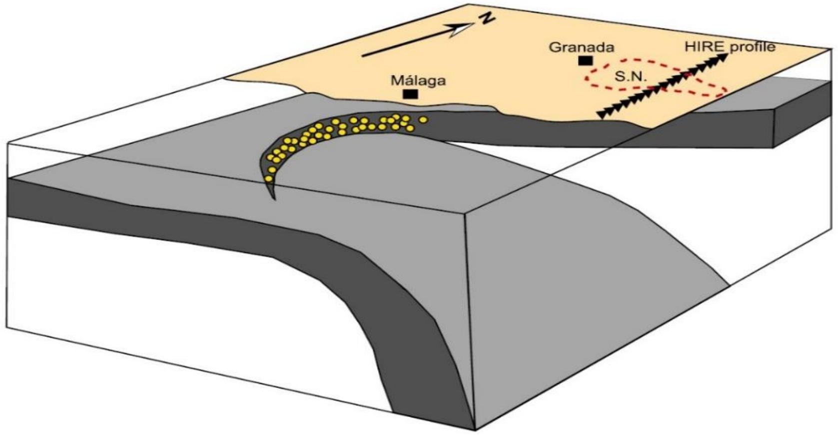

IDS: Intermidiate Depth Seismicity

- The rupture along the intermediate depth seismicity marks the onset of the lithospheric delamination, which is the result of slab pull and rollback.

Slab Subduction beneath Dinarides

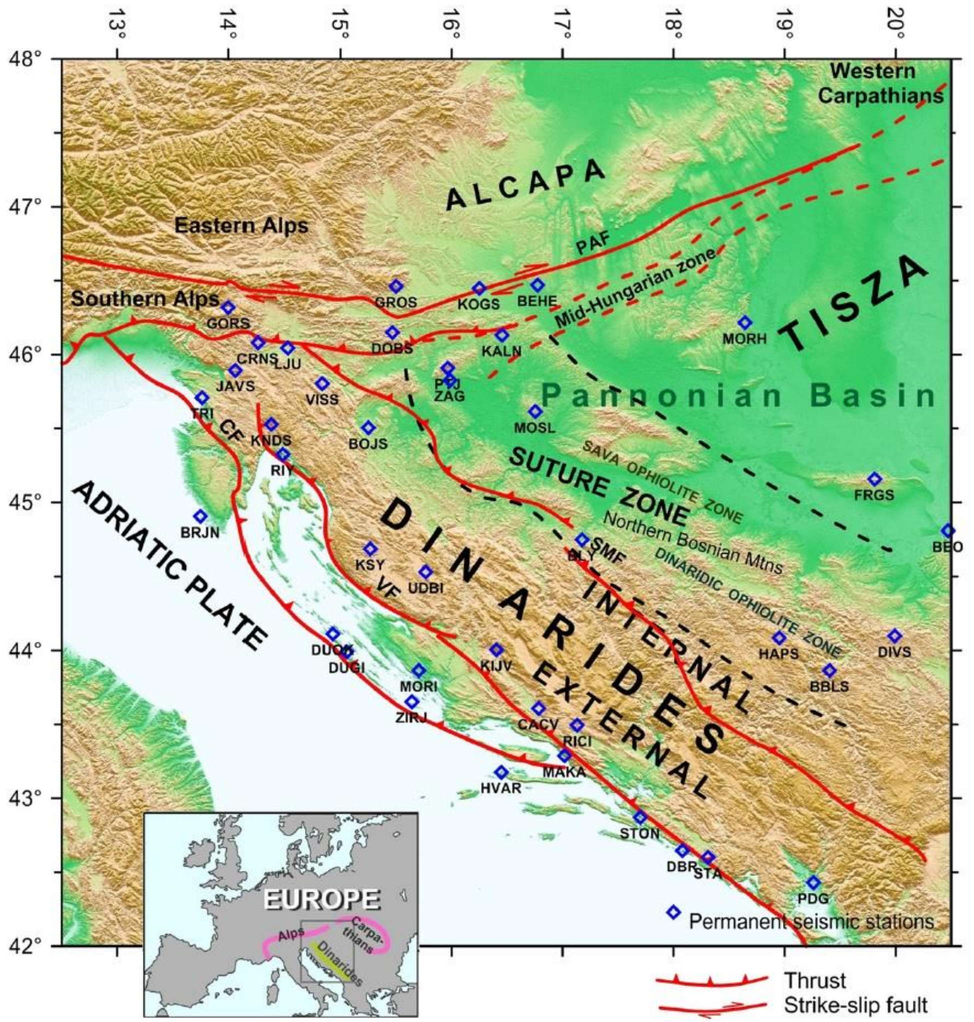

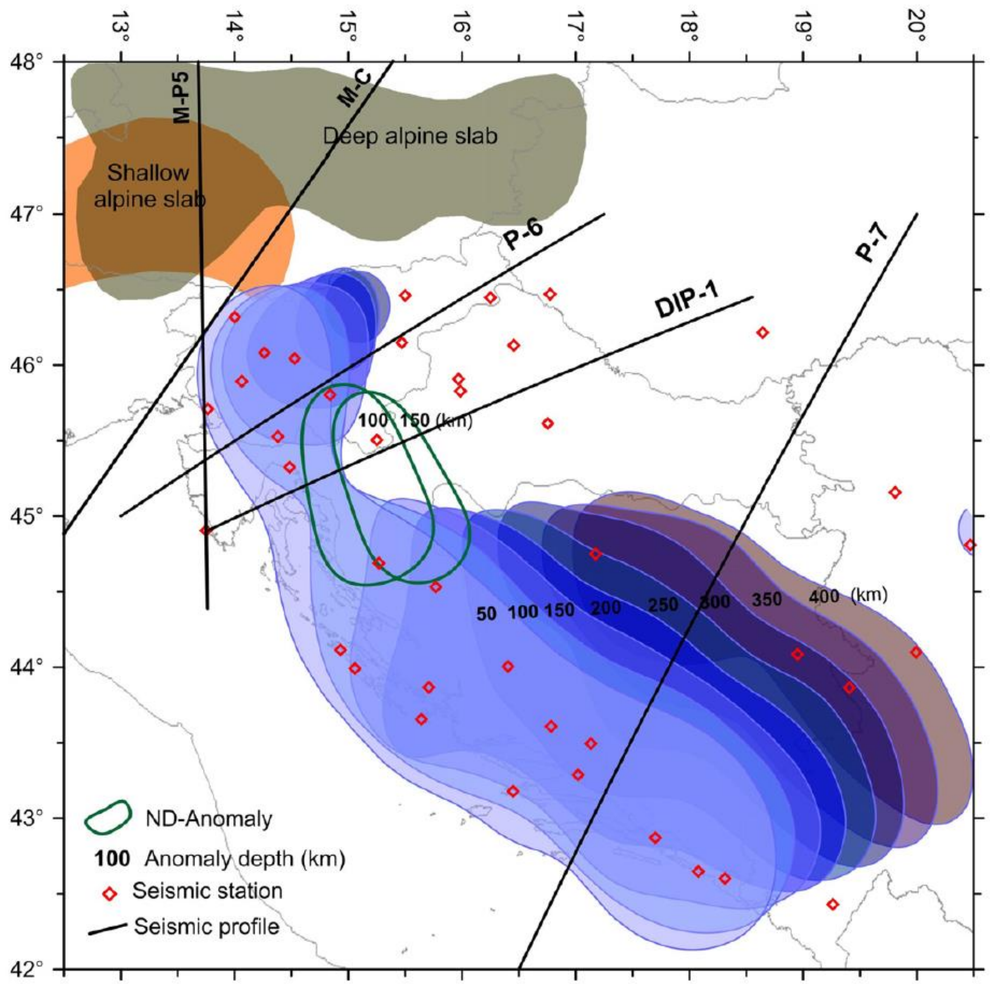

- The Dinarides are divided into External Dinarides spread along the Adriatic coast, and Internal Dinarides as narrow belt in the inland. This complex orogenic system formed because of the collision of the African and Eurasian plate.
- A fast velocity anomaly extending underneath the entire Dinarides mountain belt indicates cold, rigid materials.
- In the Northern Dinarides the anomaly, steeply sloping towards the northeast (due to the sinking of the Adria microplate underneath the Pannonian tectonic segment) extends to the depth of 250 km, whereas in the Southern Dinarides it reaches greater depths (up to 450 km).

Slab Subduction beneath Dinarides

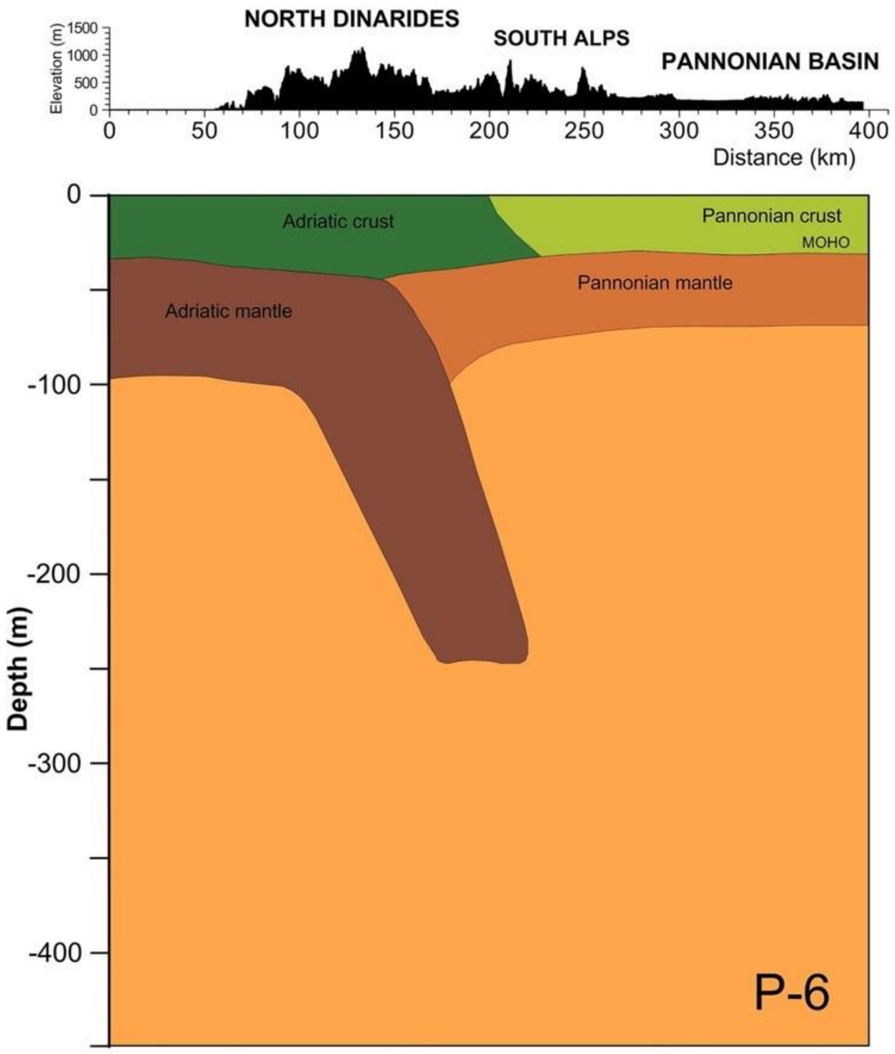

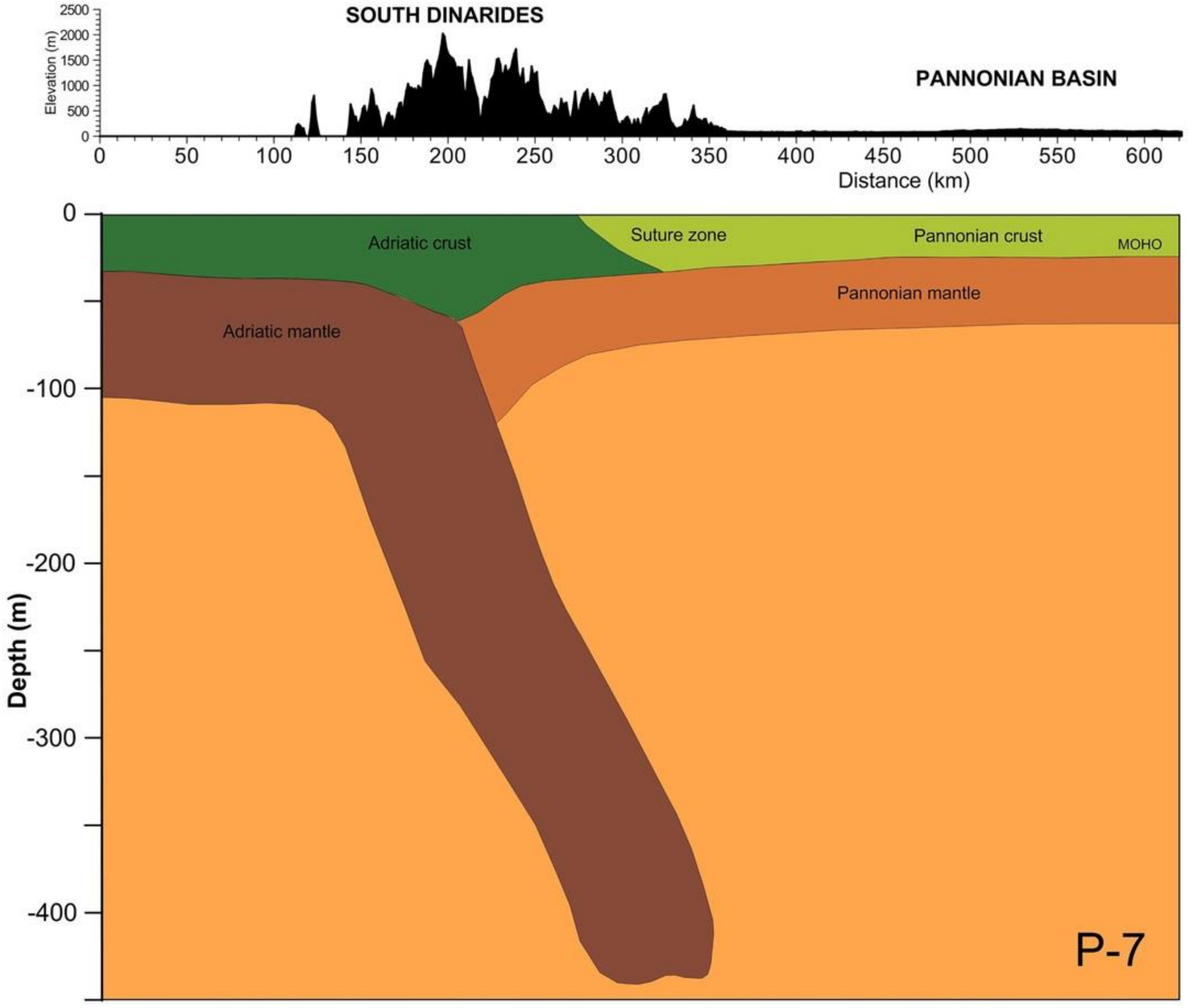

- Different slab depths are interpreted as the faster convergence of the plate in the southern Dinarides than in the northern, or the convergence of the plates had started in the southern part and systematically developed to the north.

The Alps-Carpathians-Pannonian Basin System: Vrancea Area (Romania)

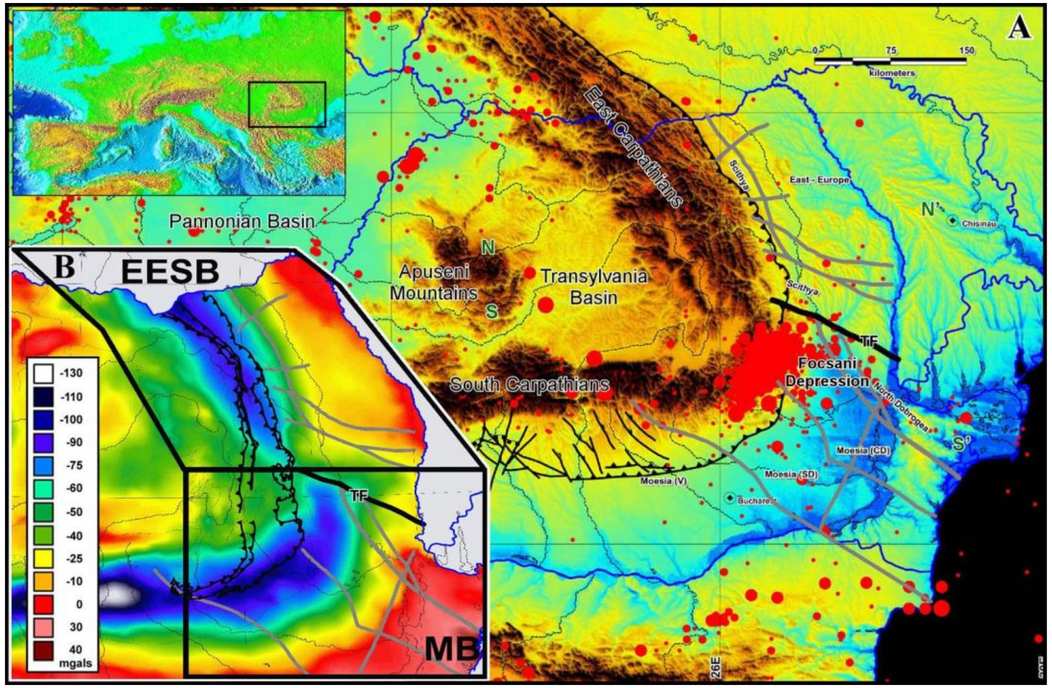

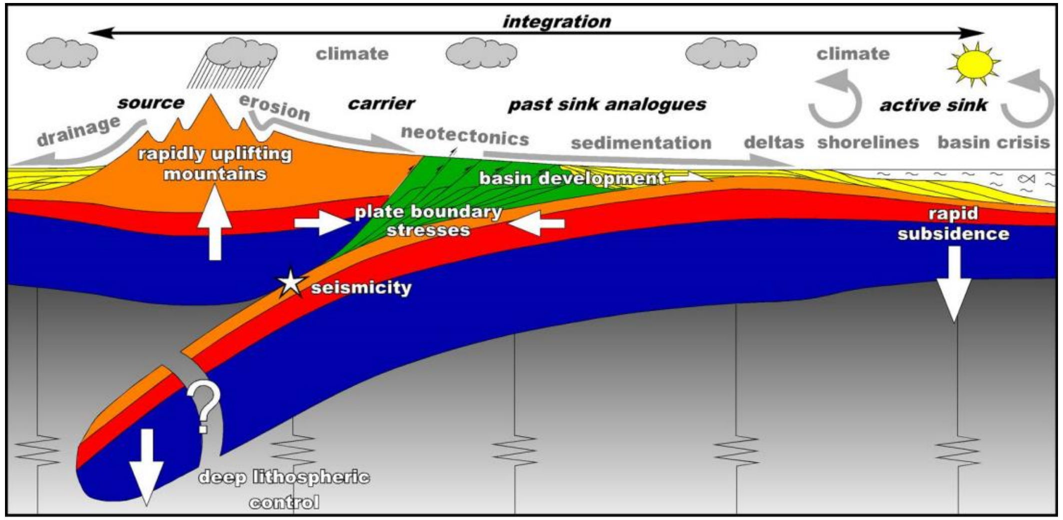

- The tectonic development of the Carpathian-Alpine system began in the Jurassic and is mostly controlled by the collision of three large continental plates: the Eurasian, African, and Arabian.
- The southeastern Carpathian Arc bend is located at the confluence of three main tectonic units (east European plate, Intra Alpine subplate and Moesian subplate) in the Vrancea region of Romania.
- The collision of this segment of the Alpine belt began in the Cenozoic as a result of the lateral eastward extrusion caused by the continuous convergence in the Alps.
- In the Vrancea region, an oceanic basin, floored by an oceanic crust, lays in the area of the present-day Carpathians which was consumed by subduction during Tertiary times.
- A complex active processes still take place beneath Vrancea in a very confined area, manifested in a cluster of intermediate seismicity beneath Vrancea in a narrow nearly vertical volume at depths below 60 km.

The Alps-Carpathians-Pannonian Basin System: Vrancea Area (Romania)

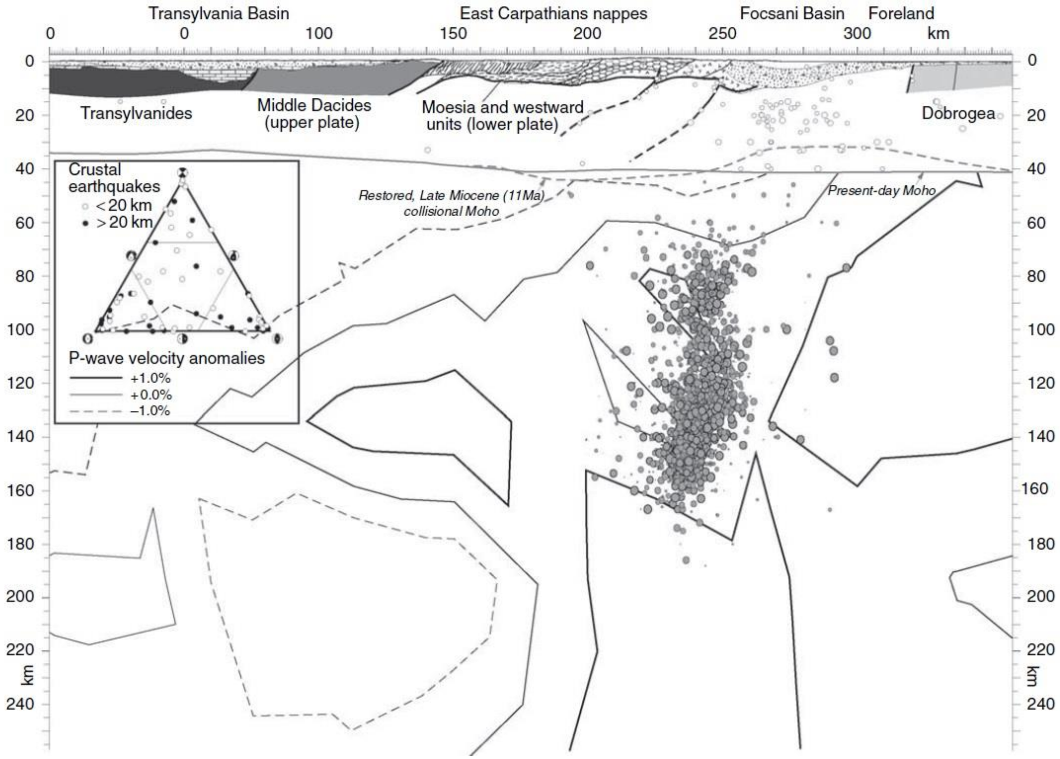

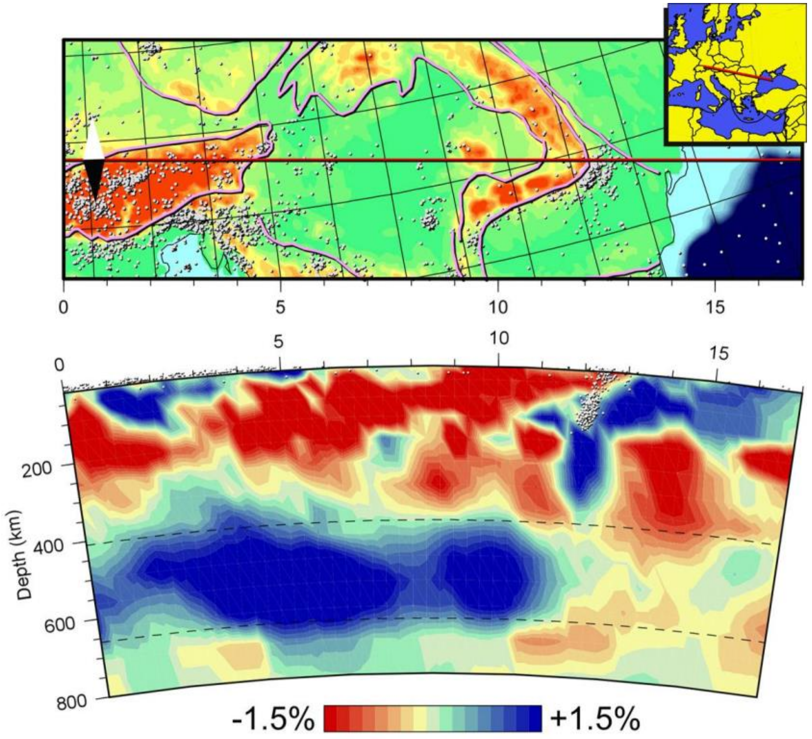

Bijwaard and Spakman, Geoph.J.Int, 2000

Wortel and Spakman, Science, 2000

The Alps-Carpathians-Pannonian Basin System: Vrancea Area (Romania)

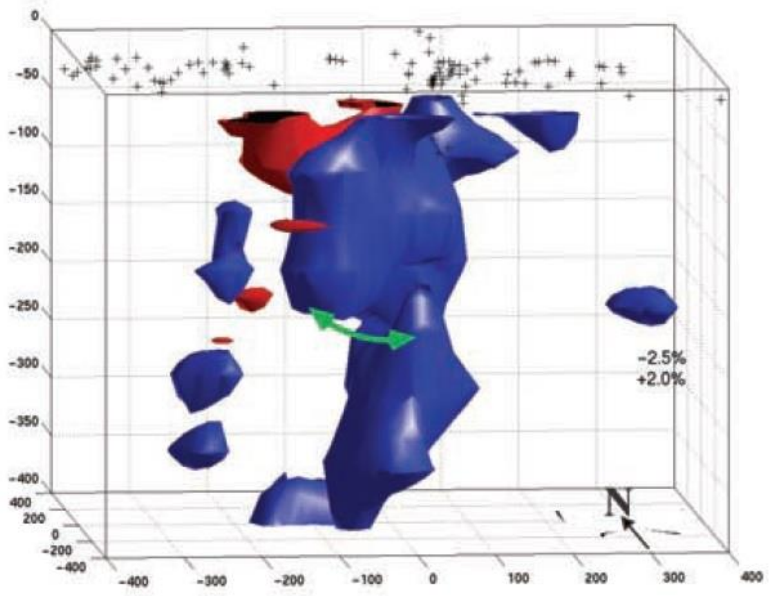

Martin et al., 2006, Geophys. J. Int., 164

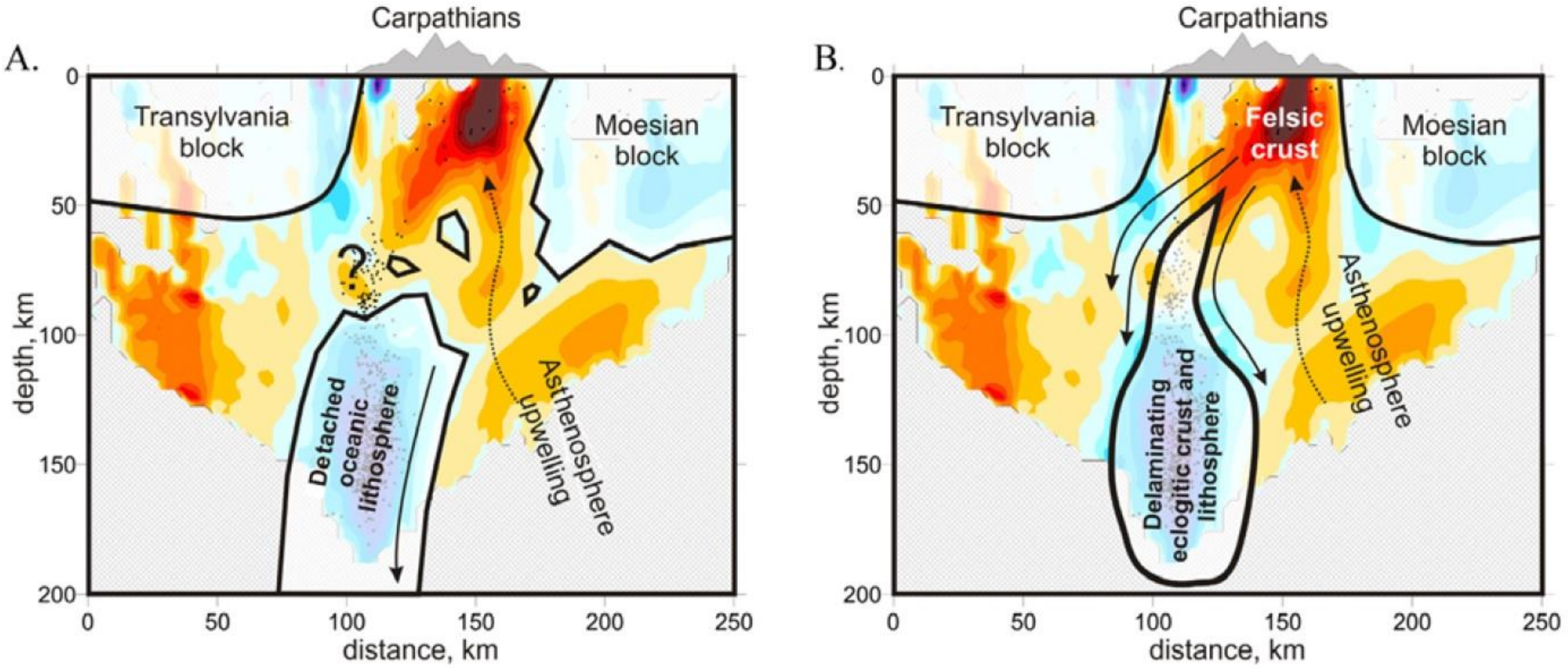

Koulakov et al., 2010, G3

- The tearing of the slab at 200 km depth accompanied by the rotation of the slab from NE–SW towards N–S orientation (green arrow)

- It is observed a falling ‘‘drop’’ consisting of eclogitic lower crust material, result of phase transition in the mafic layer due to the thickening of the crust, surrounded by untrained lithosphere material. This delamination occurs after a long stage of accumulation of denser eclogitic material in the bottom of the crust.

Eastern Mediterrenean

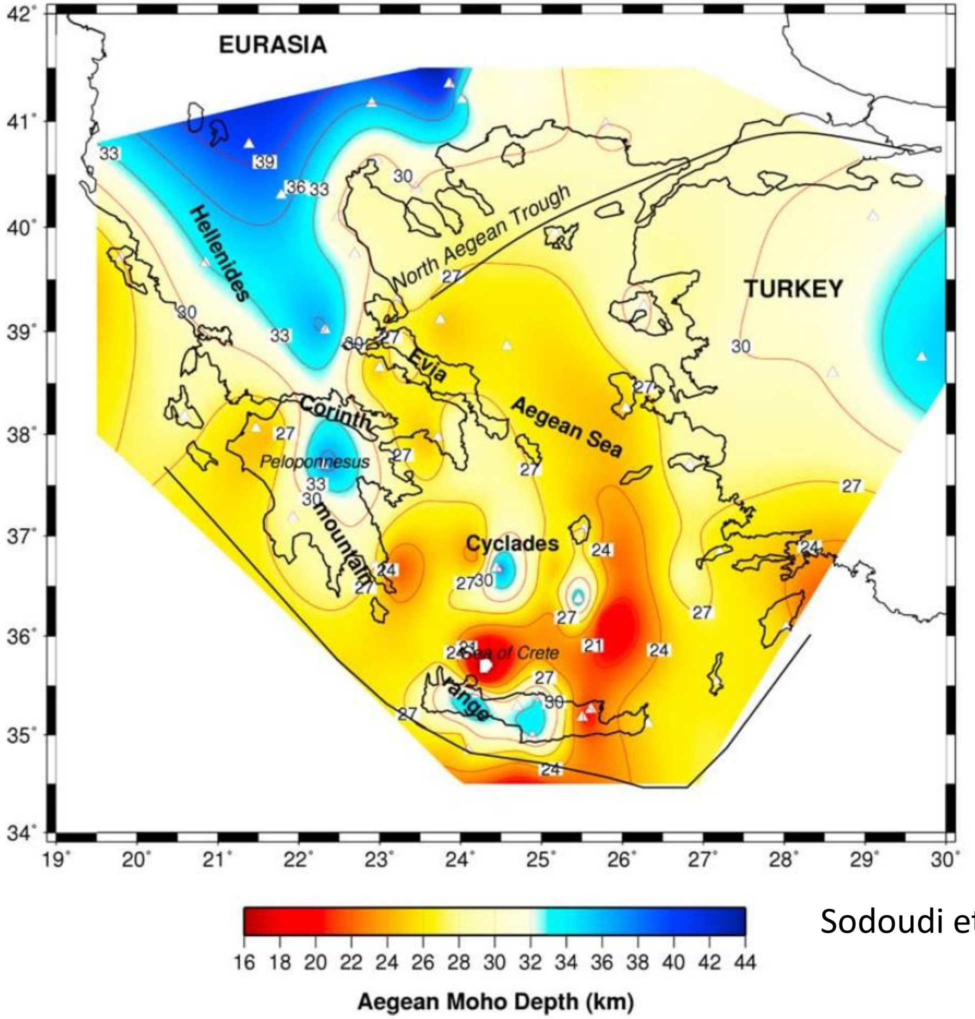

Aegean Moho depth map (in km) obtained from P and S receiver functions.

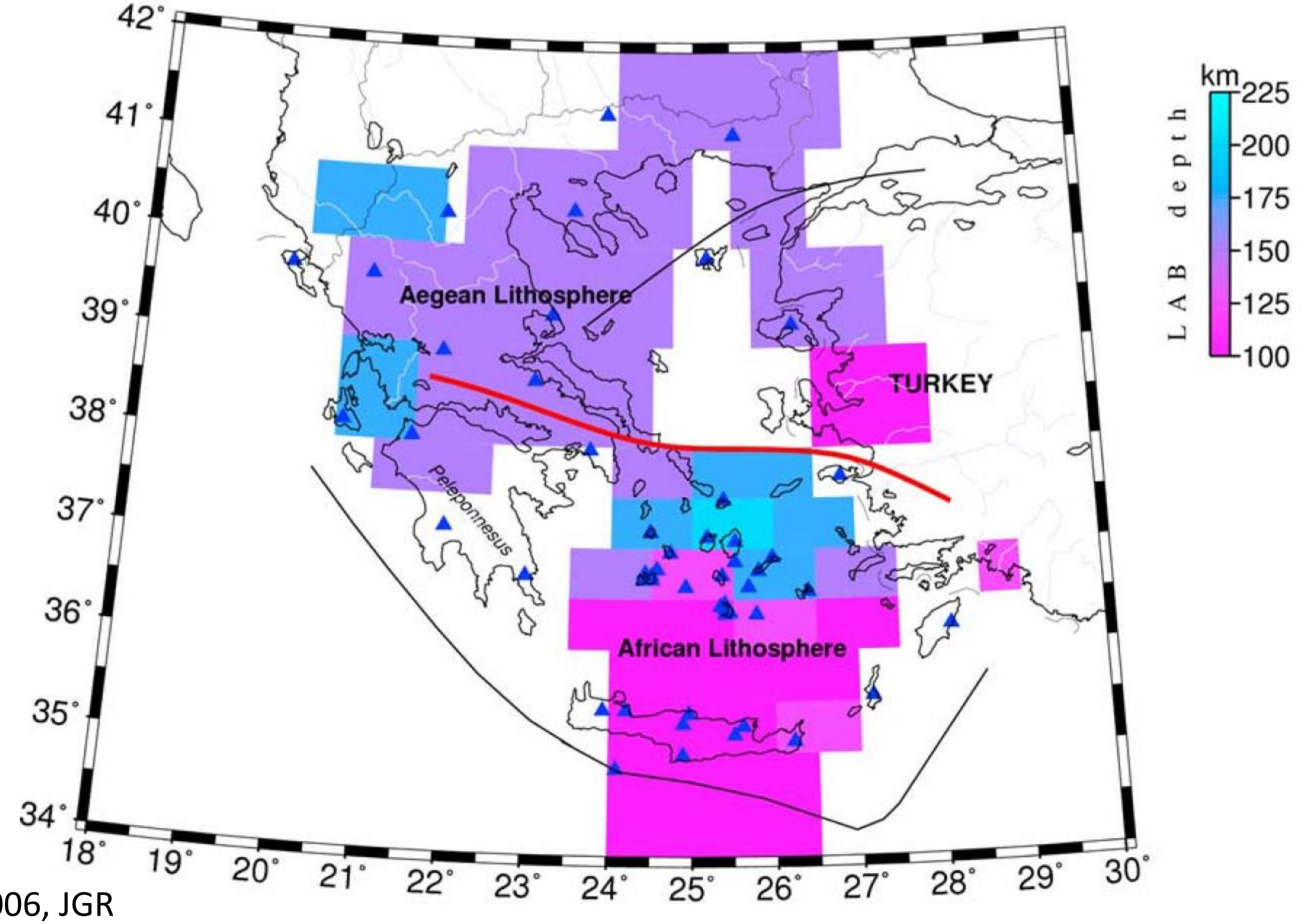

Sodoudi et al., 2006, JGR

LAB depth map obtained from S receiver function analysis in the Aegean. Red line indicates the boundary separating the observed continental Aegean lithosphere from the oceanic African lithosphere.

- The crustal structure of Aegean Sea and its surroundings is thinned and formed as an extensional backarc basin due to subduction of the African lithosphere beneath the Hellenic trench.

Eastern Mediterrenean

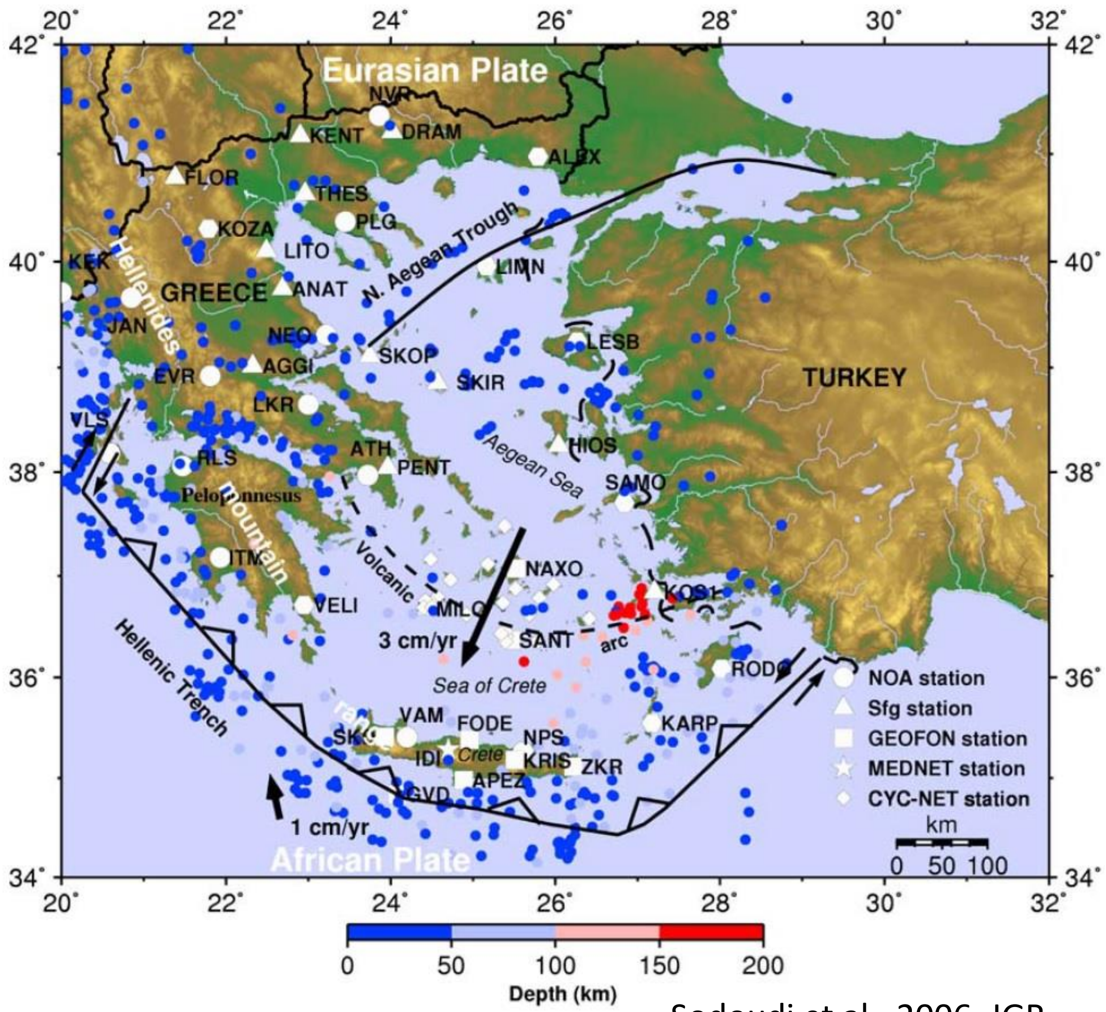

Sodoudi et al., 2006, JGR

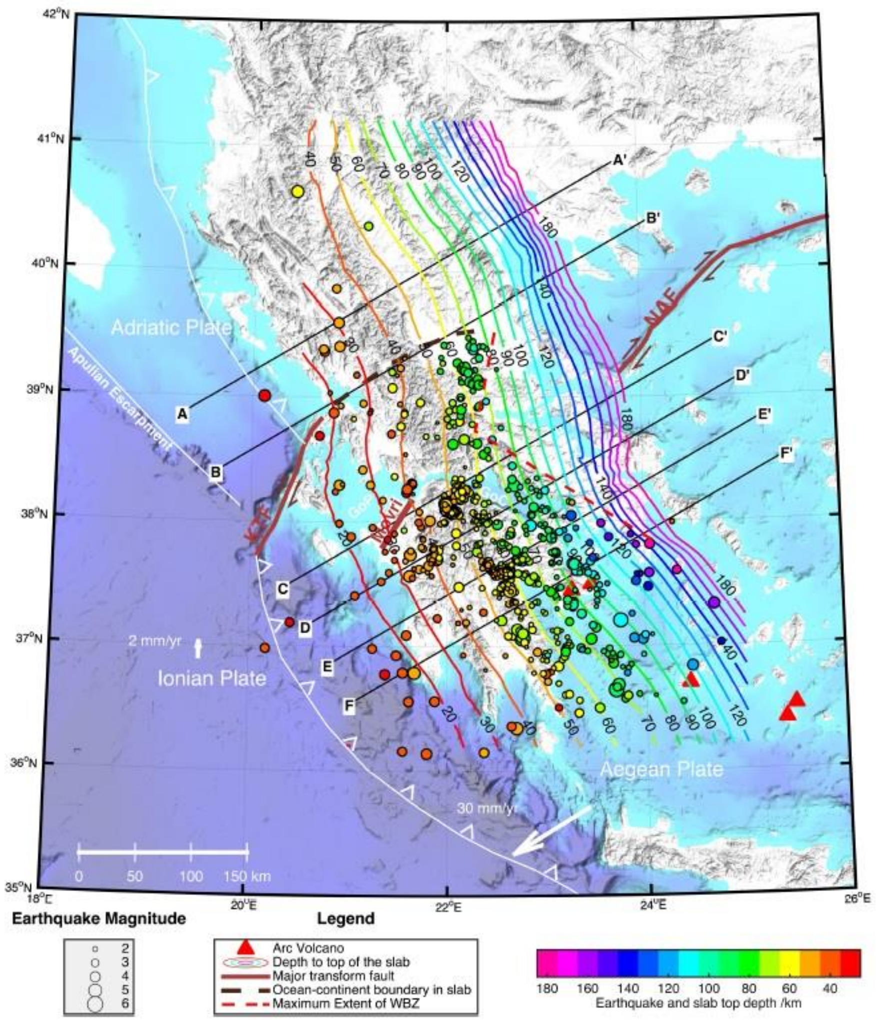

Halpaap et al., 2018, JGR

Black solid lines = locations of the Hellenic trench and the North Aegean Trough.
Dashed line =location of the volcanic arc.
Black arrows = direction of the motion relative to Eurasia
Blue circles = earthquakes with Ms>4.5

- The transition between oceanic subduction with more rollback in the south to continental subduction with less rollback in the north occurs in correspondence of Kefalonia fault and is reflected by a smoothly deformed slab, accompanied by a gap in deep intraslab seismicity (>60 km depth), probably indicative of a change in thermal regime between south and north

Eastern Mediterrenean

- The Eastern part of the Cyprus slab is extending beneath Nigde and Karaman cities and terminates beneath the quaternary volcanoes, while the western part of the Cyprus slab is extending under the Isparta Angle (IA) and Antalya Basin and is probably closed to the Hellenic slab.
- The Hellenic and Cyprus slab, divided by a tear, may simply be merged south of the Isparta Angle.
- The slow anomalies under the IA and Antalya Basin are likely to be associated with rising hot materials from asthenosphere due to major tearing between the Hellenic and Cyprus slabs.

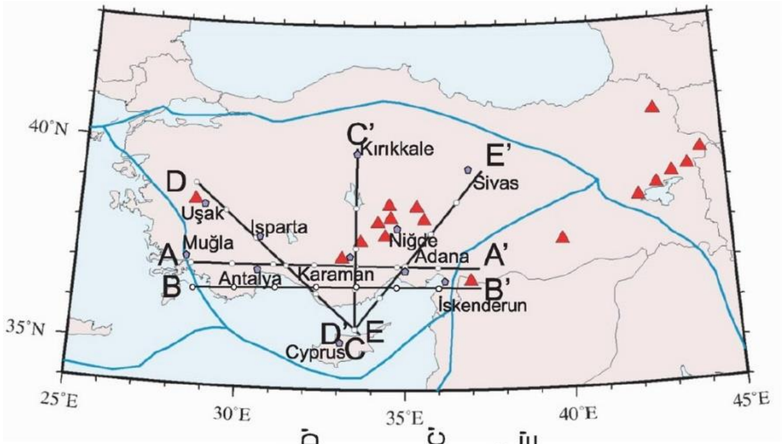

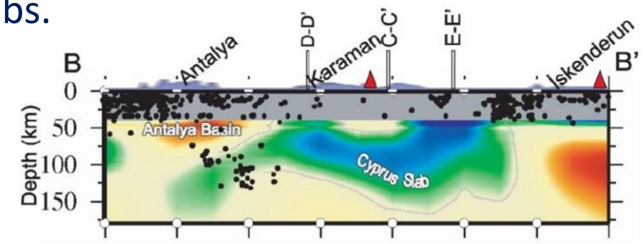

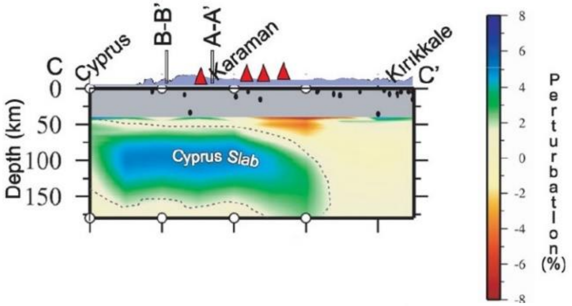

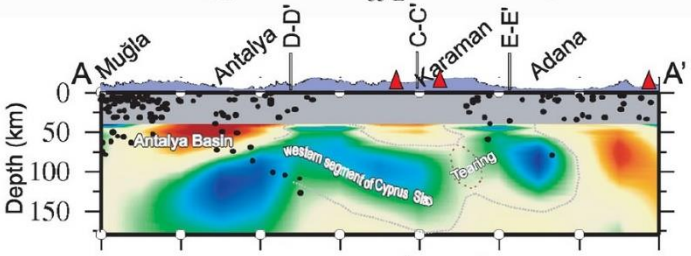

Bakirici et al., 2012, GJI

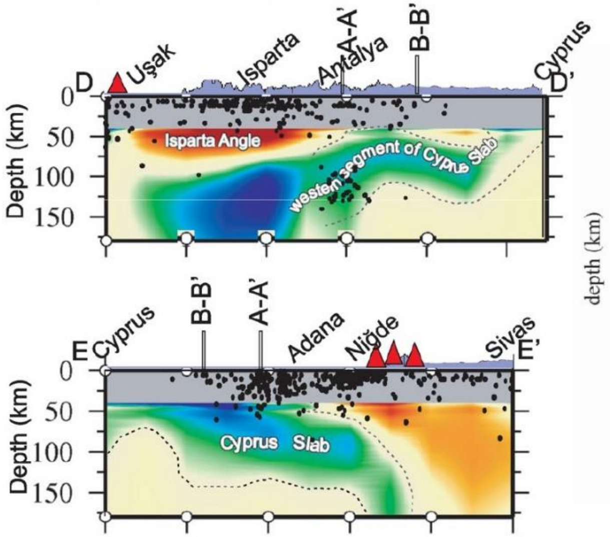

Black circles on the slices are focal depth of earthquakes with M_0 ≥3.0.

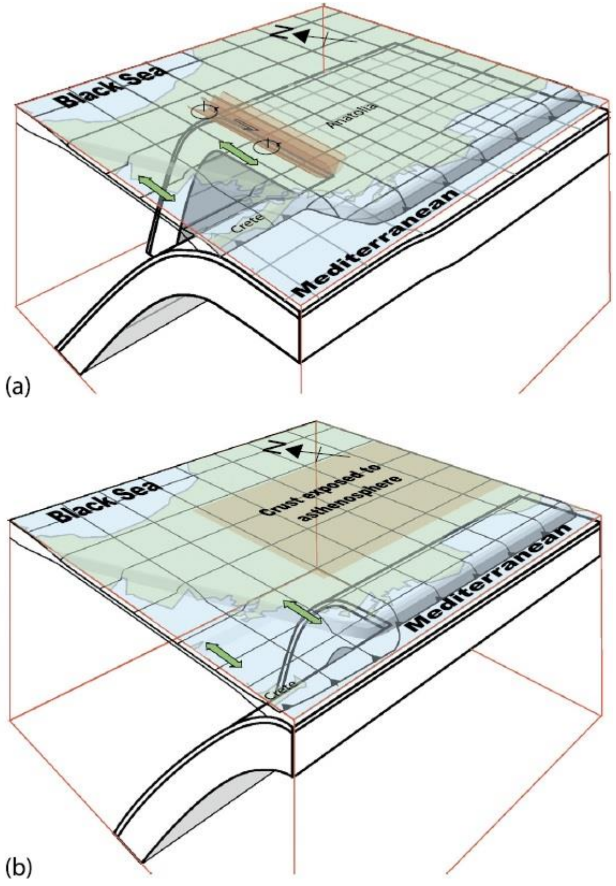

Govers and Fichtner, 2016, EPSL, 450

Eastern Mediterrenean

- The Arabian slab appears to be broken-off under the Eastern Anatolia, which may cause the widespread volcanism and uplift in the Eastern Anatolia.

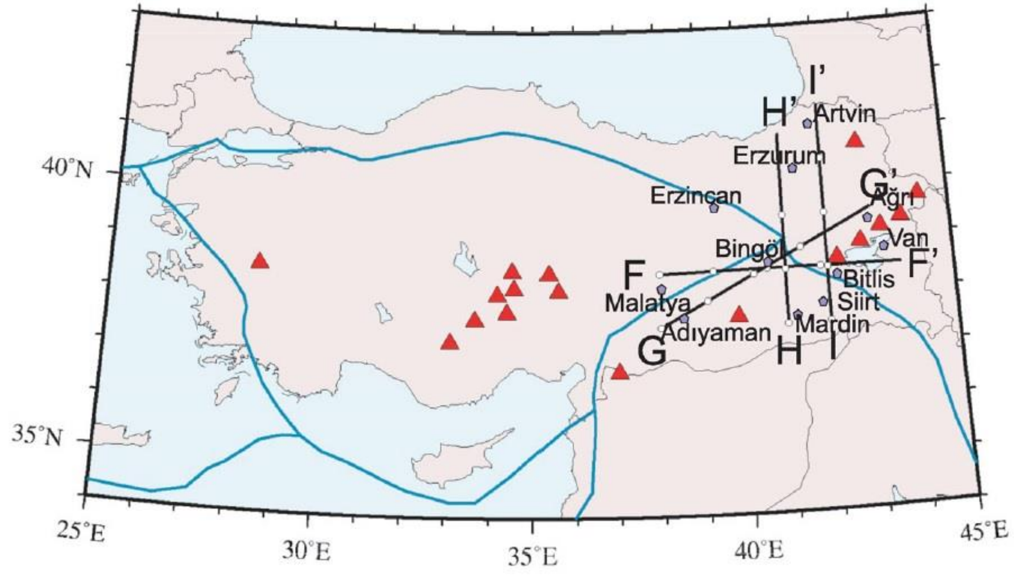

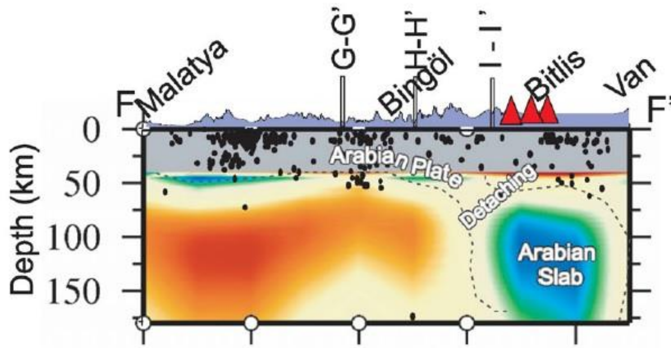

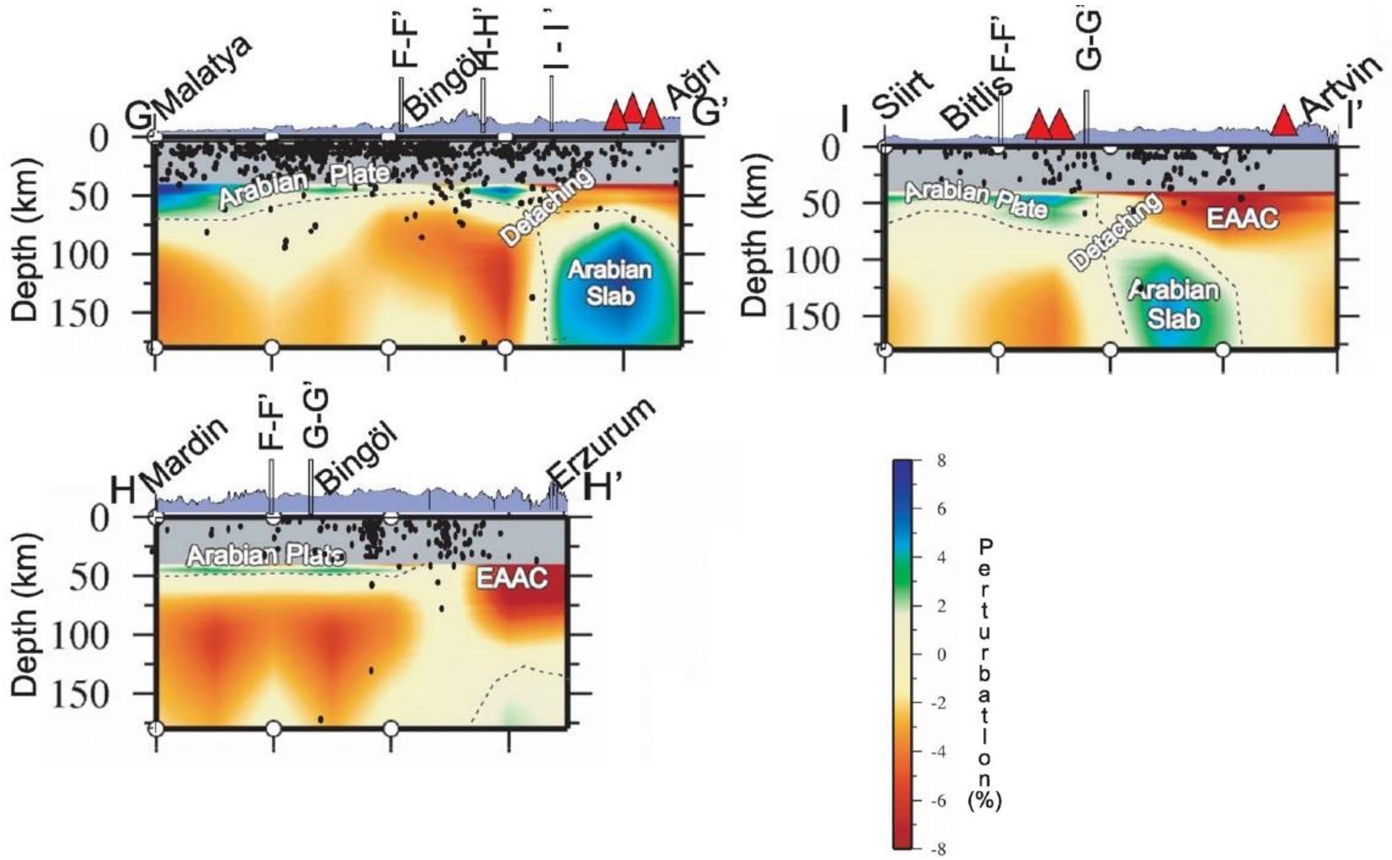

Bakirici et al., 2012, GJI

Mediterrenean Tectonics

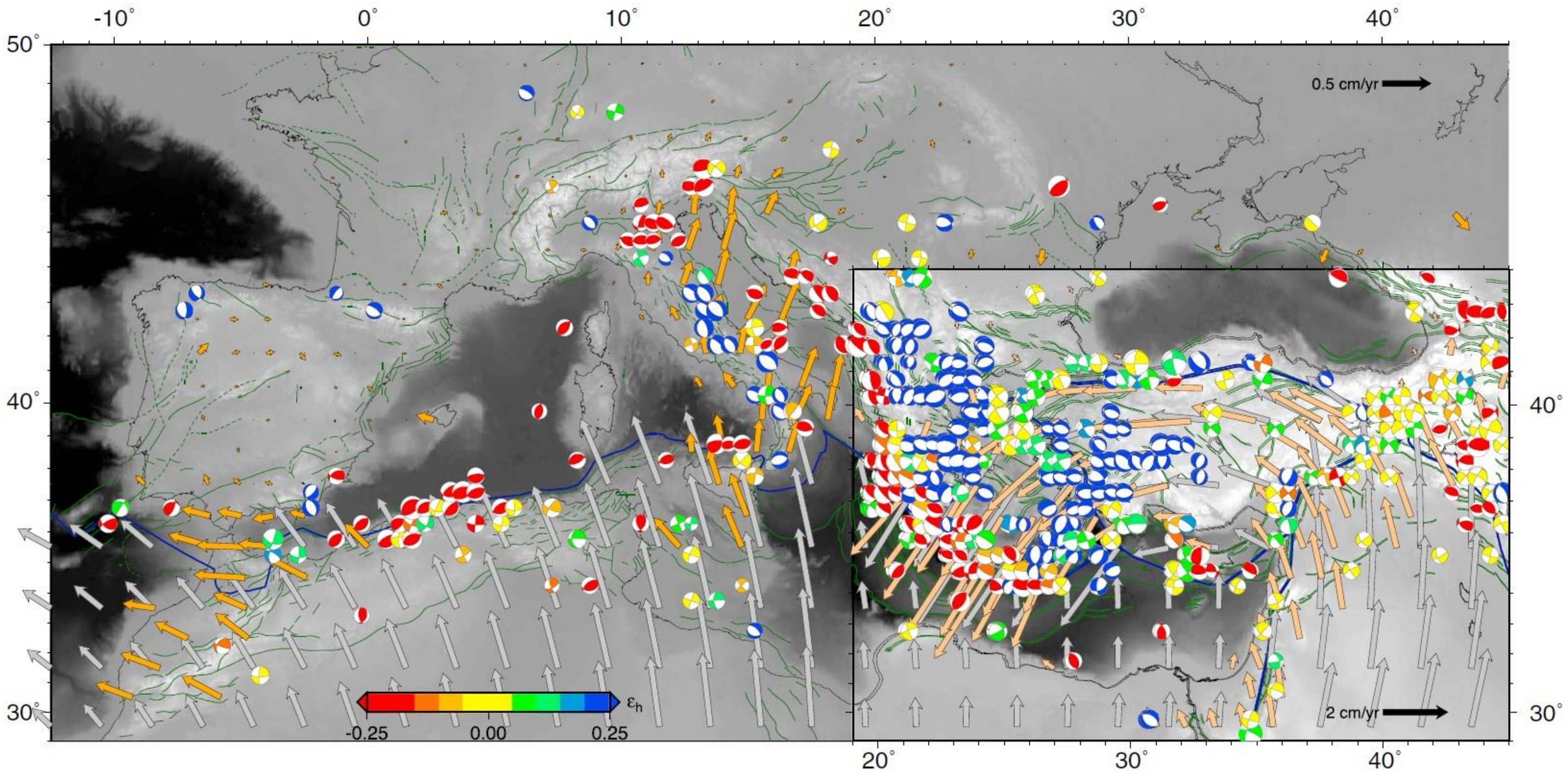

Faccenna et al., 2014, Rev. Geophys., 52

Interpolated GPS velocities (orange vectors obtained by first averaging velocities weighted by their uncertainties on a 1° × 1° grid, and then using spline-in-tension interpolation) long-term plate velocities (gray vectors, both in Eurasia-fixed reference frame). Blue, red, and green indicate extensional, compressional, and strike-slip types of deformation state.

Dynamic topography

(due to subducting slabs)

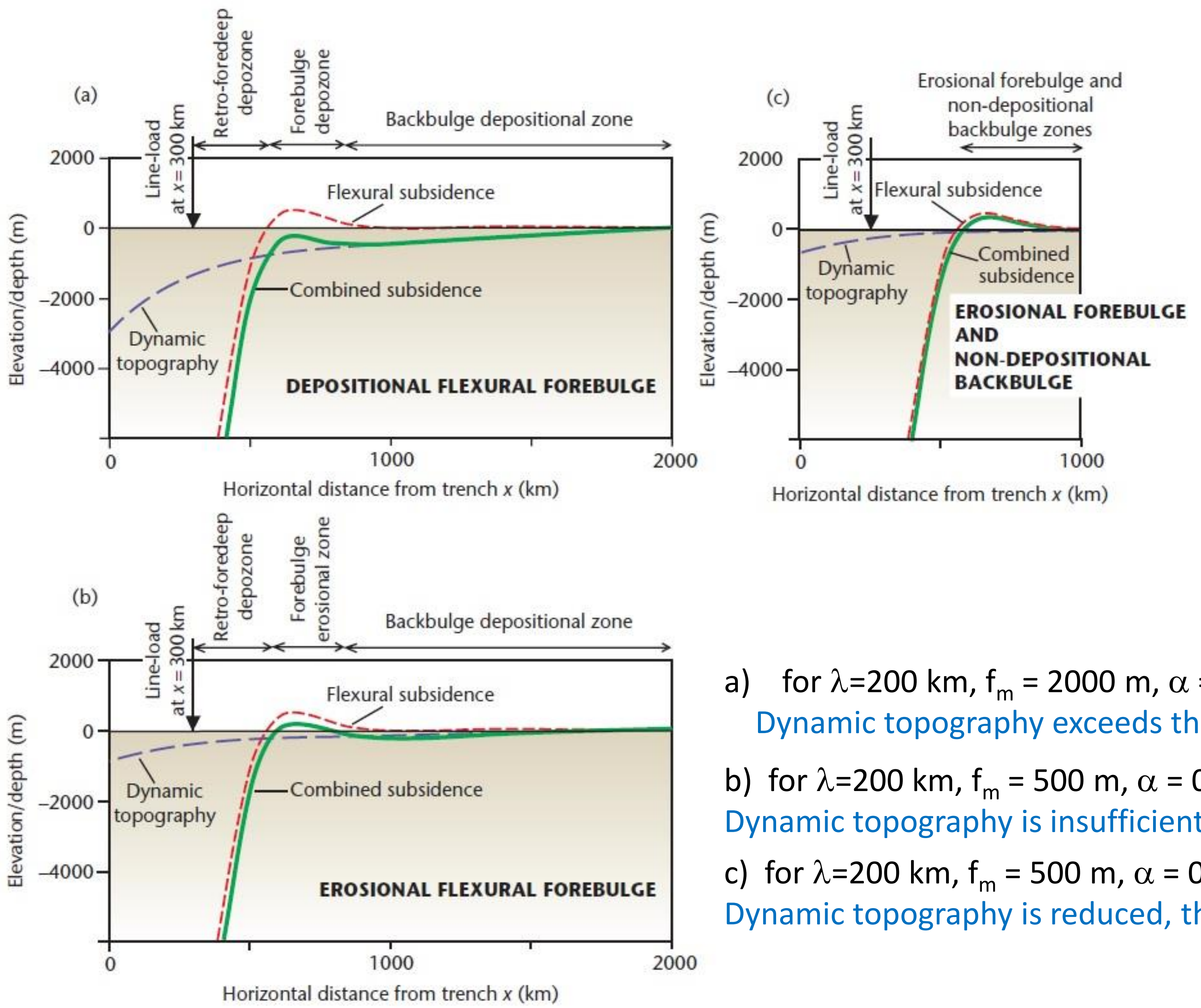

An expression for the geometric form of the dynamic topography is obtained by assuming that it is made of two components:

(i) an exponential component with an exponent λ and maximum deflection f_m.

(ii) a linear tilt with a maximum gradient α in m km^{-1} and a maximum distance from the trench at which tilting occurs η.

$$f(x) = f_m\left(e^{-x/\lambda}\right) + \alpha(\eta - x)$$

x = horizontal orthogonal distance from the trench

a) for λ=200 km, f_m = 2000 m, α = 0.5 m/km, and η = 2000 km
Dynamic topography exceeds the effects of flexural forebulge uplift.

b) for λ=200 km, f_m = 500 m, α = 0.2 m/km, and η = 2000 km
Dynamic topography is insufficient to exceed the magnitude of forebulge uplift.

c) for λ=200 km, f_m = 500 m, α = 0.2 m/km, and η = 1000 km (due to steepening of slab dip):
Dynamic topography is reduced, then back-bulge region is a non-depositional zone.

Dynamic topography

(due to subducting slabs)

- Horizontal distance into the upper plate affected by dynamic topography is likely related to the dip of the subducting slab.
- Subduction angle < 45° and a ΔT between slab and surrounding mantle of -200 K to -800 K produce deflections of the continental plate > 500 km from the trench.
- Factors influencing dynamic subsidence/uplift, besides subduction angle, are plate age, rate of subduction, flexural rigidity, and viscosity of the upper mantle.

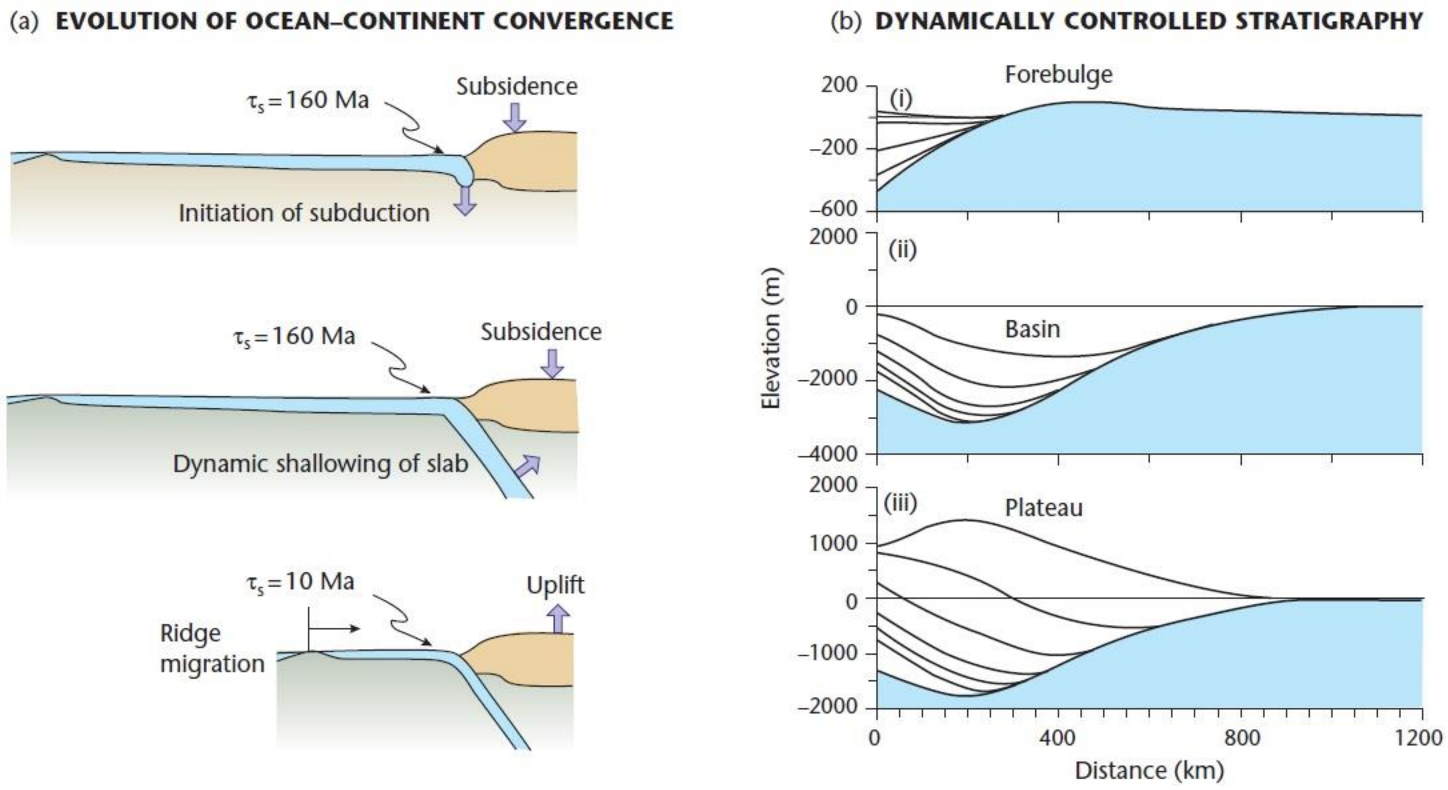

- **Subduction of young oceanic lithosphere causes long-wavelength uplift (e.g., Farallon plate beneath North America caused uplift of the Colorado Plateau).**
- **The dip of the slab generally decreases with age or when it attempts to subduct positive buoyant region (e.g., mid-oceanic ridge).**

Delamination of the subducting slab

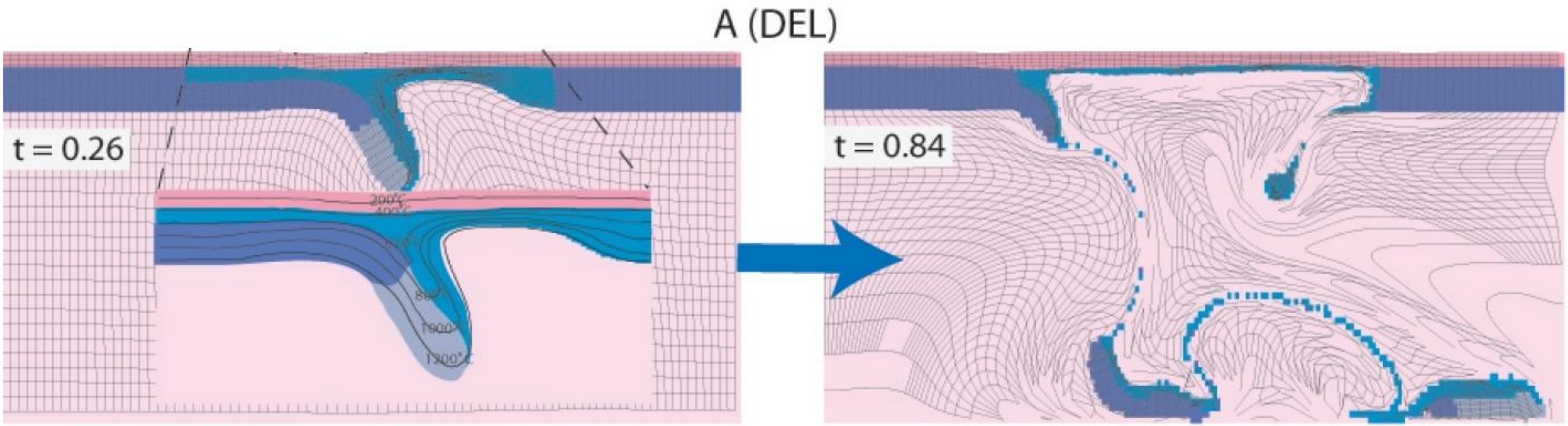

Gogus, 2010 (PhD thesis)

- As the mantle lithosphere starts to delaminate, it causes subsidence of the crust, while uplift occurs on the right side of the depression as hot mantle material is owing into the lithosphere breach vacated by the delaminating lithosphere.
- The signal of topography is becoming more asymmetrical as the delamination progresses in these very early stages.

Dripping of the subducting slab

DRIP-1 viscous dripping with nonlinear, temperature dependent rheology
DRIP-2 viscous dripping with non-linear, temperature independent rheology

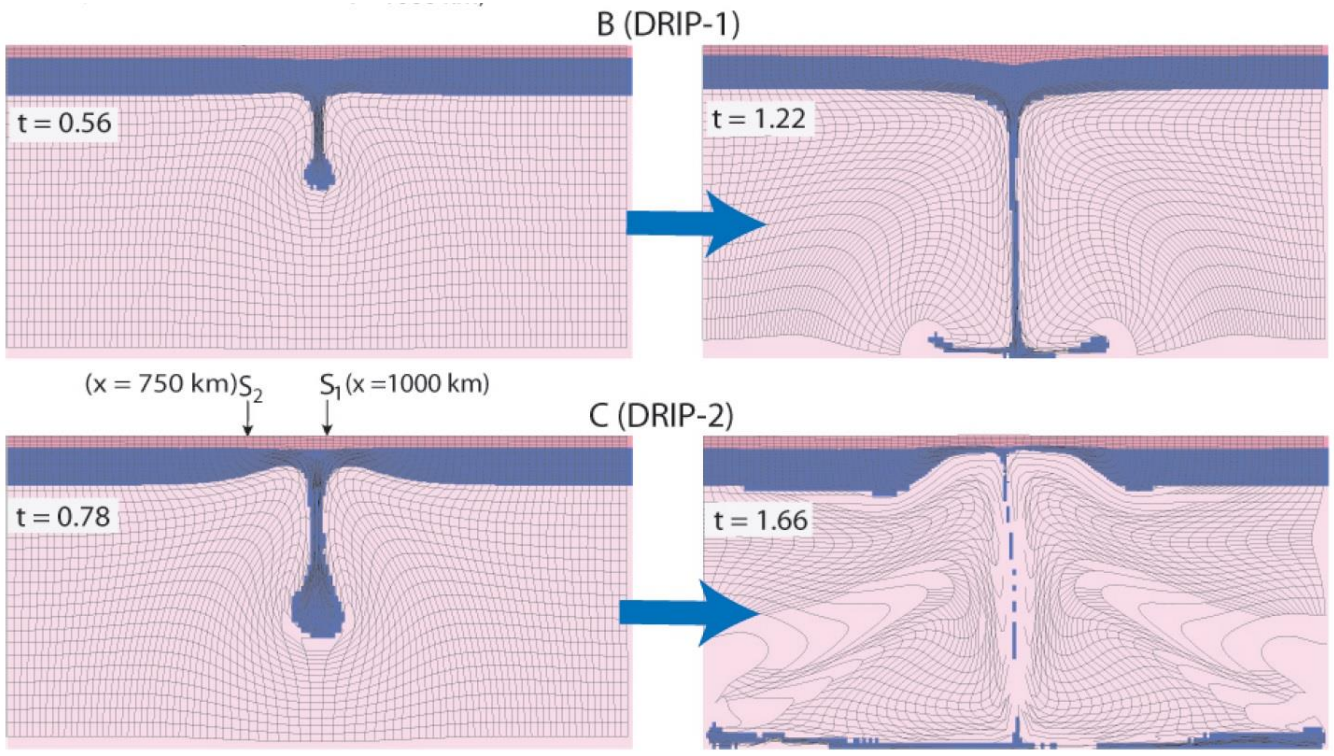

Gogus, 2010 (PhD thesis)

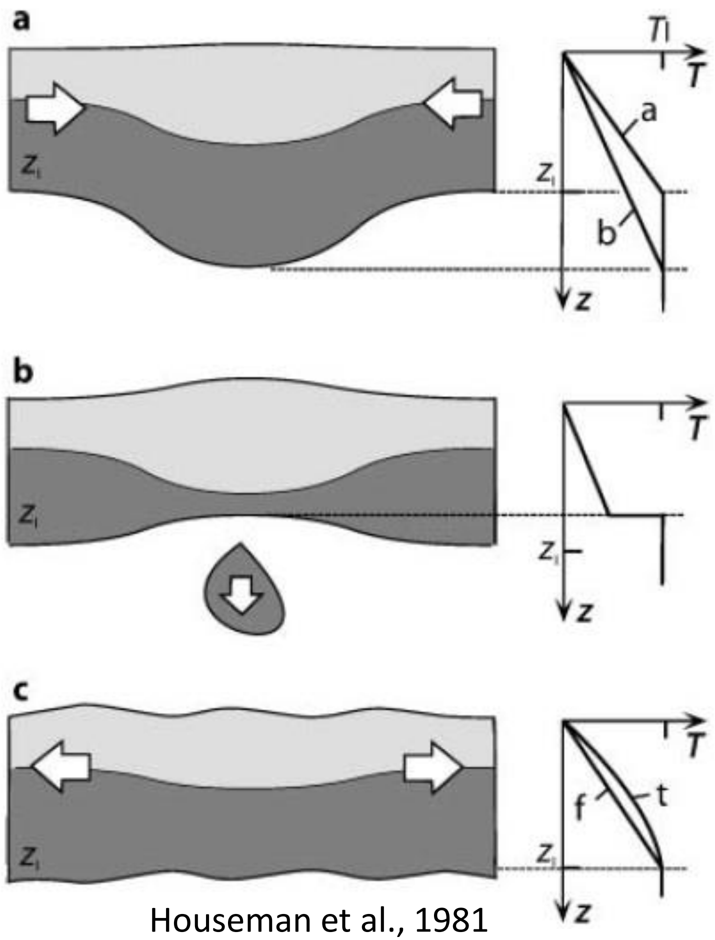

a=after thickening
b=before thickening

t=transient stage
f=final stage

Houseman et al., 1981

- A negative topography initially develops when the above the descending Raileigh-Taylor (*RT*) instability reaches a maximum depression.
- This symmetric topography is supported by the actively descending/dripping mantle lithosphere.
- The subsidence inverts to uplift as a result of the decrease in the downwelling forces as the descending mantle lithosphere is necking and narrowing, and reaches the bottom of the box.
- The topography is now dominated by isostatic uplift associated with the flow induced by crustal contraction and thickening.
- The drip models show clearly symmetrical topography signals that remain fixed in location above the downwelling mantle lithosphere (no migration of the *RT* instability).